IL-1 Activation of NF-κB Contributes to Perinatal Hypoxia/Ischemia Induced Cell Death

by
Xiaoming Hu

APPROVED BY THE SUPERVISORY COMMITTEE

_____
J. R. Perez-Polo, Ph.D.

_____
Karin W. High, Ph.D.

_____
Olivera B. Nesic-Taylor, Ph.D.

_____
David K Rassin, Ph.D.

_____
Norbert K. Herzog, Ph..D.

_____
Marjorie R. Grafe, M.D. Ph. D.

_____
Dean, Graduate School

IL-1 Activation of NF-κB Contributes to Perinatal Hypoxia/Ischemia Induced Cell Death

by
Xiaoming Hu, B.M., M.M.

DISSERTATION

Presented to the Faculty of The University of Texas Graduate School of Biomedical Sciences at Galveston
in Partial Fulfillment of the Requirements
for the Degree of

Doctor of Philosophy

Approved by the Supervisory Committee

Jose R. Perez-Polo, Ph.D.
Norbert K. Herzog, Ph..D.
Marjorie R. Grafe, M.D. Ph. D.
Karin W. High, Ph.D.
David K. Rassin, Ph.D.
Olivera B. Nesic-Taylor, Ph.D.

June, 2005
Galveston, Texas

Key words: Inflammatory cytokines, therapeutic strategies

To my mother, my husband Ye Peng, my daughter Katharine Peng and all my friends

ACKNOWLEDGMENTS

I would like to express my sincere gratitude to my mentor, Dr. J. Regino Perez-Polo, for his guidance, generosity, and commitment to my education and research work. I would also like to thank members of my Supervisory Committee, Dr. Olivera Nesic-Taylor, Dr. David Rassin, Dr. Karin High, Dr. Norbert K. Herzog, Dr. Marjorie Grafe, for their helpful inputs throughout this process. Thanks also to my friends and co-workers in Dr. Perez-Polo's lab: Dr. Jingxin Qiu, Danny Rafati, Krystyn Bourne, Julieann Lee, Diana Cittelly, Chamaine Rea, Martin Gill and Diana Ferrari. Special thanks to Lab Manager Karin Werrbach-Perez and Dr. Perez-polo's secretary Donna Masters.

I extend special thanks to Neuroscience Program Director Dr. James Blankenship for his guidance and Program Coordinator Ms. Lonnell Simmons and Ms. Cynthia Cheatham for their help in my four years graduate studies.

Finally, I would especially like to thank my mother and my husband for their love, support and encouragement to me.

IL-1 Activation of NF-κB Contributes to Perinatal Hypoxia/Ischemia Induced Cell Death

Publication No. _____

Xiaoming Hu, Ph.D.
The University of Texas Medical Branch at Galveston, 2005

Supervisor: Jose. R. Perez-Polo

IL-1 activity has been implicated in perinatal hypoxia/ischemia (HI) brain damage without the underlying mechanisms being characterized. We used a 7-day-old rat model to elucidate the role of NF-κB in HI stimulation of IL-1 signaling. HI was induced by permanent ligation of the left carotid artery followed by 90 minutes of hypoxia (7.8% O_2). We observed increased cell death and caspase 3 activity in the hippocampus and the cortex 3 to 48h post-HI. IL-1β protein expression increased began at 3h post-HI and lasted until 24h post-HI in the hippocampus and 12h post-HI in the cortex. Intracerebroventricular injection of 2μg IL-1 receptor antagonist (IL-1Ra) 2h post-HI significantly reduced cell death and caspase 3 activity. EMSA analyses for NF-κB activity showed increased p65/p50 DNA-binding activity at 24h post-HI. Western blot analyses and immunofluorescent staining showed significant nuclear translocation of p65. Protein expression levels of iNOS and COX2, known to be transcriptionally regulated by NF-κB, also increased at 24h post-HI. All these changes were reversed by IL-1Ra blockade of IL-1, consistent with IL-1 triggering of inflammatory apoptotic outcomes via NF-κB transcriptional activation. The observed increase in cytoplasmic phosphorylated IκBα and nuclear translocation of Bcl-3, was also attenuated by IL-1Ra blockade, suggesting that HI-induced IL-1 activation of NF-κB is via both degradation of IκBα and nuclear translocation of Bcl-3.

Inhibition of NF-κB via decoys containing NF-κB binding consensus sequences present in IgG-κB promoter showed selective inhibition of p65/p50 binding activity, while Bcl-x decoys selectively inhibited c-Rel/p50 (p52) binding activity. RPAs showed that IgG-κB decoys significantly decreased IL-1α, TNF-α and TNF-β mRNA levels compared to minimal changes after Bcl-x or scrambled decoy treatment, indicating a selective IgG-κB decoy effect on inflammation post-HI. Microarray data indicated that 1) Genes that were significantly down-regulated by IgG-κB decoys were not affected by Bcl-x decoys and *vice versa*, another piece of evidence for selective effects of different decoys. 2) A large number of cell death/survival related genes were affected by IgG-κB

decoys. Our results suggest that IgG-κB decoys selectively inhibit inflammatory responses to HI. However, careful design of decoy sequences is essential to acquire selective effects on cell death.

TABLE OF CONTENTS

LIST OF FIGURES

Chapter 1: INTRODUCTION

Perinatal hypoxia-ischemia (HI) brain injury is a leading cause of neonatal morbidity and mortality (Kaltschmidt et al. 1994). Although the incidence of perinatal HI brain injury is only 2 to 5 per 1000 births, the medical cost, the developmental delays, and the impact on the family and government are profound. Following HI brain injury, a large number of brain neurons will degenerate. This can cause severe impairment of brain function for those survivors. It is estimated that 20 to 30% of survivors of HI brain injury have severe long-term neurological sequelae such as cerebral palsy (Kuban and Leviton 1994); uncounted others have milder injuries that result in mental retardation, seizures, learning disorders, and behavioral disorders (Krageloh-Mann et al. 1999; Vexler and Ferriero 2001). Approximately 3,000 newborns are diagnosed with cerebral palsy every year in the United States. Although advances in obstetrical and neonatal care have improved outcomes for both term and preterm infants, they have also increased the number of infants surviving perinatal HI with moderate or severe encephalopathies who will typically exhibit at least one of several neurological disabilities. That causes problems not only for the children but for the parents as well; it is a very heavy emotional and financial burden to care for a disabled child. Society is affected as well: the lifetime cost of caring for a single disabled child approaches one million dollars. The mechanism of neuronal cell death after HI brain injury is still under investigation. Although a variety of pharmacological and physiological interventions have been proposed (Vannucci and Perlman 1997), none have proven to be effective or safe for use in human infants.

Rat Models for perinatal Hypoxia-Ischemia Brain Injury

Animal studies are important in providing information regarding mechanisms underlying perinatal HI brain injury and how the injury may be prevented or reduced through a therapeutic strategy. Until the early 1980's, studies of ischemic brain injury in rats were limited to the adult rat, called the Levine preparation (Levine, 1960). The adult model entails ligation of one common carotid artery followed thereafter by exposure to hypoxia (Levine 1960). The insult produces permanent HI brain damage restricted to the

structures ipsilateral to the carotid artery occlusion, including: cortex, corpus striatum, globus pallidus, amygdala, hippocampus, thalamus and hypothalamus.

Rice et al. (1981) adapted the Levine preparation to postnatal day 7 (P7) rats. In the Rice model, ischemia resulting from unilateral common carotid artery ligation is followed by systemic hypoxia produced by the inhalation of 8% oxygen-balanced nitrogen for 3 or more hours. The P7 postnatal rat was initially chosen for study because the anatomical development of the P7 rat brain is roughly equivalent to the development of the mid-third trimester human brain based on overall growth, cell production, neuronal migration, and white matter myelination (Dobbing and Sands 1979; Vannucci et al. 1999). Rice et al. observed brain damage in over 90% of surviving rats with greater than 50% developing infarcts in the cerebral cortex and hippocampus (Vannucci et al. 1999; Towfighi et al. 1991). The injury, largely restricted to the ipsilateral side of the brain, is observed in cerebral cortex, hippocampus, striatum subcortical and periventricular white matter (Vannucci et al. 1999).

This immature rat model of perinatal HI has been widely used to study mechanisms of brain damage, brain plasticity and therapeutic interventions. Studies focused on neurotransmitter status (Romijn et al. 1992; Przedborski et al. 1991), glutamate excitotoxicity (Silverstein et al. 1991), inflammatory responses (Bona et al. 1999; Cowell et al. 2002), brain plasticity, gene induction (Gubits et al. 1993), magnetic resonance imaging of evolving lesions, apoptosis and necrosis (Rumpel et al. 1995), have provided insights into the characteristics of HI damage in the immature brain and why the distribution of injury is different from that of the adult. There are some modifications of the original protocol involving variations in the strain (Sprague-Dawley, Wistar, Long Evans), age of animals (P2-P21), duration of hypoxia (30 minutes - 3.5 hours), concentration of oxygen (5%-12%) and temperature in the hypoxia chamber (31-37˚C).

Cell Death and Hypoxia-Ischemia

HI injury to the brain has been shown to result in cell death with a pattern of combined necrosis and apoptosis (Martin, Sieber and Traystman 2000; Pulera et al. 1998;

Northington et al. 2001; Nakajima et al. 2000). Apoptosis refers to the characteristic biochemical and morphological changes that occur in cells undergoing programmed cell death. These changes include chromatin condensation and subsequent margination against the nuclear envelope, cytoplasmic and nuclear condensation, overall cell shrinkage, cytoplasmic vacuolization, and convolution of the nuclear and cytoplasmic membranes followed by the formation of apoptotic bodies. These apoptotic bodies then undergo phagocytosis. Necrosis is characterized by overall cell swelling, chromatin clumping and organelle disruption, with early loss of membrane integrity (Hockenbery 1995; Majno and Joris 1995).

Necrotic cell death occurs early in the core of the infarction, where hypoxia is most severe, and results from abrupt energy depletion and acute cellular collapse (Ray et al. 2003). Delayed cell death, which usually starts 12 hours after the HI insult, at the infarct core and in the penumbra is mainly due to apoptosis of neurons and glia (Northington et al. 2001). In adult animal models, both apoptosis and necrosis have been reported following focal cerebral ischemia in rodents (Charriaut-Marlangue et al. 1996; Chen et al. 1997; Guegan and Sola 2000; Matsushita et al. 1998) and after global cerebral ischemia (Ni et al. 1998; Nitatori et al. 1995), often emphasizing delayed neuronal death in the selectively vulnerable regions of the hippocampus. In the present P7 rat animal model, cell death occurring immediately after HI in the core site is necrotic (Nelson and Silverstein 1994), while delayed and remote cell death in the penumbra is mostly apoptotic, as documented by ultrastructural criteria, TUNEL (terminal dUTP nick-end labeling) staining and caspase-3 activation (Nakajima et al. 2000; Northington et al. 2001). Compared with the adult rat model, a significantly higher density of apoptotic cells are observed in cortex, striatum and hippocampus in P7 rats after HI (Nakajima et al. 2000). Activation of caspase-3 activity in striatum and hippocampus is prolonged for about 7 days after HI injury, which is much longer than that in the adult rat (Cheng et al. 1998; Nakajima et al. 2000). The persistence of apoptotic cells and the prolonged activation of caspase-3 after HI suggest that apoptosis plays a more important role in

neonates than in adult brains after HI. This also provides an extended therapeutic window for interventions designed to diminish cell loss after HI.

Hypoxia-Ischemia Stimulation of IL-1

A rapidly expanding body of evidence suggests that inflammatory responses contribute substantially to the pathogenesis of perinatal HI brain injury (Hagberg et al. 1996; Bona et al. 1999; Hedtjarn et al. 2002). HI increases expression of the pro-inflammatory cytokines: interleukin-1 (IL-1)β, TNFα/β and IL-6 (Foster-Barber, Dickens, and Ferriero 2001; Lau and Yu 2001; Saliba and Henrot 2001). The best-characterized early response inflammatory cytokine after HI is IL-1 (Szaflarski, Burtrum, and Silverstein 1995). The IL-1 family includes the agonists IL-1α and IL-1β, the endogenous receptor antagonist IL-1 receptor antagonist (IL-1Ra) and a newly discovered member, IL-18/IL-1γ (Shapiro et al. 1998). IL-1β has consistently been detected in central nervous system after injury to the brain or spinal cord (Rothwell et al. 1997; Nesic et al. 2001). There are reports showing that IL-1β mRNA and protein levels increase as early as 1h after brain injury and persist during the development of infarction in various adult animal models (Minami et al. 1992; Zhang et al. 1998; Davies et al. 1999). Although an early increase in IL-1β mRNA levels has been reported in a neonatal rat model of ischemia (Hagberg et al. 1996; Szaflarski, Burtrum and Silverstein 1995), there is no information about IL-1β protein levels after neonatal HI. The exact cellular source of IL-1β after HI is still controversial. The major sources are considered to be endothelial cells and microglia (Buttini, Sauter and Boddeke 1994). However, it is reported in some studies that neurons, astrocytes, and oligodendrocytes, also express IL-1β after induction of HI (Sairanen et al. 1997). The involvement of IL-1α in the pathogenesis of HI has not been investigated extensively. Although there are some reports showing that IL-1α mRNA increases even earlier than IL-1β after both temporary and permanent occlusion of the middle cerebral artery in mice (Hill et al. 1999; Touzani et al. 1999), there is no information available concerning the role of IL-1α in HI brain injury.

Following synthesis, pro-IL-1β (31kD) remains primarily in the cytoplasm until cleaved by the IL-1β converting enzyme (ICE, Caspase-1), producing mature and active IL-1β (17kD). Caspase-1 also cleaves and activates IL-18 but not IL-1α (Dinarello 1999). There is evidence showing a correlation between increased IL-1β levels and subsequent neurodegeneration. Administration of exogenous IL-1β markedly exacerbates neuronal/glial damage in rodents exposed to focal cerebral ischemia or excitotoxin administration (Lawrence et al. 1998; Stroemer and Rothwell 1998). Decreasing effective IL-1β levels using anti IL-1β antibodies (Touzani et al. 1999) or inhibitors of ICE (Hara et al. 1997; Loddick and Rothwell 1996) decreases neuronal loss after cerebral ischemia. IL-1Ra is widely used to study the function of IL-1 in HI because it is a selective, endogenous receptor antagonist that blocks the actions of IL-1α and IL-1β (Dinarello et al. 1998). Injection, or over expression, of IL-1Ra significantly inhibits HI induced cell death (Betz, Yang and Davidson 1995; Stroemer and Rothwell 1997; Stroemer and Rothwell 1998; Yang et al. 1998). Although there is compelling evidence which validates a contribution of IL-1 to HI induced cell death, the precise mechanisms by which IL-1 may achieve its effects are unknown.

The responses to IL-1α and IL-1β are initiated by binding to IL-1 type-I receptor (IL-1RI), which then associates with an IL-1 receptor accessory protein (IL-1RAcP) (Wesche et al. 1997), leading to signal transduction (Cao, Henzel and Gao 1996; Muzio et al. 1997). IL-1RIs are expressed on both glia and neurons (French et al. 1999; Pinteaux et al. 2002). A second receptor, IL-1 type-II receptor (IL-1RII), has a much shorter cytoplasmic domain and is thought to act as a decoy (non-signaling) receptor (McMahan et al. 1991). The activation of IL-1RI stimulates ubiquitous transcription factors (NF-κB, AP-1, AFP), and some key intracellular signaling molecules (JNK, IP3 or PKC-kinases), (Auron 1998; O'Neill and Greene 1998). The specific signaling mechanisms triggered by IL-1 responsible for the effects on transcription factors and kinases are less well understood for HI-induced cell death. Based on in vitro studies, it has been suggested that

activation of the NF-κB pathway through IL-1RI binding after ischemia results in gene transcription with deleterious outcomes (Dunn et al. 2002).

NF-κB/Rel family of proteins

The transcription factor "NF-κB" consists of homo- or heterodimers of subunits which constitute a family of related proteins, including p50, p52 (also called p49), p65 (also called RelA), c-Rel and Rel-B (Figure 1). All share a highly conserved ~300 residue NH2–terminal domain for DNA binding/dimerization (Rel homology domain), which enables them to form dimers and bind to an array of homologous decanucleotide sequences with varying affinities. NF-κB/Rel proteins can be divided into two classes based on their C-terminal domain. One class includes p65, c-Rel and Rel-B proteins, all of which contain a C-terminal transactivation domain. Another class includes p50 and p52, which have no transactivation domains at their C-termini (Bours et al. 1990; Bours et al. 1992; Ghosh and Baltimore 1990; Nolan et al. 1991; Ruben et al. 1991; Ryseck et al. 1992; Schmid et al. 1991). p50 and p52 are first synthesized as the precursors p105 and p100 respectively, both of which have ankyrin-like repeats in their C-termini with close homology to that of IκB protein family. After degradation of their C-terminal regions, mature p50 and p52 will be released. Dimerization of NF-κB subunits produces species with various intrinsic DNA-binding specificities, transactivation properties, and subcellular localization (Baeuerle 1991; Siebenlist et al. 1994). NF-κB dimeric combinations must contain at least one of the transactivating members (p65, c-Rel or Rel-B) to have the ability to activate DNA transcription (Baeuerle 1991; Chen et al. 1998; Lenardo and Siebenlist 1994; Siebenlist, Franzoso and Brown 1994). The most commonly described active NF-κB subunit combinations are the p65/p50 and c-Rel/p50 heterodimers. Homodimeric combinations of p50 or p52 have no transactivation activity and often behave in vivo as transcriptional inhibitors at high affinity binding sites (Franzoso et al. 1992; Franzoso et al. 1993; Kang et al. 1992).

NF-κB is expressed in the nervous system and shows a low level of constitutive activity in neurons (Kaltschmidt et al. 1994). NF-κB is induced above constitutive levels

in the brain by various stimuli, most of which are stressful or neurotoxic. For example, rodent NF-κB is induced in the forebrain and hippocampus following HI (Koong, Chen and Giaccia 1994; Schmidt et al. 1995, Yang, Mu and Hayes 1995, Qiu et al. 2001), in the cortex after traumatic brain injury (Yang, Mu and Hayes 1995), and in the limbic structures following seizures (Rong and Baudry 1996). NF-κB is reported to regulate cell death by modulating a diverse array of genes, known to be important for cell death or survival, such as Bcl-2, Bcl-xL, manganese superoxide dismutase (MnSOD), inducible nitric oxide synthase (iNOS), cyclooxygenase 2 (COX2), and some inflammatory cytokines (IL-1α/β, TNF-α/β), (Foster-Barber et al. 2001; Lau and Yu 2001; Saliba and Henrot 2001).

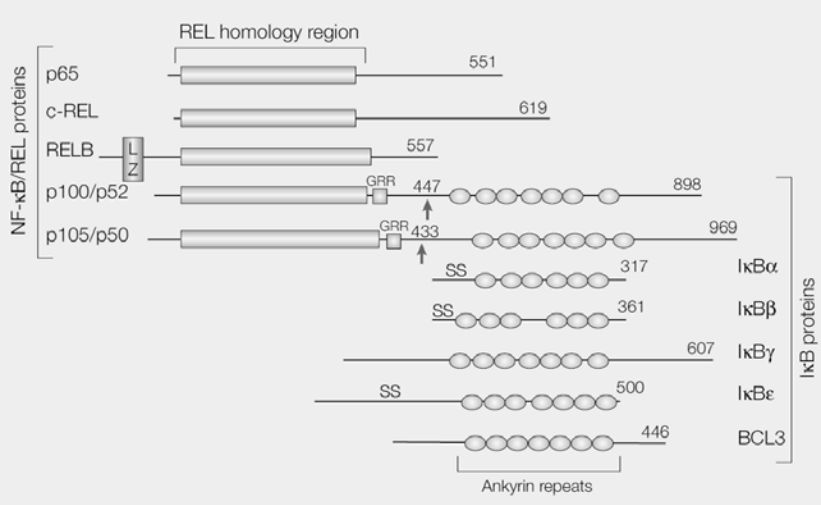

Figure 1. The NF-κB/Rel and IκB family of proteins. Members of the NF-κB/rel and IκB families of proteins are shown. The number of amino acids in each protein is shown on the right. The arrows point to the endoproteolytic cleavage sites of p100/p52 and p105/p50; LZ, leucine zipper domain of Rel-B; GRR, glycine-rich region. *(Adapted from Ghosh et al. Annu. Rev. Immunol. 1998. 16:225-260).*

NF-κB has been reported to play a role in HI-induced cell death (Clemens et al. 1997; Schneider et al. 1999; Seegers et al. 2000; Stephenson et al. 2000). The levels of activation of NF-κB vary in a complex fashion over time after HI in the adult rat brain. This complexity reflects the broad range of NF-κB binding consensus sequences present in many gene promoters regulated by NF-κB and the variability in NF-κB protein dimer

compositions present in different central nervous system (CNS) regions under different physiological conditions (Pizzi et al. 2002; Qiu et al. 2001). The extent to which NF-κB activation contributes to neuropathology vs. neuroprotection and recovery remains unresolved. In a number of experimental models, including cell lines and tissues under different stimuli, NF-κB activation appears to result in both apoptotic and anti-apoptotic outcomes (Abbadie et al. 1993; Baichwal and Baeuerle 1997; Barger et al. 1995; Barger and Mattson 1996; Grilli and Memo 1999; Grimm et al. 1996; Jung et al. 1995; Lipton 1997). It is possible that the different compositions of NF-κB protein dimers determine the outcomes of their activation. For example, the p65/p50 dimer may activate genes coding for proteins with pro-apoptotic properties, while c-Rel/p50 dimer may activate genes coding for proteins that prevent cell death (Qiu et al. 2001; Pizzi et al. 2002). Therefore, different stimuli might activate different NF-κB dimers, resulting in either beneficial or detrimental outcomes. Previous studies in our research group also suggest that transcriptional regulation of target genes by NF-κB is tissue-specific and may be gene-specific within a given tissue or cell type (Qiu et al, 2001). Therefore, different NF-κB targeted genes may respond to stress stimuli by triggering both pro- and anti-apoptotic signaling pathways with the final outcome being determined by the integrated results of the different NF-κB regulated events in different tissues.

There is a generic NF-κB DNA sequence consisting of a 10 bp consensus sequence that encompasses 128 different decameric sequences, 5'-GGGRNNTYCC-3' (G=guanine, R=purine, N=any nucleotide, Y=pyrimidine, C=cytosine, T=Thymine). Distinct NF-κB subunit exhibit different binding affinities for the multiple consensus sequence combinations, and this variation likely determines the specificity of NF-κB transcriptional regulation (Perkins et al. 1992; Kunsch et al. 1992). For example, p65 binds preferentially to the decameric sequence 5'-GGGRNTTTCC-3' (Kunsch et al. 1992) and the c-Rel binds preferentially to the decameric sequence 5'-TGAATTTTCC-3' present on the IFN-γ promoter (Sica et al. 1992). Specific combinations of NF-κB

proteins can thus distinguish among the various κB sites to selectively regulate gene expression.

Sequence-specific inhibition of NF-κB can be accomplished with synthetic double stranded (ds) phosphothiorate oligonucleotides containing a NF-κB consensus sequence, which acts *in vivo* as "decoy" *cis* elements to bind transcription factors and block the activation of cognate genes (Morishita et al. 1997; Yu et al. 1999). The principle of the transcription factor "decoy" approach is simply the inhibition of promoter activity due to the binding of endogenous transcription factors to saturating amounts of exogenous double-stranded oligonucleotides displaying the specific DNA sequences that are present in the promoter region of the genes of interest. For example, an IgG-κB decoy, which contains the NF-κB consensus sequence in the IgG-κB promoter, has been used to inhibit p65/p50 activity (Blondeau et al. 2001). However, there is little information about decoys targeted to other NF-κB heterodimers.

IκB family of proteins

One of the most important features of NF-κB proteins is that the function of NF-κB is strictly regulated by its subcellular localization. Its activation depends on the translocation from cytoplasm to nucleus. The movement of NF-κB proteins into the nucleus and/or binding to DNA is controlled by a family of inhibitor proteins called IκB (Haskill et al. 1991; Thompson et al. 1995; Zabel and Baeuerle 1990). There are several inhibitory IκB proteins (IκBα, IκBβ, IκBγ and Bcl-3, **Figure 1**), which regulate NF-κB activity. These proteins have several homologous amino acid stretches known as ankyrin repeats that specifically interact with NF-κB/Rel proteins (Bours et al. 1992; Grilli, Chiu and Lenardo 1993). IκBα and Bcl-3 are the most important two in this family. They contribute to the regulation of NF-κB activity via different mechanisms.

IκBα is present in cytoplasm, where it binds to NF-κB heterodimers to inhibit their action. In response to stimuli, including IL-1, TNF-α and bacterial lipopolysaccharides (LPS), IκB is phosphorylated by an IκB kinase, ubiquinated and

degraded by proteasomes (Ghosh and Baltimore 1990; Israel 1995; Liu, Sen and Rothstein 1993), uncovering masked nuclear localization signals on the NF-κB dimers, which are then translocated to the nucleus, bind to DNA consensus sequences on gene promoters and enhancers, and activate transcription (Ghosh 1998). In particular, it has been shown that IκBα must be phosphorylated at Serine-32 and Serine-36 and ubiquitinated at Lys-21 and Lys-22 for it to be targeted for subsequent degradation by the ubiquitin/proteasome system (Traenckner et al. 1995; Baldwin 1996). Interestingly, only the NF-κB dimers that contain at least one trans-activating member (p65, c-Rel or Rel-B) are effectively regulated by IκBα. Thus, the p52 and p50 homodimers are not usually retained in the cytoplasm by IκBα. Their activity is regulated within the nucleus by Bcl-3.

Although structurally homologous, Bcl-3 and IκBs act differently in regulating NF-κB activity. While the IκBs are primarily cytoplasmic, Bcl-3 is predominantly nuclear and has a binding specificity for p52 or p50 homodimers (Bours et al. 1993; Fujita et al. 1993; Nolan et al. 1993; Bundy and McKeithan 1997; Franzoso et al. 1993). There are two mechanisms by which Bcl-3 can regulate NF-κB activity. First, Bcl-3 can successfully compete with promoter DNA bound p50 or p52 homodimers, removing the NF-κB homodimers away from cognate binding sites on target promoter DNA sites (Nolan et al. 1993; Zhang et al. 1998; Franzoso et al. 1993; Siebenlist, Franzoso and Brown 1994), allowing p65/p50 or c-Rel/p65 to bind and activate gene transcription. Secondly, Bcl-3, together with p52 or p50 homodimer, can bind to DNA κB sites and form ternary complexes. The tethering of Bcl-3 to DNA via p52 or p50 homodimer allows the activation of gene transcription, which Bcl-3 or p50/p52 homodimers alone cannot do, since Bcl-3 has only a transactivation domain and p50/p52 has only a DNA binding domain (Bours et al. 1993; Fujita et al. 1993; Rocha et al. 2003). The different regulatory effects of Bcl-3 may depend on its phosphorylation states and concentration in the nucleus (Bundy and McKeithan 1997; Cogswell et al. 2000; Fujita et al. 1993; Nolan et al. 1993).

It is reported that NF-κB is stimulated by hypoxia via increased IκBα degradation and NF-κB nuclear translocation. A small number of studies report that an independent pathway involving Bcl-3 stimulation might also contribute to NF-κB activation after hypoxia (Gozal, Simakajomboon and Gozal 1998; Qiu et al, 2001; Zhang et al. 1998). Until now, the involvement of Bcl-3 in perinatal HI injury has not been well characterized. There is scant information about the regulation of Bcl-3 activity after injury.

Hypothesis:

A series of experiments were designed to test the hypothesis that HI-induced IL-1 contributes to cell death via the selective stimulation of NF-κB p65/p50, which could further stimulate transcription of pro-apoptotic factors, such as iNOS and COX2. Activation of p65/p50 by IL-1 is via: 1) IL-1 induction of IκBα degradation, enabling p65/p50 translocation to the nucleus; 2) IL-1 induced increases of nuclear Bcl-3, which binds p50/p50 or p52/p52 homodimers and releases the κB promoter site for binding of p65/p50. We also tested the effects of selective interventions in 1) IL-1 receptor binding or 2) injury-induced p65/p50 NF-κB activation, after HI injury. The aim of this study was to characterize the activation mechanisms by which IL-1 contributes to HI-induced cell death in the neonatal hippocampus and cortex, in order to develop rational therapeutic interventions.

CHAPTER 2: METHODS

Animals

All animal procedures were approved by the institutional Animal Care and Use Committee at the University of Texas Medical Branch at Galveston. Timed pregnant Sprague-Dawley rats were purchased from a commercial breeder (Harlan, Indianapolis, IN), housed in individual cages, and fed a standard laboratory diet *ad libidum*. Offspring were delivered spontaneously. The day of birth was defined as post-natal day 0 (P0). Litter size was culled to 10 each on P1 or P2 to minimize variation in body and brain growth. Pups were maintained with their dams until 7 days of postnatal age (P7). Pups that showed signs of respiratory or other infections were excluded from further study. The average body weight on P7 was 15 ± 3 g.

The Induction of Ischemia and Hypoxia

HI was induced as described by Rice et al. (1981) with some modifications (Grafe 1994). The P7 rats were given 4% and 2% Isoflurane in air by mask inhalation for induction of anesthesia and maintenance of anesthesia throughout surgery, respectively. Both male and female rats were used in this study since gender differences in response to the insult have not been reported (Vannucci et al. 1997). The left common carotid artery was exposed through a midline incision in the neck. The artery was isolated from surrounding tissue and was dually ligated with 7-0 prolene suture (Ethicon) to restrict blood flow to the ipsilateral side of the brain. The artery was transected between the ligatures to prevent re-establishment of blood flow. The incision was closed with 5-0 silk suture (Ethicon) and the incision site was cleaned with saline and ethanol. Bitter Apple® was applied to the sutures to deter the dam from chewing the incision site. The duration of surgery was 8-12 minutes and the total time of exposure to Isoflurane was approximately 20 minutes. The operated rats recovered from surgery for approximately 30 minutes in a 37°C chamber with bedding from the cage. The rats were then returned to the dam for 2-3 hours. Rats were transferred to a humidified hypoxia chamber where

systemic hypoxia was induced by inhalation of 7.8% oxygen balanced with nitrogen for 90 minutes. The temperature in the hypoxia chamber was maintained at 37°C by warming the gas mixture entering the chamber and by wrapping the chamber in a heated water blanket. The sham groups were handled, anesthetized and treated with room air in the cage. The rats were sacrificed 3, 6, 12, 24, 48 and 72 hours after completion of HI treatment. At sacrifice, animals were briefly anesthetized by inhaling Halothane, decapitated, and the brains removed. Hippocampus and cortex were dissected from the rest of the brain, frozen, and stored at -80ºC until use.

Oligonucleotide Preparation

Unmodified complementary single-stranded oligonucleotides used in EMSA assays were synthesized by Sigma-Genosys (Woodlands, TX).

IgG-κB sequence: 5'-AGTTGAGGGGACTTTCCCAGGC-3'.

Bcl-x sequence: 5'-TTTGTGGGGGGTCTCCAGCAT-3'.

Chemically modified complementary single-stranded "decoy" oligonucleotides containing one phosphothiorate group on both 5' and 3' end were synthesized by Sigma-Genosys (Woodlands, TX).

IgG-κB sequence: 5'-GAGGGGACTTTCCCA-3'. (Yu et al. 1999)

Bcl-x sequence: 5'-GTTGGGGGGTCTCCGG-3'. (Qiu et al. 2001)

Scrambled sequence: 5'-GATGCGTCTGTCGCA-3'. (Yu et al. 1999)

Transcription factor binding sequences within each oligonucleotide are underlined above. Fluorescein was added to the phosphothiorated oligonucleotides at the 5' end for studying the decoy oligonucleotide distribution. All single stranded oligonucleotides were annealed in sterile TEN buffer (1 mM EDTA, 50 mM NaCl, 10 mM Tris, pH 7.5) at a stock concentration of 6 nmol/μl.

Treatment

The P7 rats were given 4% and 2% Isoflurane in air by mask inhalation for induction of anesthesia and maintenance of anesthesia throughout surgery, respectively, and placed in a Kopf stereotaxic apparatus (David Kopf Instruments, Tujunga, CA) modified for P7 rat skulls. The skull was exposed and a small burr hole was made using a 24-gauge needle. A Hamilton syringe with a 26-gauge needle was used for injection. The 6 nmol/1 μl (approximately 80 μg) decoy oligonucleotide solution or 2μg/1μl (totally 2μg) IL-1Ra (R&D system, Minneapolis, MN) solution was stereotaxically injected into the left lateral ventricle of each animal at a rate of 0.5 μl/30 seconds. All the intracerebroventricular injections were performed using the stereotaxic coordinates for the p10 rat lateral ventricle (Shewood and Timiras 1970) that were adapted to the p7 rat by initial trial and error. Preliminary injections with dye were made to verify the right coordinates. The coordinates were set at 1.5 mm left of midline, 2 mm posterior to bregma, and 3 mm ventral to the skull surface. Sham animals received an injection of 1 μl sterile saline (vehicle) at the same stereotaxic positions. After the completion of each injection, the needle was left in place for an additional 5 minutes to allow diffusion of solutions, and then slowly retracted. The wound was closed and sutured, and the animals were allowed to recover on a heating pad until they awakened.

Tissue Extracts

Cytoplasmic and nuclear protein extracts were prepared according to methods previously reported, with some modifications (Qiu et al. 2001). Briefly, dissected tissues were homogenized with a Wheaton Tenbroeck® manual homogenizer on ice in ice-cold buffer containing 10mM HEPES, pH 7.9, 10mM KCl, 0.1mM EDTA, 0.1mM EGTA, 1mM dithiothreitol (DTT), 0.5mM phenylmethylsulfonylfluoride (PMSF), and 2μg/ml each of the protease inhibitors antipain, chymostatin, pepstatin, and leupeptin. The tissue mixture was centrifuged at 8,000 rpm (5,220g) for 4 min at 4ºC. The supernatant was extracted and allocated for the cytoplasmic lysate. The remaining pellet was reconstituted in 1.5 μl/mg of buffer (containing 20mM HEPES, pH 7.9, 400mM NaCl,

1mM EDTA, 1mM EGTA, 1mM DTT, 1mM PMSF, and 2μg/ml each of the protease inhibitors antipain, chymostatin, pepstatin, and leupeptin) with shaking for 20 min at 4ºC. The crude nuclear extract was centrifuged at 14,000 rpm (16,000g) for 10 min at 4ºC, and the supernatants containing the nuclear extracts were frozen, and stored at -80ºC.

Protein Concentration Determination

Protein concentration was determined by the Bradford method. Standard concentration curves were determined by mixing 800μl of 0, 5, 10, 15, 20, 25, 30 and 50μg/ml bovine serum albumin with 200 μl BioRad Protein Assay Dye Reagent Concentrate and incubated for 10 minutes. Each unknown protein sample was diluted to 1:400 (nuclear fraction) or 1:800 (cytoplasmic fraction) to a final volume of 800 μl, mixed with 200 μl BioRad Protein Assay Dye Reagent Concentrate and incubated for 10 minutes. The sample absorbance was read with a Beckman Du 7400 spectrophotometer at 590nm wavelength.

Electrophoretic Mobility Shift Assays (EMSA)

Oligonucleotides encompassing the IgG-κB enhancer sequence (GGGACTTTCC) and the Bcl-x gene NF-κB/CS4 sequence (GGGGGTCTCC) were used as probes and 5' labeled with γ-^{32}P-ATP and T4 polynucleotide kinase. A 30 μg aliquot of extracted nuclear protein was preincubated in a reaction buffer (5 mM HEPES, pH 7.9, 4% glycerol, 0.2 mM EDTA, 20 mM KCl, 0.4 mM MgCl2, 2 mM DTT, and 0.4 mM PMSF) and 2μg poly dI-dC . After 10 min of incubation on ice, approximately 1×10^5 cpm of ^{32}P end-labeled double-stranded oligonucleotide probe was added to the reaction, and the mixture was incubated for 20 min at room temperature. Reaction mixtures were loaded on a 5% nondenaturing polyacrylamide gel in 0.25× TBE buffer (pH 7.2). Gels were dried and exposed to X-ray film. Immunodepletion/supershift was done by incubation with 2μg of antibodies to the different NF-κB subunits (c-Rel, p65, p50, Rel-B and p52 from Santa Cruz Biotech, Santa Cruz, CA) overnight at 4°C before adding probe.

ELISA Cell Death Detection Assay

DNA fragmentation was measured by an ELISA assay that is specific for nucleosome-associated cytosolic DNA. The apoptosis ELISA was performed by using the Roche Cell Death Detection ELISA kit (Roche, Germany). The assay is based on sandwich-enzyme-immunoassay-principle using mouse monoclonal antibodies directed against DNA and histones, respectively. This allows the specific determination of mono- and oligonucleosomes in the cytoplasmic fraction of brain tissue. Briefly, each well of the 96-well plate was coated with 100µl anti-histone antibody solution overnight at 4°C. After removing the antibody solution from the well, 200µl incubation solution was added, followed by 30 minute incubation at room temperature. The wells were washed thoroughly with 250-300µl washing buffer three times. 100µl sample solution (50µg/100µl in incubation buffer), the cytoplasmic fraction which was isolated as described above, was added to the wells and incubated for 90 minutes at room temperature. 100µl incubation buffer alone was used as a background control. Each well was duplicated. After washing the wells three times with 250-300µl washing buffer, 100µl conjugate buffer was added for another 90 minutes' incubation at room temperature. After incubation, the wells were washed three times with 250-300µl washing buffer. 100µl substrate buffer was then added. The plate was placed on a plate shaker at 250 rpm for 10-20 minutes. The sample absorbance was read with an ELISA plate reader (Dynex, Chantilly, Virginia) at 450nm wavelength.

ELISA IL-1β Detection Assay

ELISA (Biosource, Camarillo, CA) was used to measure IL-1β protein levels in cytosolic fractions of hippocampus and cortex. The assay was performed according to the BioSource Int. protocol for solid phase sandwich ELISA using antibodies specific for rat IL-1β. The sample absorbance was read with an ELISA plate reader adjusted to 450 nm, and the concentration was determined based on a standard IL-1β curve established with recombinant rat IL-1β.

Caspase 3-Like Activity Assay

Caspase-3-like enzymatic activity was measured using a colorimetric assay from R & D systems (Minneapolis, MN). Cell lysates (100μg cytosolic fraction) were incubated with a DEVD substrate peptide conjugated to p-nitroanaline. The cleavage of the peptide by active caspase 3 releases the chromophore pNA, which induces a color change that is directly proportional to the level of caspase 3 activity. After incubating plates in the dark at 37°C overnight, color change was quantitated spectrophotometrically at a wavelength of 405 nm.

Decoy Distribution Study

Fluorescein labeled IgG-κB oligonucleotides were injected into the left lateral ventricle of P7 rats. Animals were sacrificed at 2 or 7 hours after injection. At sacrifice the rat pups were anaesthetized with ketamine (40 mg/kg i.p) and perfused with 10ml heparinized saline (via the left ventricle), followed by 20ml 4% paraformaldehyde in 0.1 M phosphate buffer (pH 7.4, 100 ml/100g body weight). The entire rat head (with opened skull) was postfixed for 2 hours in the same solution. Brains were removed and cryoprotected in 30% sucrose/PBS solution overnight. Brain blocks were embedded in Optimal Cutting Temperature compound (OCT), immediately frozen with dry ice for 1-2 minutes then stored at -80^{o}C. Brain blocks were sectioned (10μm coronal) with a freezing microtome and observed immediately using a fluorescence microscope.

Western Blot Analysis

Samples containing 30 μg protein were boiled for 10 minutes in an equal volume of sample buffer (100 mM Tris, pH 6.8, 250 mM 2-mercaptoethanol, 4% SDS, 0.01% bromophenol blue, 20% glycerol), placed on ice, and then loaded into a 10% polyacrylamide gel. Samples were separated by electrophoresis in Tris-glycine buffer (25mM Tris, 250mM glycine, 0.1% SDS) at 130 volts. Proteins were subsequently transferred overnight to polyvinylidene difluoride membranes (Millipore, Billerica, MA) at 4ºC, 25 volts, in a transfer buffer containing 20% methanol, 20mM Tris, and 150 mM glycine, at pH 8. Membranes were incubated for one hour at room temperature in

blocking buffer containing 5% powdered milk in TBS-Tween (20mM Tris, 137mM NaCl, 0.1% Tween-20), followed by incubation for one hour in primary antibody diluted in 50% blocking buffer in TBS-Tween, and then washed for 20 minutes in TBS-Tween, twice. Membranes were subsequently incubated in horseradish peroxidase-conjugated IgG (Biorad laboratories, Hercules, CA), diluted 1:3000 in 50% blocking buffer for one hour, and then washed three times in TBS-Tween for 15 minutes. Peroxidase activity was detected using the Amersham enhanced chemiluminescence lighting system (ECL, Amersham, Buckinghamshire, England) and exposed to X-ray film. Protein bands were quantitated using a densitometer. p65 polyclonal and IκB polyclonal antibodies were purchased from Santa Cruz Biotechnology (Santa Cruz, CA). iNOS antibody was purchased from BD Transduction Laboratories (San Diego, CA). COX2 antibody was purchased from Cayman Chemical (Ann Arbor, MI). Phospho-IκB antibody was purchased from Cell Signaling Transduction (Beverly, MA).

Histology

The rats were euthanized with an intraperitoneal injection (i.p.) of 120-mg/kg pentobarbital (Nembutal) and then perfused through the left ventricle with saline followed by 4% paraformaldehyde. Brains were removed and postfixed in 4% paraformaldehyde overnight at 4^{o}C. The brains were blocked in the coronal plane and the right sides were notched. The brains were then dehydrated, cleared, and embedded in paraffin. Six-micron thick tissue sections were made at the level of the mid-hippocampus and the tissues were stained with hematoxylin and eosin (H&E).

Immunofluorescence Staining

Coronal sections including hippocampus and cortex were cut at a thickness of 6μm, heated in the oven at 55^{o}C overnight, then deparaffinized and re-hydrated. Sections were microwaved in 10mM sodium citrate buffer (pH 6.0) for 20 minutes for antigen retrieval, replacing evaporated buffer every 5 min. Slides were cooled for 20 minutes, and then washed 4 times in ddH_2O, 3 times in 0.1M TBS/Triton 100, and 1 time with TBS. Sections were blocked with signal enhancer (Molecular Probes, Eugene, OR) for 30

minutes at room temperature. Sections were then incubated separately with 1:200 primary antibodies (Rabbit-anti-rat IL-1RI or Rabbit-anti-rat p65, Santa Cruz Biotechnology, Santa Cruz, CA) in diluent buffer (TBS+ Triton-X-100 +1% NGS) at room temperature overnight inside a moisture chamber. After washing with TBS 3 times (7 minutes each time), sections were incubated with fluorescent labeled secondary antibody (1:1000 Alexa Fluor 568 (Red) Goat-anti Rabbit IgG) for 2 hours at room temperature, in the dark. Sections were washed with TBS 5 times, each for 12 minutes, coverslipped using fluorescence mounting medium with DAPI, and sealed with clear nail polish. For double staining the sections were incubated with a mixture of two primary antibodies from different species followed by two secondary antibodies giving fluorescence of different colors. For the neuronal marker, 1:5000 neuronal-specific nuclear antigen, NeuN (Mouse-anti rat) antibody was used as the primary antibody and 1:1000 Alexa Fluor 488 (green) Goat-anti mouse IgG was used as the secondary antibody. For the oligodendrocyte marker, 1:200 CC1 antibody (Mouse-anti rat) was used as the primary antibody and 1:1000 Alexa Fluor 488 (green) Goat-anti mouse IgG was used as the secondary antibody. Negative control omitted the primary antibody. Sections were observed immediately using a fluorescence microscope. NeuN primary antibody and all fluorescent labeled secondary antibodies were purchased from Molecular Probes (Eugene, OR). The CC1 primary antibody was purchased from Calbiochem (San Diego, CA).

RNA Isolation

Total RNA was prepared from frozen tissues using TRI-Reagent (Molecular Research Center, Cincinnati, OH). Tissues were homogenized in 1 ml of TRI-Reagent until tissue clumps were no longer visible. 0.2 ml of chloroform was added to each sample and the tubes were vortexed for 1 minute. The samples were left at room temperature for 10 minutes and then centrifuged at 4°C for 15 minutes at 12,000g. The aqueous phase was transferred to a new 1.5 ml RNase-free Eppendorf tube and 0.5ml of isopropanol was added to each tube. The tubes were again vortexed and incubated at room temperature to allow the RNA to precipitate. The samples were centrifuged at 4°C

for 8 minutes at 12,000g. The supernatant was carefully removed without disturbing the RNA pellet. The pellet was washed with 70% ethanol, vortexed for 1 minute and centrifuged for 5 minutes at 14,000g at room temperature. The supernatant was removed and the pellet was air dried for approximately 10 minutes. RNA concentration was determined by mixing 1µl RNA sample with 99µl nuclease-free water and the sample absorbance was read with a Beckman Du 7400 spectrophotometer at 260nm wavelength.

Ribonuclease Protection Assay

The Riboquant rCK-1 RPA kit (Pharmingen, San Diego, CA) contains probes for eleven inflammatory cytokines (IL-1α, IL-1β, TNF-β, IL-3, IL-4, IL-5, IL-6, IL-10, TNF-α, IL-2 and IFNγ) and two housekeeping genes (L-32 and GADPH). Assays (RPAs) were performed with this commercial kit as described by the manufacturer. Templates, supplied as unlabelled cDNAs cloned into plasmids containing the bacteriophage promoter T7, were used to generate a ^{32}P-labeled anti-sense RNA probe set. The RPA probe set was incubated with 100 µCi ^{32}P-UTP, GACU nucleotide pool, dithiothreitol (DTT) and 5X transcription buffer for one hour at 37°C. The transcription reaction was terminated by the addition of 2µl DNase and incubation at 37^{o}C for 30 minutes. 26µl 20 mM EDTA, 25µl Tris-saturated phenol, 25µl chloroform:isoamyl alcohol (50:1) and 2µl yeast tRNA were added and mixed. Phases were separated by centrifugation at 10,000 rpm (9,300g) for 5 minutes. The upper aqueous phase was extracted and mixed with 50µl chloroform:isoamyl alcohol (50:1). Phases were separated by centrifugation at 10,000 rpm (9,300g) for 2 minutes. The upper aqueous phase was extracted and mixed with 50µl 4M ammonium acetate and 250µl 100% ice-cold ethanol. The mixture was placed at –70^{o}C for 30 minutes and followed by centrifugation at 14,000 rpm (16,100g) at 4^{o}C for 15 minutes. The supernatant was removed after centrifugation and the pellet was washed with 70% ethanol. The pellet (RPA probe) was desolved into 50µl hybridation buffer. 1µl probe sample was counted with a Beckman LS 7500 liquid scintillation counter. $3x10^5 – 3x10^6$ cpm/µl without scintillation fluid is expected.

Total RNA (20μg) was frozen at –70^{o}C for 15 minutes followed by 30-60 minutes drying in a vacuum evaporator centrifuge without heating. RNA was resolubilized into 8μl hybridization buffer. 2μl diluted RPA probe ($3x10^{4}$) was added into the above RNA hybridization buffer. One drop of mineral oil was used to cover the 10μl buffer. The buffer was placed into a PCR machine (M.J. Research Inc. Waltham, MA) for RNA-RNA hybridization: 90^{o}C for 30 seconds, let temperature drop 1^{o}C per minute to 56^{o}C and incubate at 56^{o}C for 12-16 hours, let temperature drop 1^{o}C per minute to 37^{o}C and incubate for 15 minutes. 100μl RNase cocktail (for 20 samples: 2.5 ml RNase buffer + 6μl RAase A) was added into the lower aqueous layer and incubated for 45 minutes at 30 ^{o}C. The aqueous layer was extracted and mixed with 18μl proteinase K cocktail (for 20 samples: 390μl proteinase K buffer + 30μl proteinase K + 30μl yeast tRNA) and incubated at 37^{o}C for 15 minutes. 65μl Tris-saturated phenol and 65μl chloroform:isoamyl alcohol (50:1) were added and mixed. Phases were separated by centrifugation at 8,000rpm (5,900g) for 5 minutes. The upper aqueous phase was extracted and mixed with 120μl 4M ammonium acetate and 650μl 100% ice-cold ethanol. The mixture was placed at –70^{o}C for 30 minutes and followed by centrifugation at 14,000 rpm (16,100g) at 4^{o}C for 15 minutes. The supernatant was removed after centrifugation and the pellet was washed with 70% ethanol. The pellet (RPA probe) was resolved into 5μl 1x loading buffer. The buffer was boiled at 90^{o}C for 3 minutes and put in ice immediately.

The denaturing 5% polyacrylamide sequence gel was prepared during the RNase treatment period. 9.375 ml 40% acrylamide (19:1), 7.5 ml 10x TBE, 35.82g urea were mixed and the volume was adjusted to 74.5 ml by ddH_2O. 450μl 10% ammonium persulfate and 60μl Temed were added into the solution. The solution was immediately poured into a sequencing gel mold. 0.4mm spacers and 32 well comb were used. 0.5x TBE was used as a running buffer. The Gel was pre-run at 40 watts for 45 minutes before the sample was loaded. A probes only lane (1000-2000 cpm/lane) was used as a size marker. The gel was run at 50 watts until the bromophenol blue (front dye) reached

30 cm. The gel was carefully removed from the plate and vacuum dried for 30 minutes at 80^{o}C. The gel was exposed to a Storage Phosphor Screen.

The gel image was scanned and analyzed with Storm 820 Phosphor Imager (Molecular Dynamics) and bands were quantified by densitometry. Relative mRNA levels were calculated by normalizing to the ribosomal RNA L32 band included in the set of probes, as the housekeeping RNA.

DNA Microarray

The Affymetrix rat U34A DNA microarray that contains 8,799 gene specific probes was used as described elsewhere (Nesic et al, 2002). Approximately 10 μg of total RNA was used for each target. RNA was reverse-transcribed into double-stranded cDNA with a T7 promoter-containing primer using Superscript II (Life Technologies), as recommended by Affymetrix. Following extraction with phenol-chloroform and ethanol precipitation from ammonium acetate, the cDNA was used as a template in a biotin-labeled *in vitro* transcription reaction (Enzo BioArray, Affymetrix). Resulting target cRNA was collected on RNeasy columns (Qiagen) and then fragmented for hybridization to the microarrays. The rat microarray from Affymetrix was used in all hybridizations. Probes consist of 16 pairs of 25-mer oligonucleotides. One member of each pair contains a point mutation, and the signals of the pair are compared to assess specificity of hybridization. Biotinylated target cDNA was hybridized onto the array and then processed using the Affymetrix Genechip Fluidics Workstation 400, following the Mini Euk 2v2 protocol, except that only 3 μg of fragmented cRNA is added to the hybridization cocktail. Following binding with phycoerythrin-coupled avidin, microarrays were scanned on a Hewlett Packard GeneArray Scanner. Results were analyzed with Affymetrix GeneChip Analysis Suite 5.0 software. Individual microarrays were scaled to produce mean signal intensity (average difference) of 2,500, excluding the top and bottom 2 percentile to remove outliers. The “average difference” describes the signal intensity difference between the match and mismatch probes for each gene averaged over the number of probe sets. Barring systematic error, the average difference

reflects the amount of mRNA detected or expression level for each gene probed. The average expression was calculated as the mean of expression values in the three samples to represent the mRNA level for any given gene in any given experimental group.

To analyze the genomic data we performed: (1) cluster analysis of expression levels in order to classify similar groups of genes; (2) detection of genes with statistically significantly changed expression levels in the three experimental groups, as explained in Nesic et al., 2002; Svrakic et al, 2003. (a) Clustering of genes. Different genes were clustered according to similarities in their expression levels. By using these cluster-analysis tools it is possible to identify potential co-regulated genes and genes with related functions. We performed cluster analysis using the recently released CLUSFAVOR software developed by L.E. Peterson for the cluster and factor analysis of DNA microarray data. This software is freely available at: http://mbcr.bcm.tmc.edu/ genepi/. (b) Statistical significance: Cluster analysis of expression levels of single genes can detect coherent patterns of gene expression (Eisen et al., 1998), but provides little information about the level of statistical significance present among different expression levels of the genes in the different experimental groups. Finding genes with significantly changed expression levels in one of the compared groups was done by using Statistical Analysis of Microarrays (SAM) (Tusher et al., 2001), a robust statistical method devised specifically for the analysis of microarray data. The complete version of SAM software is available for downloading from: http://www-stat.stanford.edu/~tibs/SAM/index.html. This method computes the percentage of falsely identified genes for each dataset, or false discovery rate (FDR), by averaging the number of genes called significant over the appropriately chosen permutations of data among experimental groups. With the single tuning parameter (called Δ in the original work) the FDR for the dataset can be reduced, at the expense of a reduction in the number of significant genes. In our analysis, we selected the adjustable parameter Δ such that FDR was <5% for the list of significant genes. Note also that this method reliably identifies genes as statistically significant even in those instances where expression levels show relatively unremarkable fold changes. We introduced an additional cutoff to the list of significantly changed – according to the

modified t-test – expression levels. We accepted only those mRNA values with a fold change that was higher than 1.3 for up-regulated genes and lower than 0.77 for down-regulated genes.

Statistical analysis

Mean values (±SEM) for each experiment were determined. For two-group comparasion, values statistically different were calculated using two-tailed student t-test. For multiple-group comparasion, data were analyzed using one way analysis of variance (one way ANOVA). The LSD multiple comparisons post-hoc test was used to determine *p* values. *p* values less than 0.05 were considered significant.

CHAPTER 3: RESULTS

HI causes cell death in hippocampus and cortex

The well-characterized P7 rat model of HI was used to study perinatal HI injury. In order to measure cell death levels after HI and characterize its features, we measured cytoplasmic histone-DNA complexes and caspase 3 activity. During the process of apoptosis, chromosomal DNA is degraded first into large DNA fragments and then small oligonucleosomal fragments. A quantitative ELISA, which is based on a sandwich-enzyme-immunoassay-principle and allows specific determination of mono- and oligonucleosomes in the cytoplasmic fraction of brain tissue, was used to detect the presence of histone-DNA complexes, a marker for apoptosis, in the cytoplasm (**Figure 2**). There was significantly increased cell death in the hippocampus (**Figure 2A**) and the cortex (**Figure 2B**) as early as 3h after injury. Cell death continued to increase over time, peaking at 12h after HI at levels that persisted until 48h post-HI and then decreased to sham levels at 72h after injury.

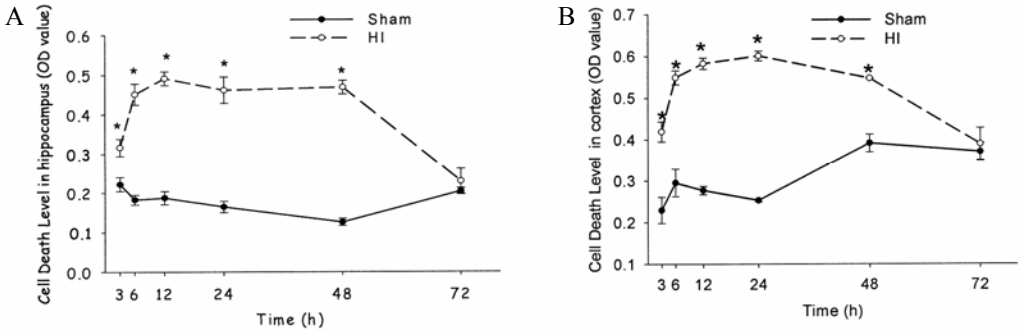

Figure 2. Hippocampal and cortical cell death levels over time after HI in the P7 rat brain. DNA fragmentation was measured by a cell death ELISA assay kit specific for nucleosome-associated cytosolic DNA. Results are given for animals at different time points (3, 6, 12, 24, 48, 72h) of recovery after HI or sham treated (n=3 for each group). Values are mean ± SEM and are expressed as optical density (OD). Cytoplasmic histone-DNA complex level in the hippocampus (A) and the cortex (B) significantly increased at 3, 6, 12, 24 and 48h after HI. * $p<0.05$ compared with sham-treated animal at corresponding time point (one way ANOVA).

Upon initiation of the apoptotic process, members of a family of cysteine aspartic acid-specific proteases known as caspases are activated, resulting in the cleavage of

various cellular protein substrates (Vaux and Strasser 1996). Among them, caspase 3 is the executor enzyme, which then goes on to cleave and activate other effector caspases or other cellular substrates. Using a caspase 3-like activity assay kit, we found Caspase 3 activity significantly increased in hippocampus (**Figure 3A**) and cortex (**Figure 3B**) 3h after HI. It kept increasing and reached the highest levels at 24h after HI. At 72h post-injury, there were no differences in caspase 3 activity between sham-treated and HI-treated pups. The histone-DNA complex cytoplasmic levels and caspase-3 activity in sham-treated tissues did not change significantly during the time course of these assessments (**Figure 2 and 3**).

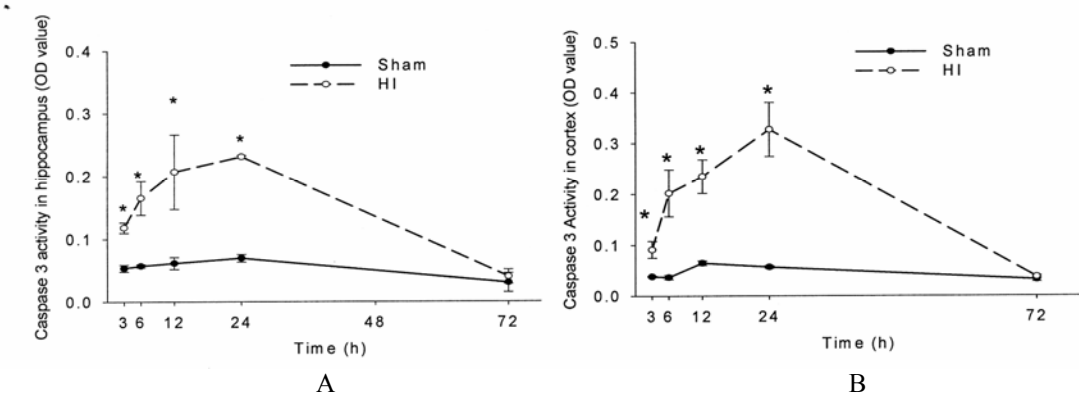

Figure 3. Hippocampal and cortical caspase-3 activity over time after HI in the P7 rat brain. Caspase 3 enzymatic activity, caspase 3 cleavage of a DEVD substrate peptide conjugated to p-nitroanaline and release of the chromophore pNA, was detected by a colorimetric assay. Results are given for animals at different time points (3, 6, 12, 24, 72h) of recovery after HI or sham treated (n=3 for each group). Values are mean ± SEM and are expressed as optical density (OD). The levels of caspase 3 activity were significantly elevated above sham-treated level at 3, 6, 12 and 24h after injury in the hippocampus (A) and the cortex (B). * $p<0.05$ compared with sham-treated animal at the corresponding time point (one way ANOVA).

Coronal sections of the P7 rat brain were made at the level of the mid-hippocampus. The morphological changes that occur during HI induced cell death were observed by H&E staining (**Figure 4**). In the sham-operated rats, occasional dying cells were seen in the developing hippocampus and cortex (**Figure 4C and 4G**). These cells were typically smaller, rounder and more nuclear basophilic than surrounding normal cells. Clusters of dying cells were observed 24h after HI (**Figure 4B, 4D, 4F, 4H).** The

dying cells in these clusters had two types of ischemic morphologic changes. Some of them were small, round and nuclear basophilic, similar as the dying cells we saw in the sham-treated animals. Others were triangle shaped cells with dark stained nuclei (**Figure 4D and 4H)**.

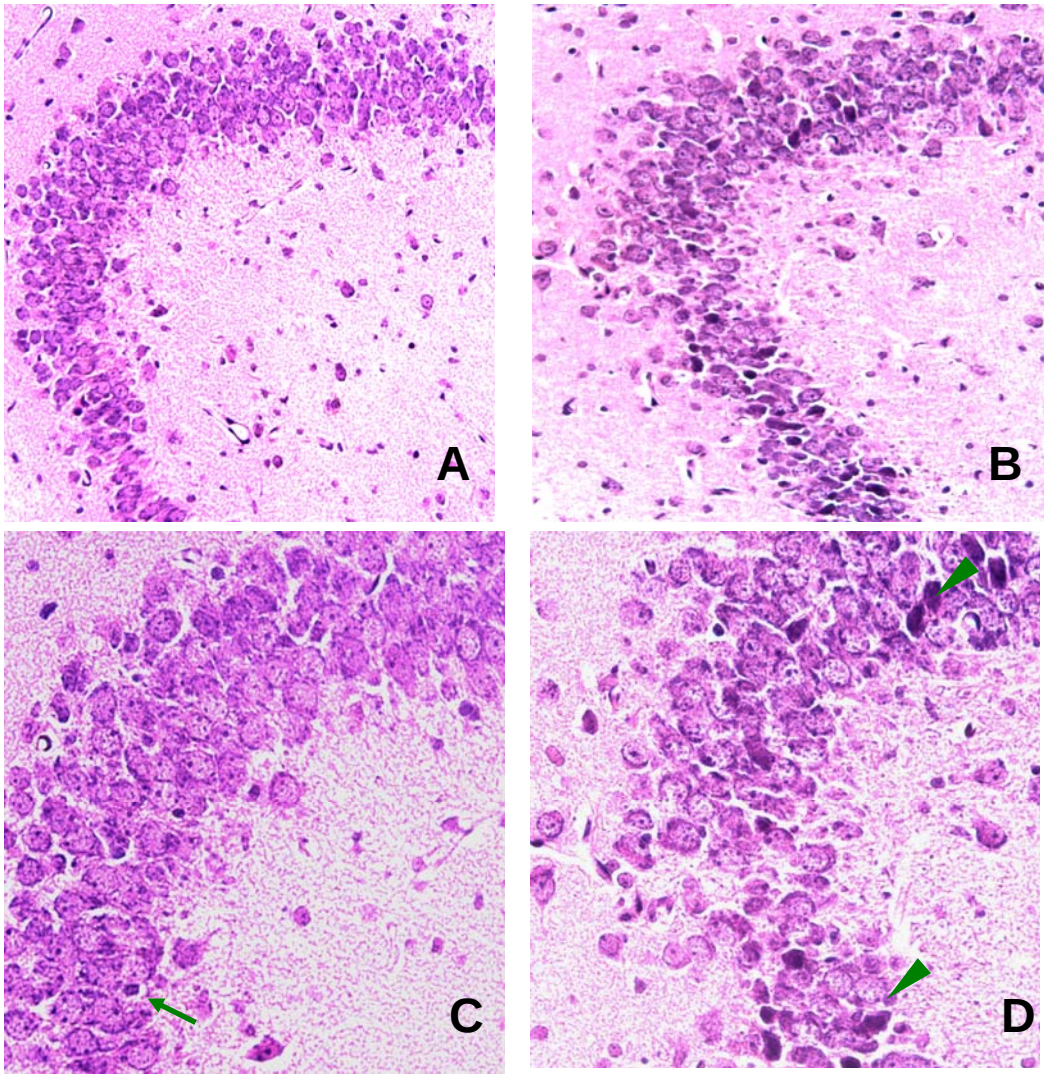

Figure 4 (A-D). H&E staining of hippocampal cells in injured and uninjured P7 rat. (A and C): CA3 region of hippocampus in a sham-operated P7 rat; (B and D): Damaged hippocampal cells 24h after HI. Arrows point to dying cells in sham-treated animal. Arrow heads point to ischemic cell changes after HI injury. Magnification: (A, B, E, F) 200×; (C, D, G, H) 400×.

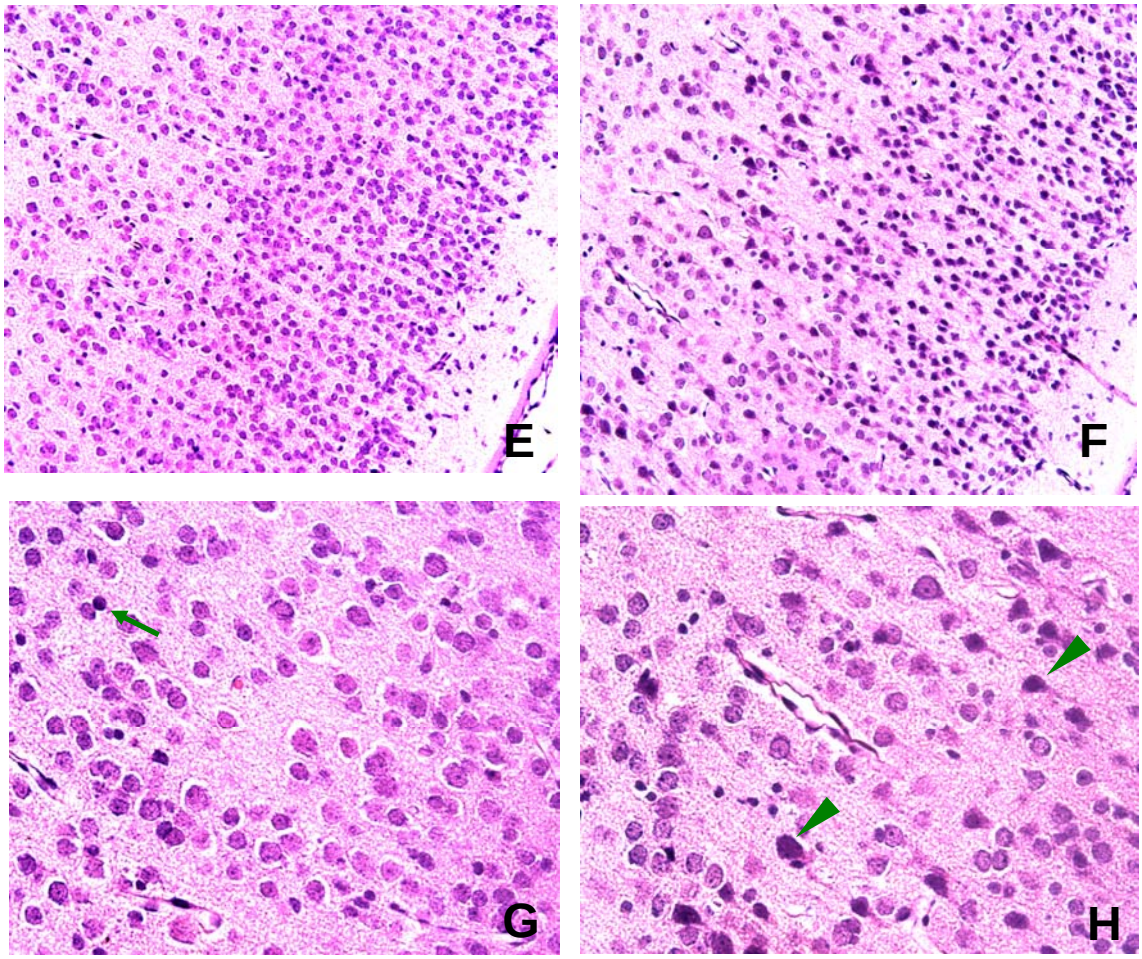

Figure 4(E-G). H&E staining of cortical cells in injured and uninjured P7 rat. (E and G): Cortex in a sham-operated P7 rat; (F and H): Damaged cortical cells 24h after HI. Arrows point to dying cells in sham-treated animal. Arrow heads point to ischemic cell changes after HI injury. Magnification: (A, B, E, F) 200×; (C, D, G, H) 400×.

HI stimulates IL-1 expression in hippocampus and cortex

Recent clinical and experimental evidence indicates that the inflammatory response contributes substantially to the pathogenesis of perinatal HI brain injury (Hagberg et al. 1996; Silveratein et al. 1997; Bona et al. 1999; Hedtjarn et al. 2002). IL-1 is one of the most important inflammatory cytokines. According to the literature, IL-1 mRNA increases significantly early after HI injury (Hill et al. 1999; Hagberg et al. 1996; Szaflarski, Burtrum and Silverstein 1995). This was confirmed when we measured IL-1

expression at the mRNA level using RPA techniques. We detected significant increases in both IL-1α and IL-1β mRNA level in hippocampus 12h after HI (**Figure 5**). However, IL-1 mRNA levels may not reflect protein levels since much of the mRNA is not translated but undergoes degradation. Until now, there has been no information about IL-1 protein levels after HI injury in P7 rat model. So here ELISAs were performed on cytoplasmic fractions from ipsilateral (left) hippocampus and cortex after HI and from sham-treated pups to measure IL-1β protein levels. IL-1β protein levels in sham-treated tissues did not change significantly during the time course of assessments (**Figure 6A, 6B**). Three hours after HI, IL-1β hippocampal protein levels increased and remained elevated up to 24h post-HI (**Figure 6A**). In the cortex (**Figure 6B**), HI-induced IL-1β protein increases were also significant at 3h post-HI, as in hippocampus, and decreased to sham levels at 24h post-HI. The maximal IL-1β cortical HI-induced increases occurred 6h after HI, almost a three fold increase compared to the sham-treated cortex.

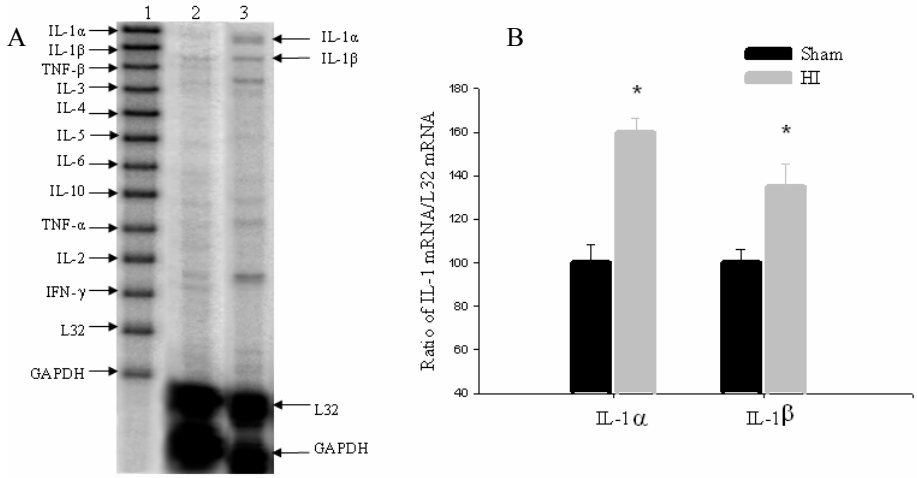

Figure 5. IL-1 mRNA expression 12h after HI in hippocampus. (A). Representative Ribonuclease protection assays (RPA) results of HI induced IL-1 mRNA expression. Lane 1: Free probe; Lane 2: Sham-treated; Lane 3: HI-treated. (B). Histogram graph of RPA results. IL-1α and IL-1β mRNA levels significantly increased after HI compared with sham-treated groups (* $P<0.05$, two-tailed student t-test).

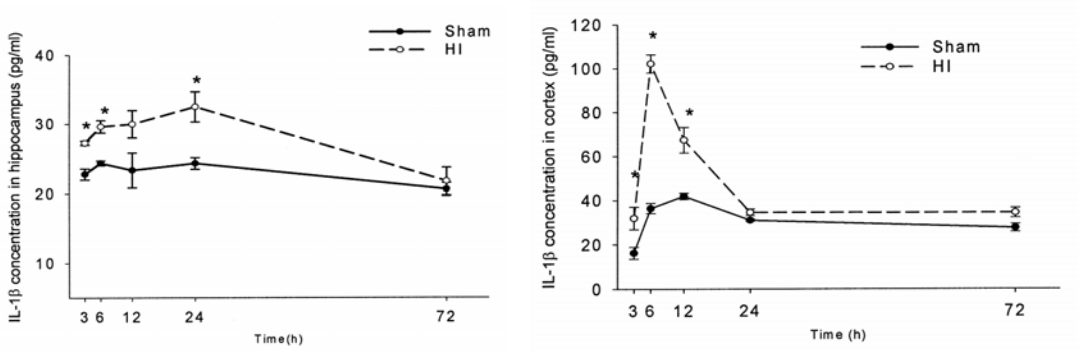

Figure 6. Hippocampal and cortical IL-1β protein levels over time after HI in the P7 rat brain. Cytoplasmic extractions from hippocampal (A) and cortical (B) tissues were used in an ELISA assay to detect the presence of IL-1β protein. Results are given for animals at different time points (3, 6, 12, 24, 72h) of recovery after HI or sham treated (n=3 for each group). IL-1β protein expression was induced beginning 3h after injury and lasting until 24h post-HI in hippocampus (A) and 12h post-HI in cortex (B). Values are mean ± SEM. * $p<0.05$ compared with sham-treated animals of corresponding time point (one way ANOVA).

HI induction of IL-1 in P7 pups contributes to hippocampal and cortical cell death

When we compared the time course of IL-1β protein levels to the time course of cell death and caspase 3 activity after HI injury, we observed parallel increases in the three variables over time, consistent with the hypothesis that IL-1 plays a role in HI-induced cell death. In order to verify this hypothesis, we first examined the distribution of IL-1RI, the effective receptor for IL-1, in neurons and oligodentrocytes of the P7 rat brain by double immunofluorescent staining (**Figure 7 and 8**). There was strong IL-1RI immunoreactivity in neurons (**Figure 7D and 7E**). NeuN mainly stains nuclei of neurons. We observed co-localization of NeuN and DAPI staining in **Figure 7E** while the staining of IL-1RI surrounds NeuN staining without overlap (**Figure 7D and 7E**), which indicates the distribution of IL-1RI on the cell membrane and cytoplasm of neurons. There was also strong IL-1RI immunoreactivity in membrane and cytoplasm of oligodendrocytes (**Figure 8D and 8E**). CC1 stains the cell bodies of mature oligodendrocytes but not the fiber. In **Figure 8D and 8E**, we observed co-localization (yellow) of IL-1RI and CC1

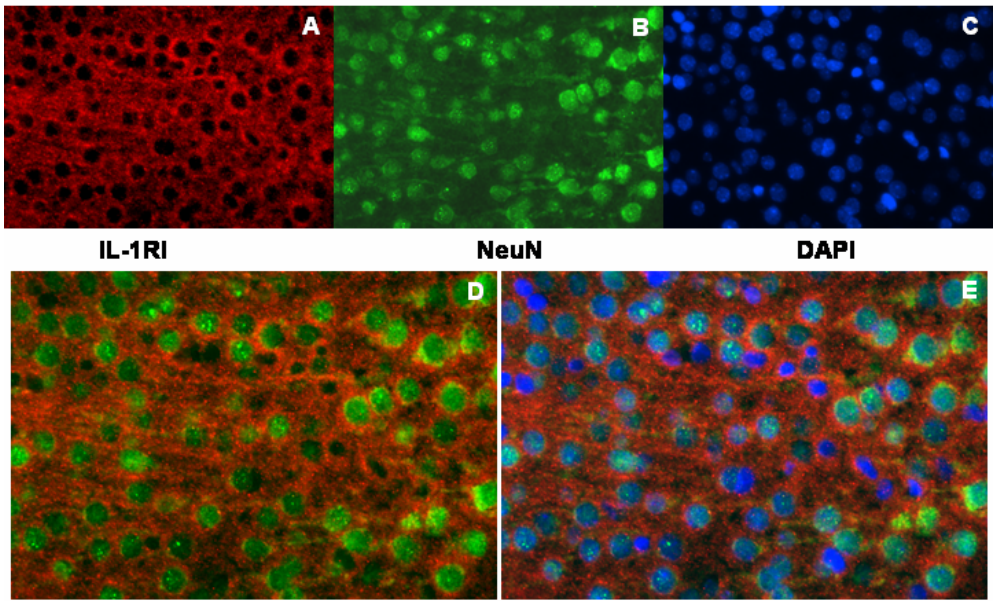

Figure 7. Immunolabeling of sham-treated P7 rat cortex shows distribution of IL-1 Receptor Type I (IL-1RI) on neurons. (A) IL-1RI (red); (B) The neuronal marker NeuN (green); (C) Nuclear DAPI staining (blue); (D) Overlap of IL-1RI and NeuN; (E) Overlap of IL-1RI, NeuN and DAPI.

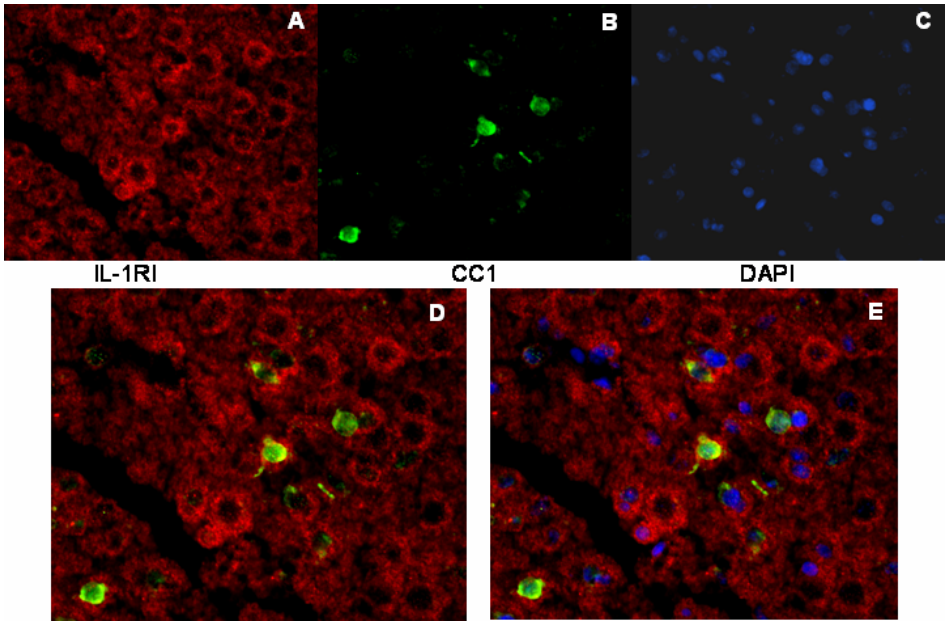

Figure 8. Immunolabeling of sham-treated P7 rat cortex shows distribution of IL-1 Receptor Type I (IL-1RI) on oligodendrocyte. (A) IL-1RI (red); (B) The mature oligodendrocyte marker CC1 (green); (C) Nuclear DAPI staining (blue); (D) Co-localization (yellow) of IL-1RI and CC1; (E) Co-localization of IL-1RI, CC1 and DAPI.

staining but not co-localized with DAPI. There were also IL-1RI staining surround CC1 staining. No immunoreactive products were observed in the negative control sections in which the primary anti-IL-1RI antibody was omitted (Data not shown).

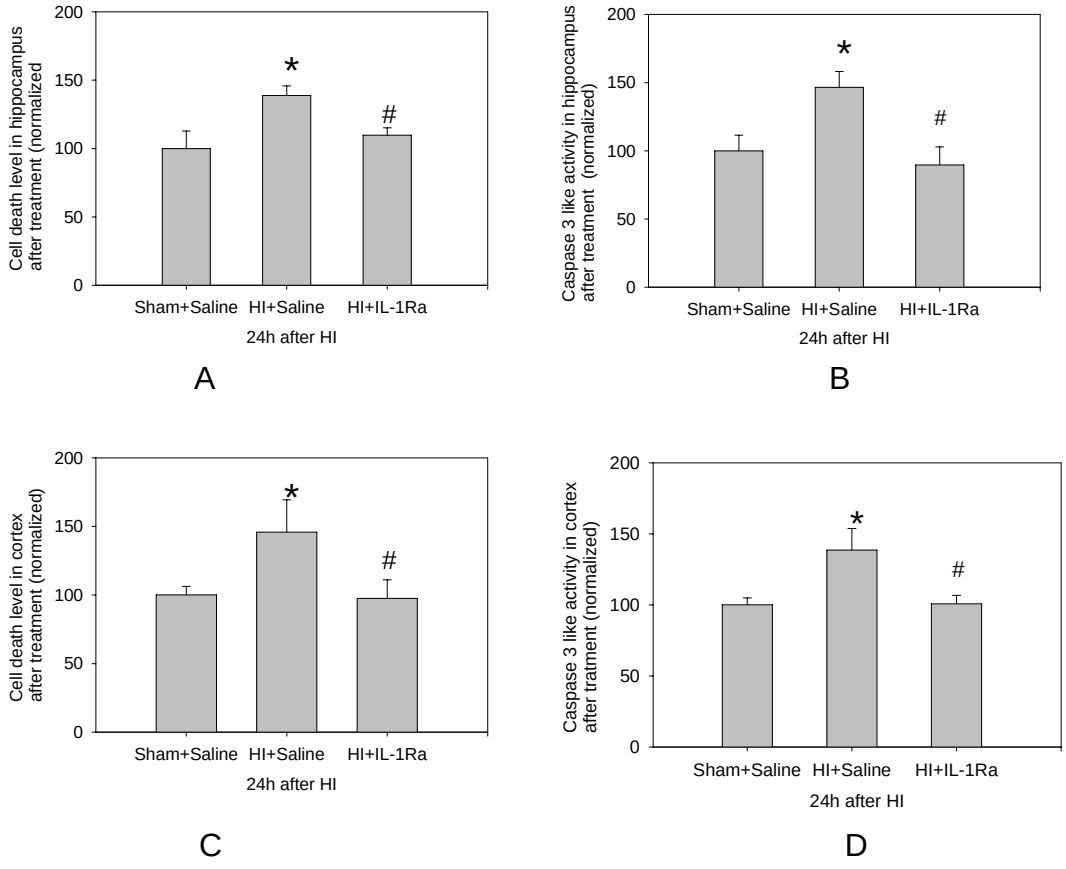

Figure 9. Effect of IL-1Ra on cell death levels and caspase 3 activity 24h after HI injury. IL-1Ra (2μg) treatment was given intracerebroventricularlly 2h after HI. Vehicle (saline) injected animals with HI were used as control. Using cell death ELISA assay, we determined that IL-1Ra injection can significantly decrease the cytoplasmic histone-DNA complex levels in the hippocampus (A) and the cortex (C) when compared with vehicle-treated group after HI. Using caspase 3 activity assay, we determined that IL-1Ra injections can significantly decrease caspase 3 activity in the hippocampus (B) and the cortex (D) when compared to the vehicle-treated group after HI. Values are mean ± SEM and are normalized to sham-treated + saline injection group. N=6 for each group. * $p<0.05$ compared with Sham-treated + Saline injection group. #: $p<0.05$ compared with HI + Saline injection group (one way ANOVA).

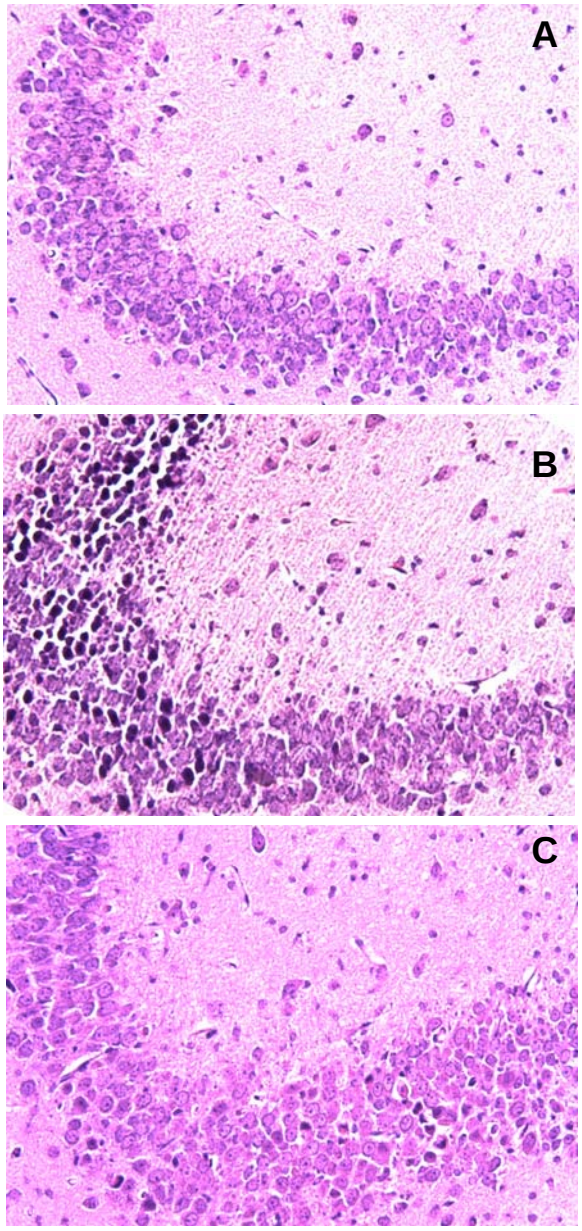

Figure10. Effect of IL-1Ra on P7 rat hippocampus 24h after HI injury was observed by H&E staining. (A) CA3 region of hippocampus in a sham-operated P7 rat; (B) Hippocampal cells in vehicle (saline) injected animals with HI. (C) Hippocampal cells in IL-1Ra (2μg) injected animals with HI. There was significant cell death in hippocampus 24h after HI (B). IL-1Ra injection significantly decreased the number of dying cells (C). Magnification: 200×.

IL-1Ra was then injected into the left cerebral ventricle 2h after HI injury to block IL-1 signaling. In Figure 9, we showed that administration of IL-1Ra significantly decreased cell death levels and caspase 3 activity in the ipsilateral hippocampus (**Figure 9A and 9B**) and cortex (**Figure 9C and 9D**) 24h after HI injury. Likewise, H&E staining showed a markedly increased number of dying cells in the hippocampus 24h after HI injury (**Figure 10B**). IL-1Ra injection protected the brain and markedly reduced the number of dying cells (**Figure 10C**). 24h post-HI was chosen as the time point to assess the effect of IL-1Ra on cell death because this is one of the time points with maximal cell death and it is easy to see the effects of treatment.

HI-induced IL-1 stimulates NF-κB p65/p50 transcriptional activity

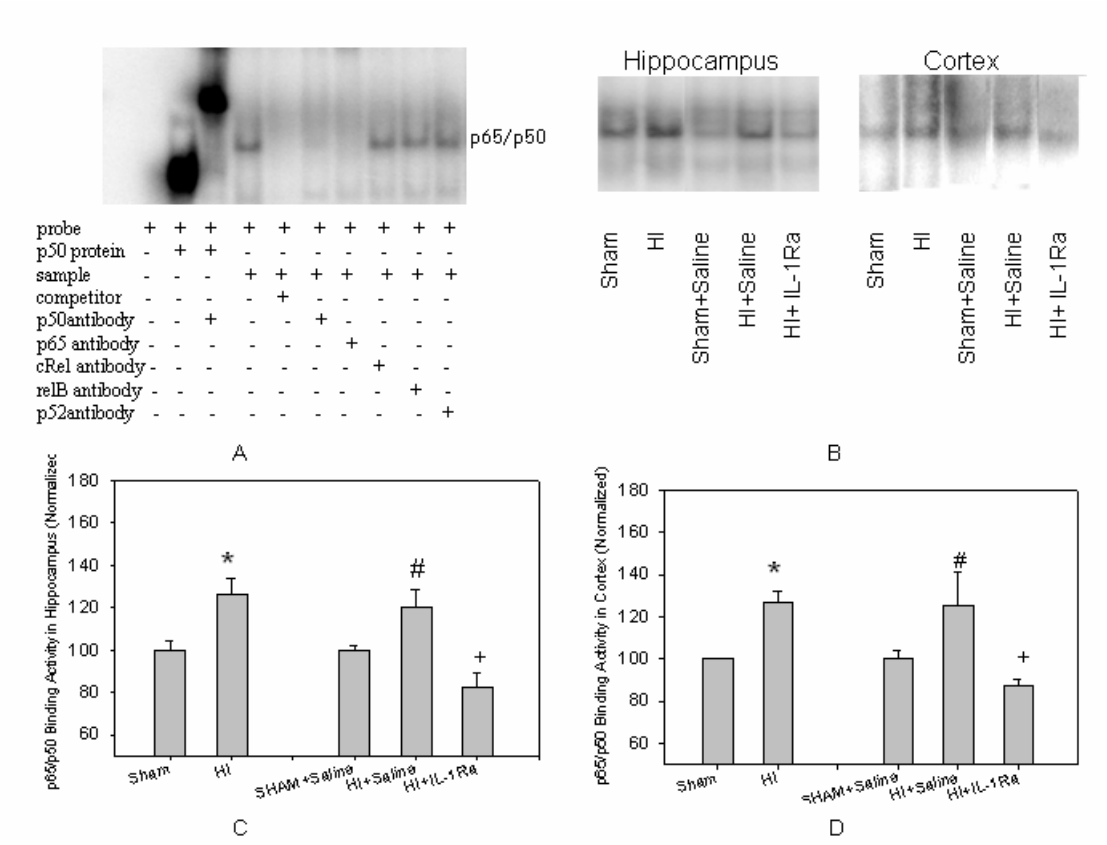

Figure 11. EMSA and supershift/immunodepletion analysis of nuclear NF-κB binding activity in hippocampus and cortex to the IgGκB enhancer consensus sequence. Nuclear extractions from hippocampal and cortical tissues were used. (A) Supershift /immunodepletion was performed with antibodies directed against p50, p65, C-Rel, Rel-B and p52. Competition was performed with a 10-fold unlabeled probe. (B) Representative EMSA analysis of p65/p50 binding activity 24h after HI + IL-1Ra treatment in hippocampus (left panel) and cortex (right panel). The bar graph shows densitometric analysis of EMSA results obtained from hippocampal samples (C) and cortical samples (D). p65/p50 binding activity significantly increased after HI injury; IL-1Ra injections reversed that increase. Values are mean ± SEM and are normalized to sham-treated or sham-treated + saline injection group. *: $p<0.05$ compared with sham-treated group (two-tailed student t-test). #: $p<0.05$ compared with Sham-treated + Saline injection group (one way ANOVA). +: $p<0.05$ compared with HI + Saline injection group (one way ANOVA).

To assess whether HI activates NF-κB activity, we first measured NF-κB binding activity by Electrophoretic Mobility Shift Assays (EMSAs) in hippocampal and cortical tissue nuclear fractions. There were significant increases in NF-κB binding activity 24h

after HI (**Figure 11B, 11C, 11D**). Pups subjected to HI had a mean NF-κB binding activity level that was 26% and 27% higher than that of sham-treated P7 hippocampus and cortex, respectively (**Figure 11C and 11D)**. To identify the participating NF-κB proteins, nuclear fractions were incubated with antibodies to the different NF-κB proteins prior to the EMSA analyses (**Figure 11A**). The anti-p50 and anti-p65 antibodies induced supershifts, indicative of the presence of p65 and p50 in the DNA-protein complexes, most likely as p65/p50 dimers.

To test the hypothesis that HI-induced IL-1 activity stimulates NF-κB activation, we injected 2μg rIL-1Ra intraventricularly and detected a significant decrease in p65/p50 binding activity when compared to the HI-treated group injected with saline (**Figure 11B,**

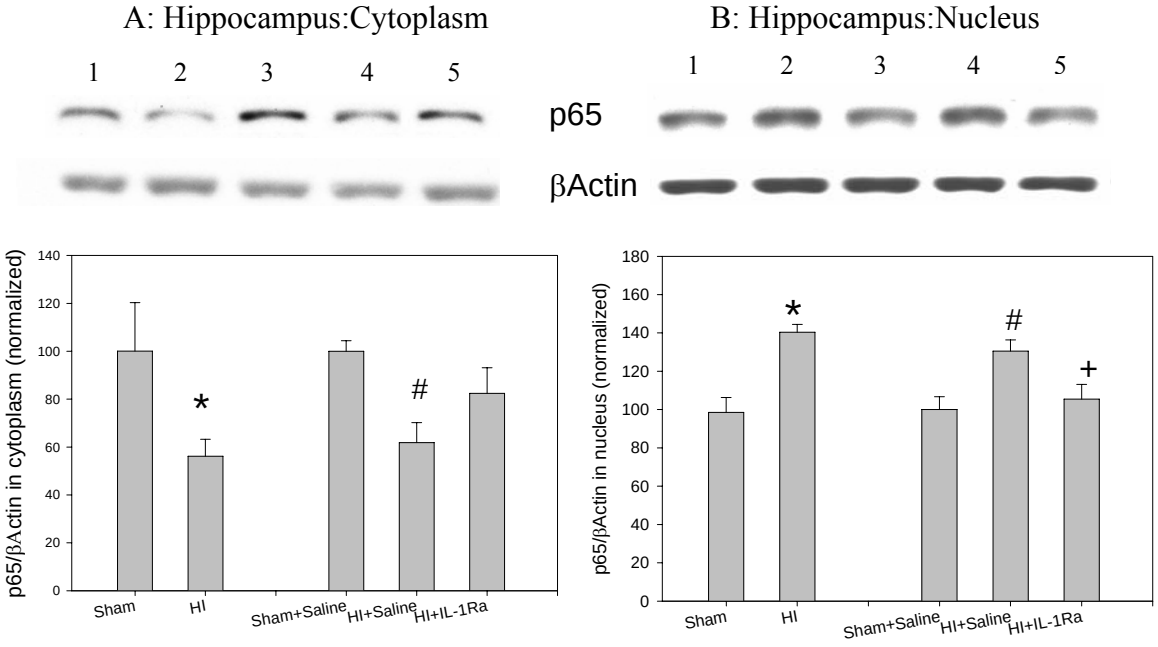

Figure 12. Hippocampal levels of p65 protein in cytoplasm and nuclei 24h after HI + IL-1Ra treatment. Western blots were used and expression of p65 was quantified by densitometry analysis, illustrated in bar charts. Values are mean ± SEM and are normalized to sham-treated or sham-treated + saline injection group. N=6 for each group. (A) Cytoplasmic p65 in hippocampus; (B) Nuclear p65 in hippocampus. β-actin was used as loading control. Lane 1: sham-treated; lane 2: HI; lane 3: sham-treated + saline; lane 4: HI + saline; lane 5: HI + IL-1Ra. *: $p<0.05$ compared to sham-treated group(two-tailed student t-test).. #: $p<0.05$ compared with sham + saline injection group (one way ANOVA). +: $p<0.05$ compared with HI + saline injection group (one way ANOVA).

11C and 11D). There was also a 20% (hippocampus) and 25% (cortex) increase in p65/p50 binding activity in HI pups treated with saline compared to sham animals treated with saline. IL-1Ra injection 2h after HI injury markedly decreased p65/p50 binding activity both in hippocampus (38% decrease, **Figure 11C**) and cortex (38% decrease, **Figure 11D**) in pups when compared to the saline injected group at the same time point.

HI-induced IL-1 stimulates p65 translocation from cytosol to nucleus

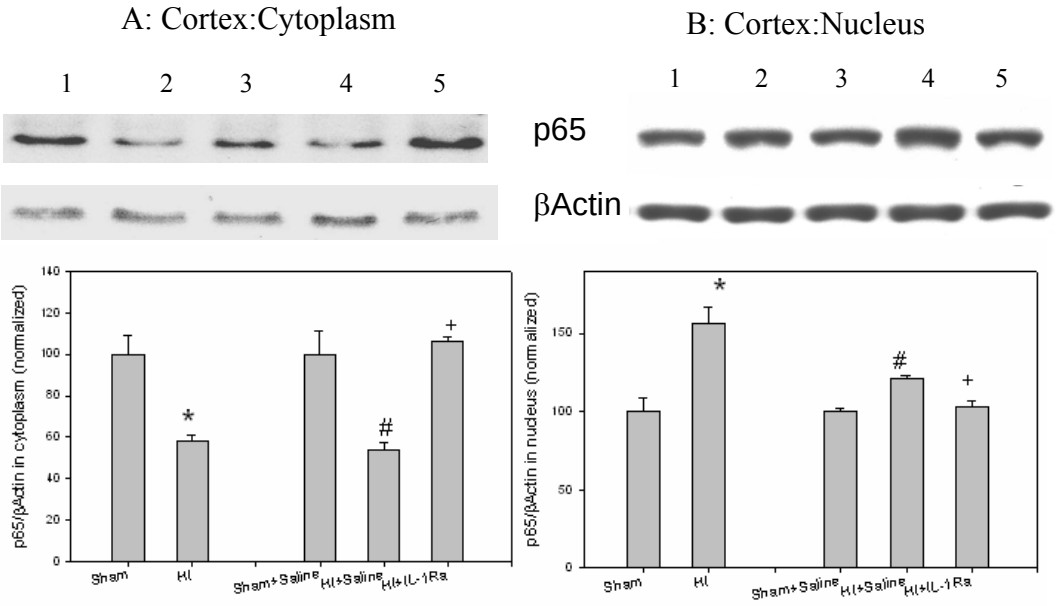

Figure 13. Cortical levels of p65 protein in cytoplasm and nuclei 24h after HI + IL-1Ra treatment. Western blots were used and expression of p65 was quantified by densitometry analysis, illustrated in bar charts. Values are mean ± SEM and are normalized to sham-treated or sham-treated + saline injection group. N=6 for each group. (A) Cytoplasmic p65 in cortex; (B) Nuclear p65 in cortex. β-actin was used as loading control. Lane 1: sham-treated; lane 2: HI; lane 3: sham-treated + saline; lane 4: HI + saline; lane 5: HI + IL-1Ra. *: $p<0.05$ compared to sham-treated group (two-tailed student t-test). #: $p<0.05$ compared with sham + saline injection group (one way ANOVA). +: $p<0.05$ compared with HI + saline injection group (one way ANOVA).

To confirm that the observed increases in NF-κB activity paralleled increased p65 nuclear translocation, we measured cytosolic and nuclear levels of p65. Western blot analyses showed a significant decrease in p65 levels in cytosol 24h after HI in the hippocampus (**Figure 12A**) and cortex (**Figure 13A**). At the same time, nuclear p65 expression levels increased significantly (**Figure 12B** and **Figure 13B**), consistent with

increased translocation of p65 from cytosol into nucleus after HI. IL-1Ra injections appeared to perturb translocation as there was increased retention of p65 in the cytosolic fractions (**Figure 12 and 13**).

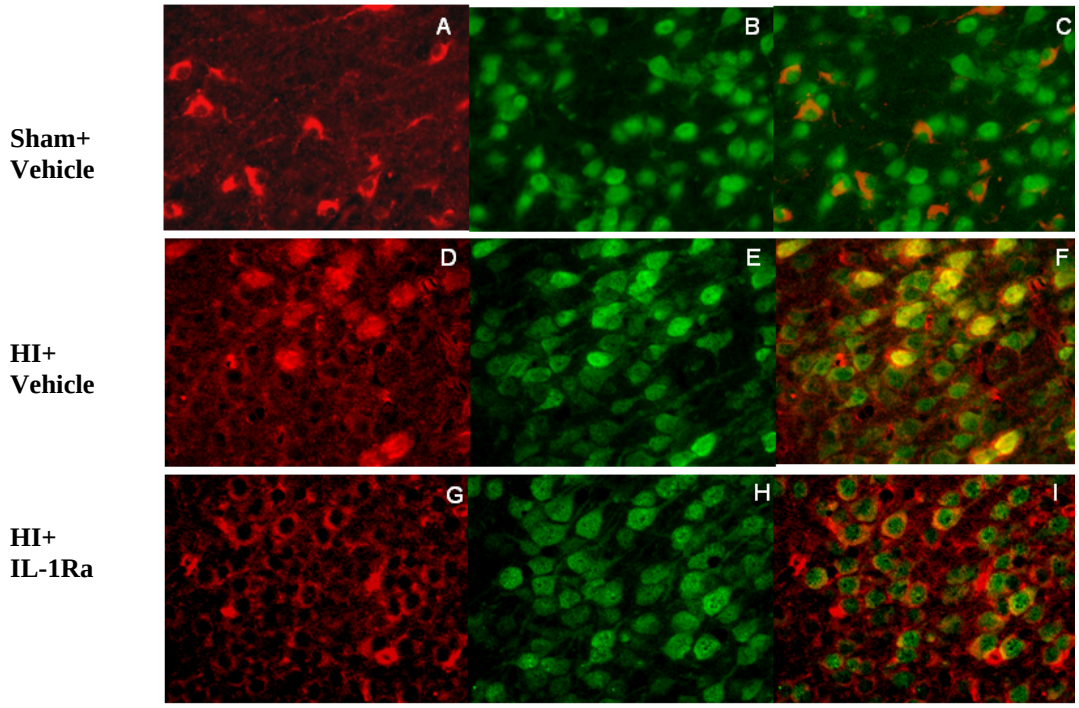

Figure 14. Double immunofluorescence staining of P7 brain sections for Neuron (green) and NF-κB p65 (red) 24h after HI + IL-1Ra treatment. Co-localization of NF-κB p65 immunoreactivity with NeuN (neuron-specific marker) is indicated by yellow color. A-C: NF-κB p65 (A), NeuN (B), and their colocalization (C) in Vehicle-treated sham. D-F: NF-κB p65 (D), NeuN (E), and their colocalization (F) in Vehicle-treated HI. G-I: NF-κB p65 (G), NeuN (H), and their colocalization (I) in IL-1Ra-treated HI. Sections were examined at 400× magnification.

Furthermore, brain sections taken at 24h post-HI were analyzed for p65 translocation using Double immunofluorescence staining. As depicted in **Figure 14**, p65 mainly resides in cytoplasm of neurons and oligodendrocytes in sham-treated rats (**Figure 14C and 15C**). 24h after HI, a greater number of NeuN-positive cells and CC1-positive cells expressed p65 in their nuclei compared to those in vehicle-treated sham (**Figure 14F and 15F**), which indicate nuclear translocation of p65 24h after HI. The increased nuclear localization of p65 was attenuated markedly in IL-1Ra-treated HI rats

(**Figure 14I and 15I**), indicative of retention of p65 in the cytoplasm after HI by IL-1Ra treatment.

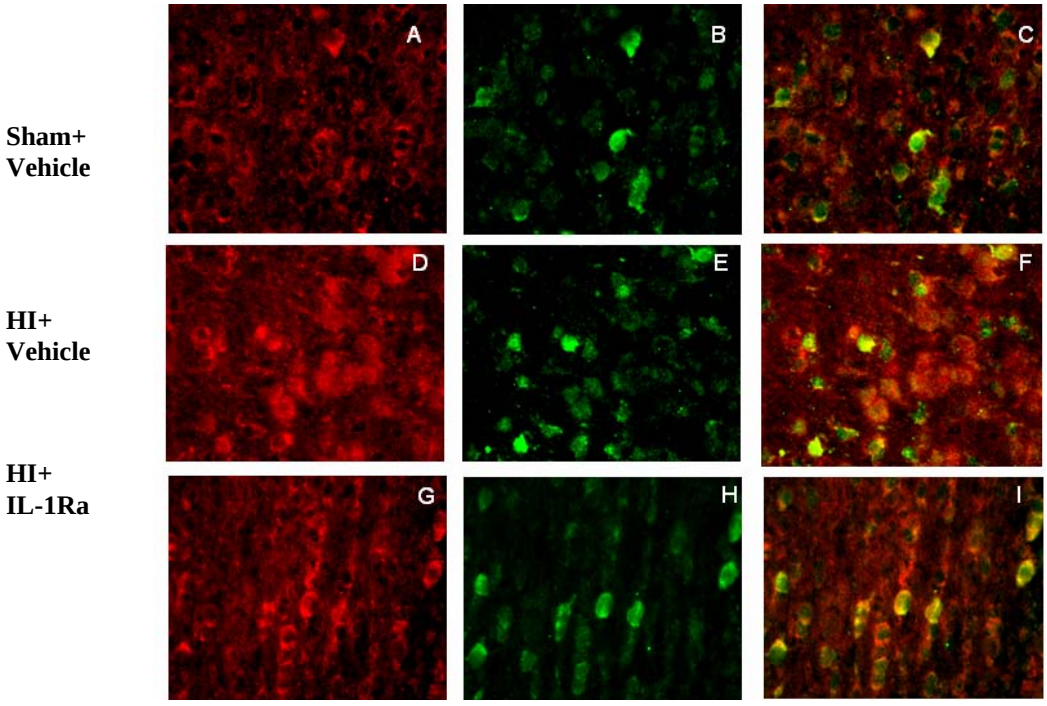

Figure 15. Double immunofluorescence staining of P7 brain sections for Oligodendrocyte (green) and NF-κB p65 (red) 24h after HI + IL-1Ra treatment. Co-localization of NF-κB p65 immunoreactivity with CC1 (mature oligodendrocyte-specific marker) is indicated by yellow color. A-C: NF-κB p65 (A), CC1 (B), and their colocalization (C) in Vehicle-treated sham. D-F: NF-κB p65 (D), CC1 (E), and their colocalization (F) in Vehicle-treated HI. G-I: NF-κB p65 (G), CC1 (H), and their colocalization (I) in IL-1Ra-treated HI. Sections were examined at 400× magnification.

HI-induced IL-1 activity stimulates NF-κB p65/p50- dependent gene expression

Two well-known NF-κB p65/p50 target genes that promote cell death in CNS trauma are iNOS and COX2. iNOS presence was shown as a major band at approximately 130KD in western blot analyses. The expression of iNOS was significantly increased 24h after HI in hippocampus (**Figure 16A and 16B**) and cortex (**Figure 17A and 17B**). After rIL-1Ra treatment, iNOS/β-actin expression ratios decreased significantly in hippocampus (81% decrease) and cortex (110% decrease). This

was also the case for COX2. The antibody against COX2 displayed a band on western blots with a molecular weight of about 72KD. COX2 expression also significantly increased in hippocampus (**Figure 16A and 16C**) and cortex (**Figure 17A and 17C**) 24h after HI. The induction of COX2 was significantly decreased after rIL-1Ra injection (76% decrease in hippocampus and 73% decrease in cortex).

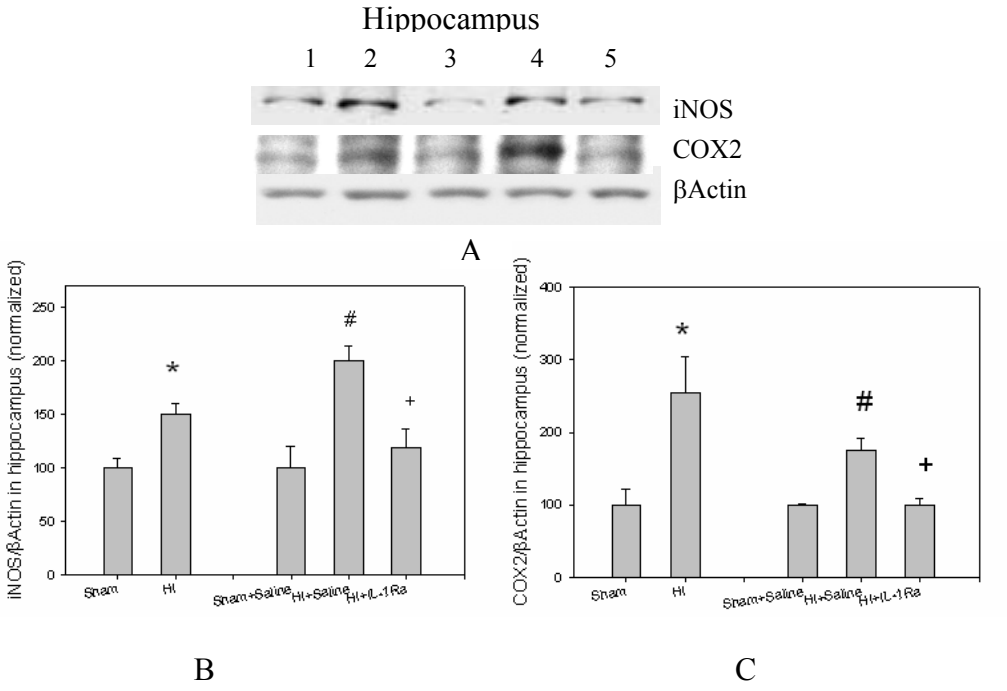

Figure 16. Hippocampal levels of iNOS and COX2 protein 24h after HI + IL-1Ra treatments. (A) Representative results on western blot with detection of a 130KD band of iNOS and a 72KD band of COX2 in hippocampus. β-actin was used as control for equal loading. Lane 1: sham-treated; lane 2: HI; lane 3: sham-treated + saline; lane 4: HI + saline; lane 5: HI + IL-1Ra. Expression of iNOS and COX2 were quantified by densitometry analysis and illustrated in bar charts. Values are mean ± SEM and are normalized to sham-treated or sham- treated + saline injection group. The expression of iNOS (B) and COX2 (C) increased significantly after HI in hippocampus. After IL-1Ra injection, iNOS and COX 2 expression levels markedly decreased. N=6 for each group. *: $p<0.05$ compared with sham-treated group(two-tailed student t-test). #: $p<0.05$ compared with sham-treated + saline injection group (one way ANOVA). +: $p<0.05$ compared with HI + saline injection group (one way ANOVA).

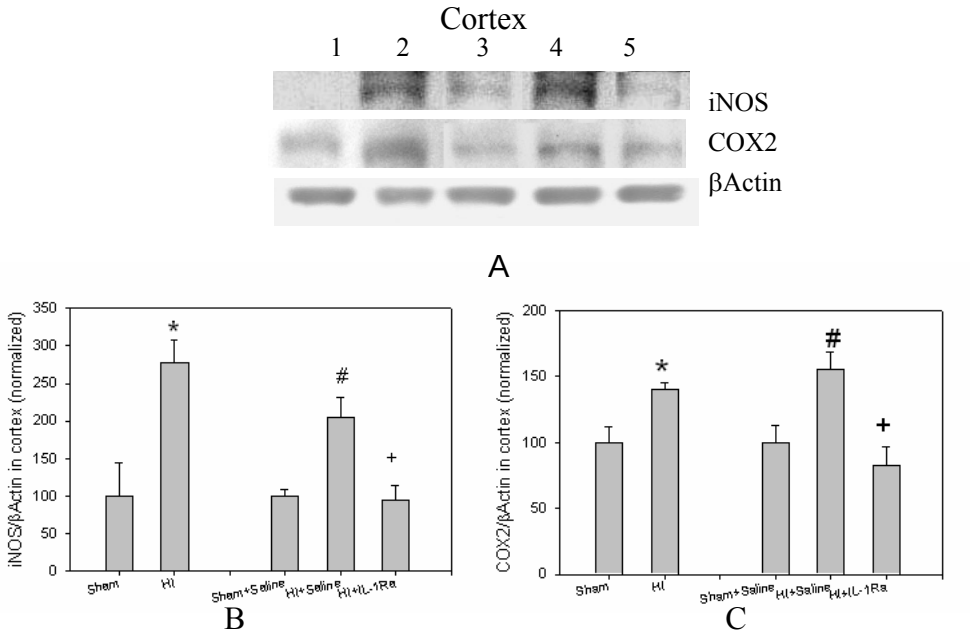

Figure 17. Cortical levels of iNOS and COX2 protein 24h after HI + IL-1Ra treatments. (A) Representative results on western blot with detection of a 130KD band of iNOS and a 72KD band of COX2 in cortex. β-actin was used as control for equal loading. Lane 1: sham-treated; lane 2: HI; lane 3: sham-treated + saline; lane 4: HI + saline; lane 5: HI + IL-1Ra. Expression of iNOS and COX2 were quantified by densitometry analysis and illustrated in bar charts. Values are mean ± SEM and are normalized to sham-treated or sham- treated + saline injection group. The expression of iNOS (B) and COX2 (C) increased significantly after HI in cortex. After IL-1Ra injection, iNOS and COX2 expression levels markedly decreased. N=6 for each group. *: $p<0.05$ compared with sham-treated group (two-tailed student t-test). #: $p<0.05$ compared with sham-treated + saline injection group (one way ANOVA). +: $p<0.05$ compared with HI + saline injection group (one way ANOVA).

HI-induced IL-1 increase promotes IκBα degradation

Another index of NF-κB activation is the phosphorylation and degradation of IκB as monitored in terms of measurement of phosphorylated IκBα using antibodies to the phosphorylated protein (phosphor-Ser-32) in cytosolic fractions from sham- and HI-treated hippocampus and cortex. Although the presence of phosphorylated IκBα was barely detectable in sham-treated pups, there was a significant increase in phosphorylated IκBα in the hippocampus (**Figure 18A**) and cortex (**Figure 18B**) of HI-treated pups,

determined as a distinct band at 41KD. There was no obvious change in total cellular IκBα (both unphosphorylated and phosphorylated) expression, resulting in a marked increase in the ratio of phosphorylated IκBα to total IκBα after HI. IL-1Ra injections significantly decreased the phosphorylated component of IκBα levels and ratios of phosphorylated IκBα to total IκBα in hippocampus and cortex 24h after HI.

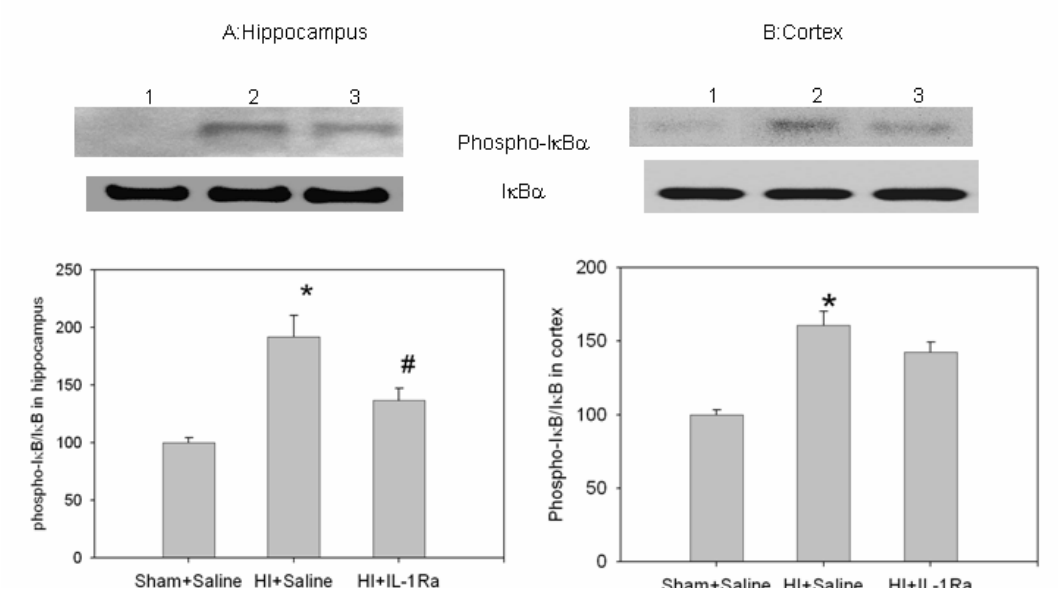

Figure 18. Results of western blot assays for cytoplasmic IκBα and phosphorylated IκBα levels in the hippocampus (A) and the cortex (B) 24h after HI + IL-1Ra treatment. The ratio of mean densitometry values of phosphorylated IκBα and IκBα was illustrated in a bar chart. Values are mean ± SEM and are normalized to sham-treated + saline injection group. Lane 1: sham-treated + saline group; lane 2: HI + saline; lane 3: HI + IL-1Ra. N=6 in each group. *: $p<0.05$ compared to sham-treated + saline group. #: $p<0.05$ compared to HI + saline injection group (ANOVA).

HI-induced IL-1 stimulates nuclear Bcl-3 levels

Bcl-3, an IκB family member, can bind to p50/p50 or p52/p52 homodimers in its phosphorylated state; thus removing these homodimers from cognate NF-κB binding promoter sites and allowing transactivating NF-κB heterodimers to bind and activate gene transcription. Bcl-3 migrates in SDS-PAGE as a major band with an apparent molecular weight of approximately 63KD and a minor band of approximately 55KD. The

faster migrating band (not shown) may be a nonphosphorylated species (Hunter et al. 2002). At 24h after HI, the Bcl-3 immunoreactive band intensity was markedly decreased in cytoplasmic fractions in both hippocampus (**Figure 19A**) and cortex (**Figure 20A**), and increased in nuclear fractions in the HI-treated pups when compared to sham-treated pups (**Figure 19B and 20B**). After rIL-1Ra treatment, nuclear Bcl-3 levels in hippocampus and cortex decreased significantly when compared to the saline-injected pups. Cytosolic Bcl-3 levels increased significantly after IL-1Ra treatment in cortex (**Figure 20A**) but not in hippocampus (**Figure 19A**).

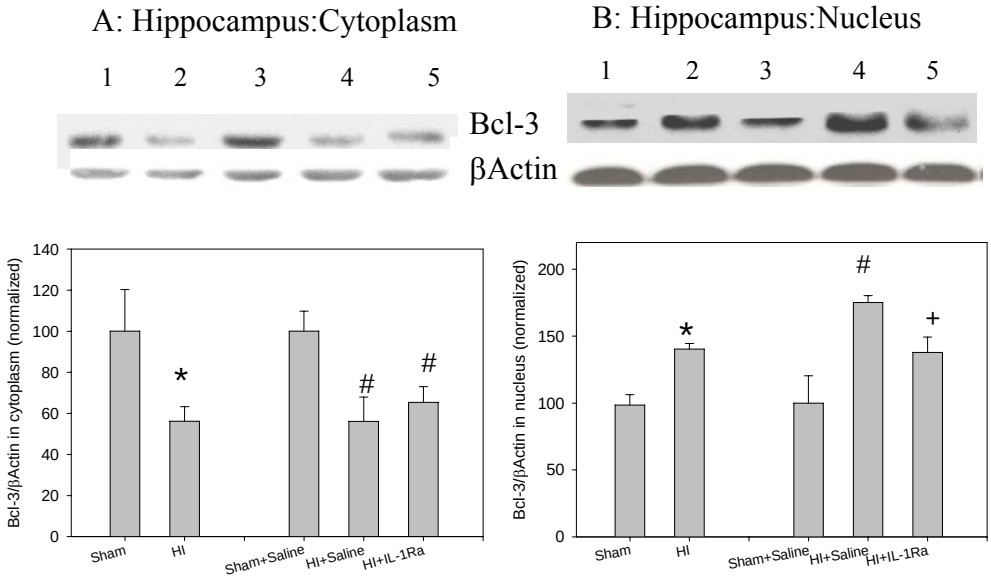

Figure 19. Hippocampal Bcl-3 protein levels in cytoplasm and nuclei 24h after HI + IL-1Ra treatment. Western blots were used to measure Bcl-3 expression levels. Expression of Bcl-3 was quantified by densitometry analysis and illustrated in bar charts. Values are mean ± SEM and are normalized to sham-treated or sham-treated + saline injection group. N=6 in each group. (A) Cytoplasmic Bcl-3 in hippocampus; (B) Nuclear Bcl-3 in hippocampus. β-actin was used as loading control. Lane 1: sham-treated; lane 2: HI; lane 3: sham-treated + saline; lane 4: HI + saline; lane 5: HI + IL-1Ra. *: $p<0.05$ compared to sham-treated group (two-tailed student t-test). #: $p<0.05$ compared to sham-treated + saline injection group (one way ANOVA). +: $p<0.05$ compared to HI + saline injection group (one way ANOVA).

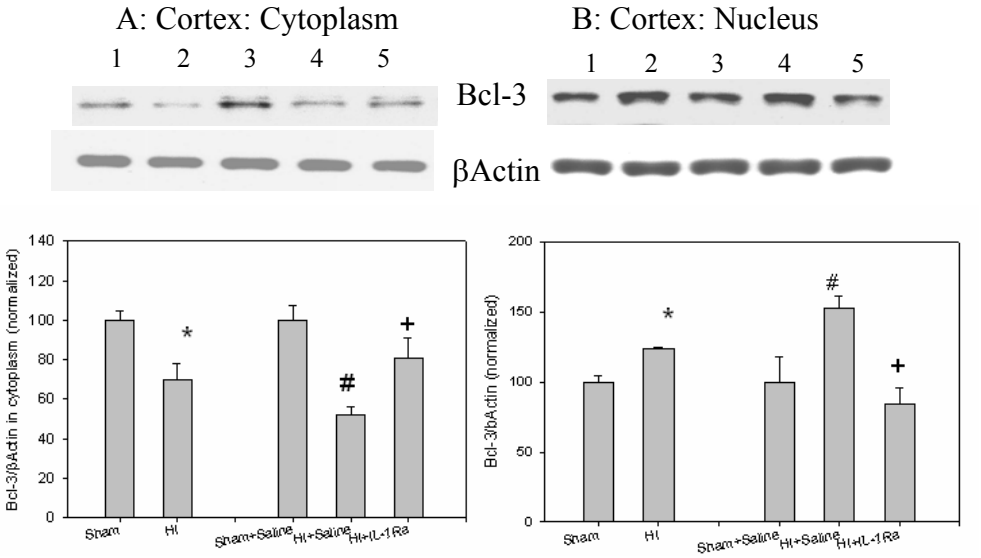

Figure 20. Cortical Bcl-3 protein levels in cytoplasm and nuclei 24h after HI + IL-1Ra treatment. Western blots were used to measure Bcl-3 expression levels. Expression of Bcl-3 was quantified by densitometry analysis and illustrated in bar charts. Values are mean ± SEM and are normalized to sham-treated or sham-treated + saline injection group. N=6 in each group. (A) Cytoplasmic Bcl-3 in cortex; (B) Nuclear Bcl-3 in cortex. β-actin was used as loading control. Lane 1: sham-treated; lane 2: HI; lane 3: sham-treated + saline; lane 4: HI + saline; lane 5: HI + IL-1Ra. *: $p<0.05$ compared to sham-treated group (two-tailed student t-test). #: $p<0.05$ compared to sham-treated + saline injection group (one way ANOVA). +: $p<0.05$ compared to HI + saline injection group (one way ANOVA).

Injected NF-κB decoys permeate hippocampal cells

We stereotaxically injected into the lateral ventricles of P7 pups 5′-fluorescein-labeled IgG-κB oligonucleotide "decoys" to determine cellular occupancy, nuclear penetration and the duration of their cellular presence in hippocampi. As early as two hours after injection, we could detect decoys in cell nuclei and significant cellular clearance by 7 hours (**Figure 21**). These data indicate that decoys successfully entered the cell from the lateral ventricle. We could thus deliver discrete "pulses" of decoy inhibition, a useful feature to ascertain the consequences of NF-κB selective activation.

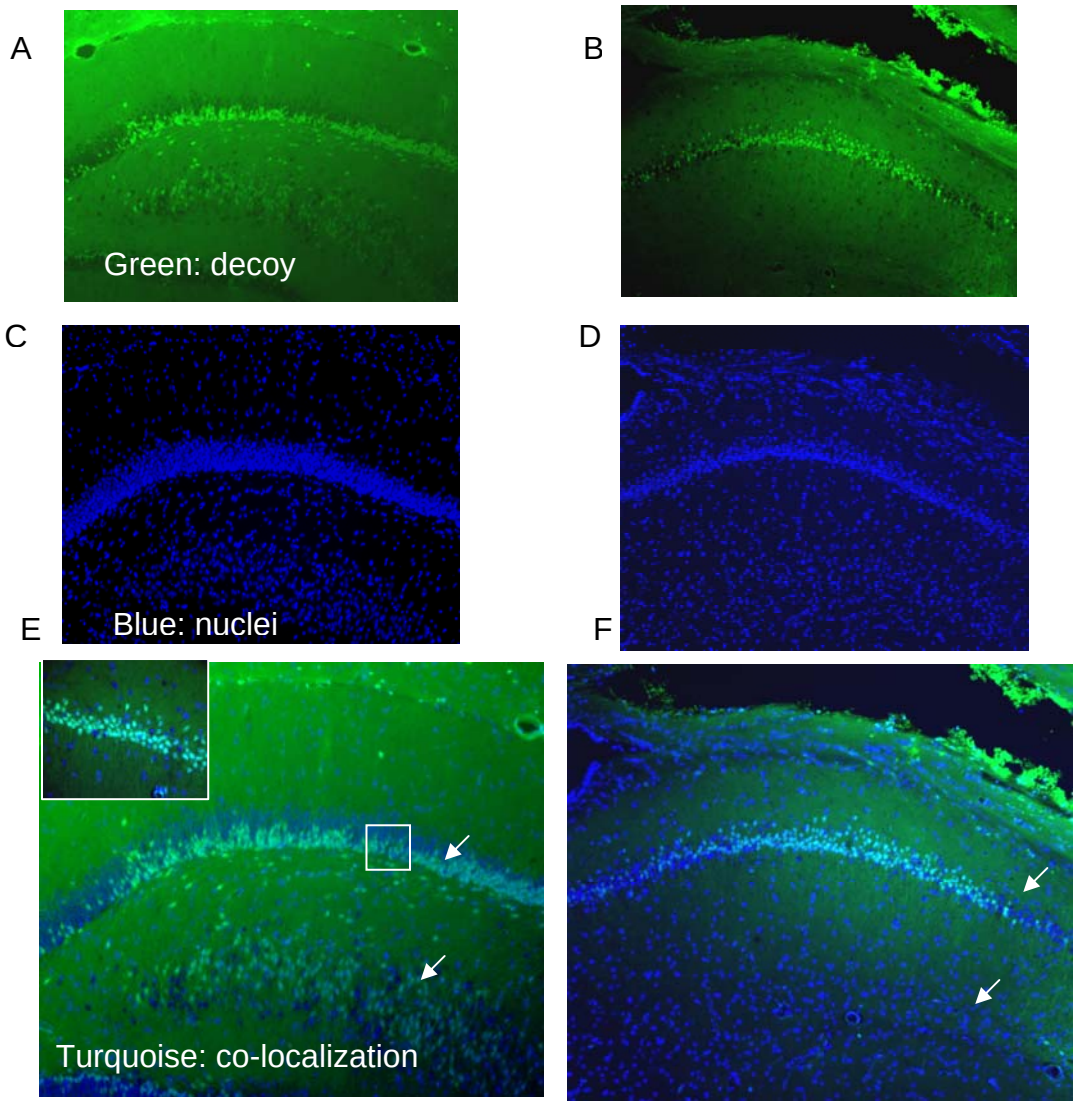

Figure 21. Decoy deoxyoligonucleotides' distribution in the hippocampus. 6 nmol/μl (approximately 80 μg) of 5'-fluorescein labeled phosphothiorated IgG-κB decoy oligonucleotides were injected into left lateral ventricle of P7 rat. Hippocampi were collected 2h and 7h after injection. A) and B): Fluorescence staining of decoy (green) 2hrs and 7hrs after injection, respectively. C) and D): Counter-staining of nuclear DNA (blue) 2h and 7h after injection, respectively. E) Co-localization of decoy staining and counterstaining 2h after injection. The inset is higher magnification (400×) of the marked area. F): Co-localization of decoy staining and counterstaining 7h after injection. Arrows indicate the areas where we can see more co-localization of green and blue color at 2h after injection as compared to those 7h after injection.

IgG-κB or Bcl-x decoys have different effects on NF-κB binding

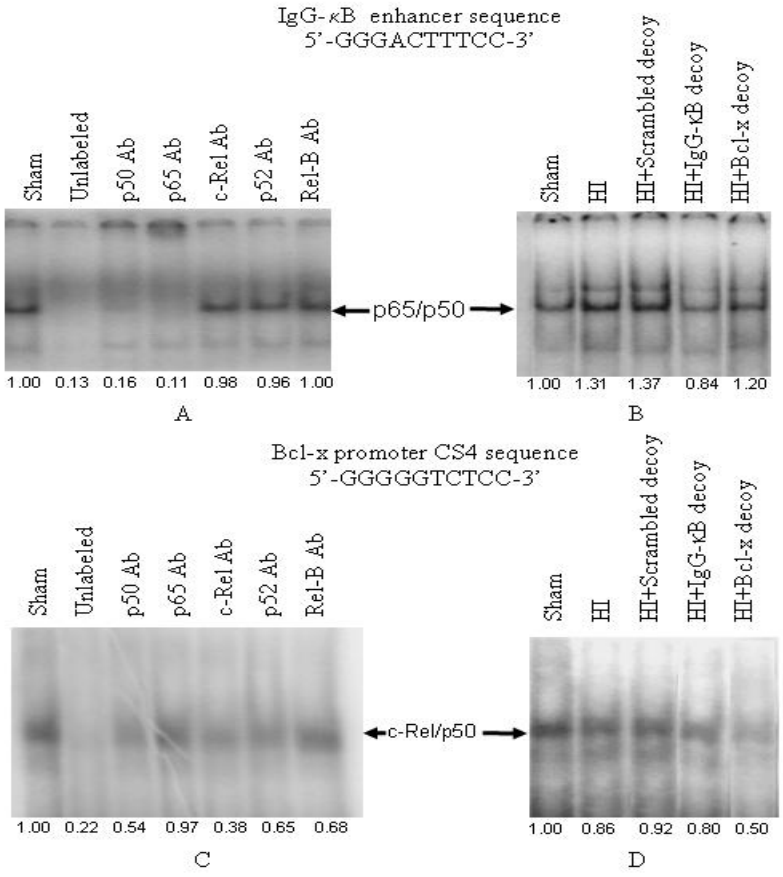

Figure 22. IgG-κB and Bcl-x decoy differentially regulate NF-κB activity. NF-κB binding activity to consensus sequences was detected by Electrophoretic Mobility Shift Assays and supershift in nuclear extracts collected from hippocampi 12h after HI. Numbers below show the fold change in band radioactivity when normalized to shams. A) Supershift results showing that IgG-κB probe preferentially binds to p65/p50 dimer. B) p65/p50 binding activity increased 12h after HI. IgG-κB decoy strongly inhibited the nuclear NF-κB binding to the IgG-κB probe. Bcl-x decoy only weakly inhibited the NF-κB binding to the IgG-κB probe. Scramble decoy did not affect NF-κB binding to the IgG-κB probe. C) Supershift result showing that Bcl-x probe preferentially binds to c-rel/p50 dimer. D) c-Rel/p50 binding activity increased 12h after HI. Bcl-x decoy strongly inhibited the NF-κB binding to the Bcl-x probe. IgG-κB decoy weakly inhibited the nuclear NF-κB binding to the Bcl-x probe. Scramble decoy did not affect NF-κB binding to the Bcl-x probe.

It has been reported that sequence-specific inhibition of transcription factor activation can be accomplished with synthetic double stranded (ds) phosphothiorate oligonucleotides (decoys) containing a NF-κB consensus sequence, which acts *in vivo* as a decoy *cis* element to bind the transcription factors and block the activation of cognate genes (Tomita et al. 1998; Yu et al. 1999). To determine whether the decoys have an inhibitory effect *in vivo*, we conducted decoy injection experiments with phosphothiorated oligonucleotides. We applied 6 nmol/μl (approximately 80 μg) decoy oligonucleotide solutions stereotaxically into the P7 rat lateral ventricle. EMSAs were used to measure NF-κB nuclear binding in nuclear extracts from P7 hippocampi samples collected 12 hours after HI.

Our results in **Figure 22B and 22D** showed that injected decoy oligonucleotides containing the IgG-κB promoter sequence (IgG-κB decoy) strongly inhibited NF-κB binding to the IgG-κB probe but had only a weak inhibitory effect on NF-κB binding to the Bcl-x probe. Alternatively, injected decoy oligonucleotides containing the Bcl-x promoter sequence (Bcl-x decoy) had a weak inhibitory effect on NF-κB binding to the IgG-κB promoter probe but strongly inhibited NF-κB binding to the labeled Bcl-x promoter probe. Injected decoy oligonucleotides containing the scrambled sequence (scramble decoy) had no effect on NF-κB binding to the Bcl-x probe or the IgG-κB probe

To determine the extent to which endogenous NF-κB protein dimers present in hippocampi bind with different affinities to the NF-κB binding consensus sequences present on the Bcl-x and IgG-κB promoters, we measured DNA-binding activities in hippocampal nuclear fractions from P7 pups treated with decoys using EMSA with immunodepletion/supershift. Antibodies (2μg) to the different NF-κB subunits (c-Rel, p65, p50, Rel-B and p52) were added to the nuclear extracts prior to incubation with probes **(Figure 22A and 22C)**. Our results suggest that the IgG-κB promoter specific consensus sequence preferentially binds the endogenous p65/p50 **(Figure 22A)**. Bcl-x promoter specific consensus sequence preferentially binds the endogenous c-Rel/p50 (**Figure 22C**). For the Bcl-x promoter specific consensus sequence, the shifted band

decreased slightly in the presence of p52 antibody **(Figure 22C)**. We cannot exclude the possibility that c-Rel/p52 heterodimers also bind to the Bcl-x consensus sequence.

Specific effect of IgG-κB decoy treatment

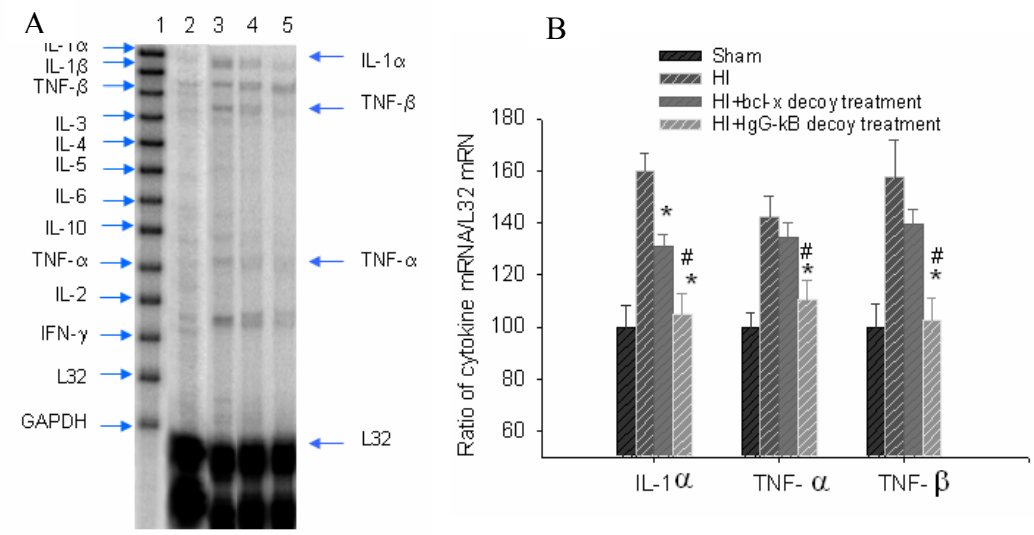

Figure 23. IgG-κB decoy treatment selectively downregulated cytokine mRNA expression in hippocampi 12h after HI injury. The effect of decoy treatments on cytokine mRNA expression after HI was measured using RPAs. A). Result of RPA. Lane 1: Free probe. Lane 2: Sham-treated. Lane 3: HI. Lane 4: Bcl-x decoy treatment. Lane 5: IgG-κB decoy treatment. B). Statistically analysis (one way ANOVA) of RPA results. IL-1α, TNF-α and TNF-β mRNA levels significantly increased after HI compared with sham groups ($P<0.05$). IgG-κB targeted decoy treatment significantly decreased IL-1α, TNF-β and TNF-α mRNA levels ($P<0.05$) compared with HI groups. Bcl-x targeted decoys significantly decreased IL-1α mRNA levels ($P<0.05$) compared with HI groups but had no effect on other cytokines mRNA levels. *: $p<0.05$ as compared with HI group. #: $p<0.05$ as compared with Bcl-x decoy treatment group.

IgG-κB decoy treatment selectively down-regulates inflammatory cytokine expression. Cytokine expression (Interleukins, TNFα/β, interferon [IFN]-γ) has been reported to be elevated transiently after HI (Szaflarski et al. 1995) and the increase has been related to the occurrence of cell death after HI (Hagberg et al. 1996; Martin et al. 1994). This finding is consistent with protection from cell death after HI in neonatal IL-1 null mice (Liu et al. 1999). NF-κB decoy treatments have been used to suppress cytokine

expression in a variety of pathological conditions (Tomita et al. 1998; Tomita et al. 2000; Tomita et al. 2001). As presented in **Figure 23**, we measured the effects of decoy treatment on cytokine expression after HI using RPAs and found that IL-1β, IL-1α, TNF-α and TNF-β mRNA levels were significantly increased ($p<0.05$) 12h after HI. IgG-κB decoy treatment significantly decreased IL-1α, TNF-α and TNF-β mRNA levels without any effect on IL-1β, IL-6 and IL-10 mRNA levels (data not shown). Bcl-x decoys significantly decreased only IL-1α mRNA levels without affecting any other cytokine mRNA level. The undigested RNA probes contain a stretch of plasmid sequence and are therefore larger than the mRNA which they "protect" from the action of RNase by duplex formation. Therefore they migrate slower than the protected fragments.

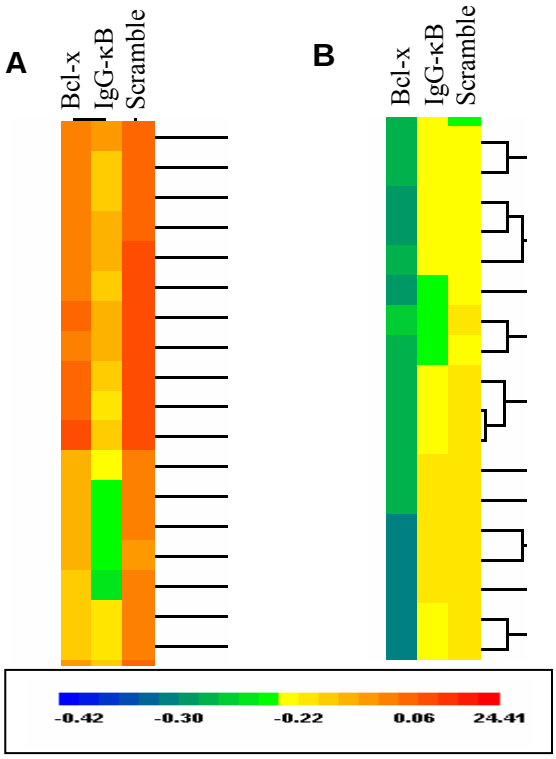

Figure 24. Partial presentation of Cluster analysis using average expression levels in three experimental groups (HI hippocampus treated with scramble decoys, depicted in the column "scramble", HI hippocampus treated with IgG-κB decoy, in the column "IgG-κB" and HI samples treated with Bcl-x decoy, in column "Bcl-x", n=3 for each group). The mRNA levels of the individual genes are presented in rows. High levels of mRNA expression are depicted in red colors, while low mRNA levels are depicted in blue-green colors. Genes that are down-regulated by IgG-κB alone are presented in the panel A: note the yellow color in the IgG-κB column that differs from red color in the scramble and Bcl-x columns. Panel B shows a representative example of genes that are down-regulated in the presence of Bcl-x only (blue versus green color)

Global effect of IgG-κB decoy treatments

To determine the global effects of decoy treatments on hippocampal transcriptional profiles, we used an Affymetrix DNA microarray that contains 8,799 gene specific probes. Total RNA was extracted from 3 experimental groups:1) P7 hippocampi

exposed to HI and scrambled decoy injections; 2) P7 hippocampi exposed to HI and IgG-κB decoy injections; and 3) P7 hippocampi exposed to HI and Bcl-x decoy injections (n=3 for each group). Analyses of the DNA microarray data showed that both IgG-κB decoys and Bcl-x decoys affected the mRNA levels of a large number of genes. A total of 224 genes and ESTs were upregulated and 206 genes and ESTs were downregulated by the IgG-κB decoy treatments (Data partially presented in **Table 1)**. Only one gene was upregulated and 55 genes and ESTs were downregulated by the Bcl-x decoy treatments. IgG-κB decoy treatment specifically affected a number of genes that were not affected by the Bcl-x decoy treatment. As shown in **Figure 24A**, genes that were down-regulated by IgG-κB decoys, were not affected by Bcl-x decoys, and *vice versa* (**Figure 24B**). The only exceptions were the mRNAs of two genes: GluR-A receptor and Glutamate receptor subunit 4C, whose mRNA levels changed in the presence of both decoys, although the IgG-κB and Bcl-x decoy treatments exerted opposite effects on the respective mRNA levels.

Table 1. Selected mRNAs which levels were affected by IgG-κB or Bcl-x decoy treatment. The genes were selected based on their possible role in regulating cell death/survival.

Genes	IgG-κB decoy Fold	Bcl-x decoy Fold
AF077354 Rattus norvegicus ischemia responsive 94 kDa protein	↑2.42x	--
S67722 cyclooxygenase isoform COX-2	↑2.17x	--
X54656 Rat GluR-K3 gene for the glutamate receptor	↑2.05x	--
M36420 Rat glutamate receptor (GluR-C) mRNA	↑1.80x	--
M81183 Rat insulin-like growth factor I gene, 3 end of exon 6	↑1.72x	--
Z27118 R.rattus mRNA for heat shock protein 70	↑1.61x	--
M35826 Rat mitochondrial NADH-dehydrogenase (NDI) gene	↑1.44x	--
X17184 Rattus norvegicus mRNA for glutamate receptor, AMPA subtype, GluR1	↑1.40x	--
X63744 R.norvegicus mRNA for glutamate/aspartate transporter protein	↑1.40x	--
M36418 Rat glutamate receptor (GluR-A) mRNA	↑1.35x	↓0.70x
S94371 Glutamate receptor subunit 4c	↑1.28x	↓0.72x
D14015 RATCYCLE Rat mRNA for cyclin E	↓0.50x	--
AB003991 rat mRNA for SNAP-25A	↓0.57x	--
U93306 Rattus norvegicus VEGF receptor-2/FLK-1 mRNA	↓0.58x	--
Z48444 RNDIGMETP R.norvegicus mRNA for disintegrin-metalloprotease	↓0.59x	--
Y12009 R.norvegicus mRNA for chemokine co-receptor CKR5	↓0.60x	--
M74223 Rat VGF mRNA	↓0.61x	--
U49930 Rattus norvegicus ICE-like cysteine protease mRNA	↓0.63x	--
Y00497 Rat mRNA for manganese-containing superoxide dismutase (MnSOD)	↓0.63x	--
AB004267 Rattus norvegicus mRNA for Ca2+/calmodulin-dependent protein kinase I beta 2	↓0.65x	--
U34684Rattus norvegicus interleukin-1-beta-converting enzyme and ced-3 homolog-1	↓0.66x	--
U01227 RSU01227 Rattus sp. 5HT3 receptor subunit mRNA	↓0.66x	--
L10072 Rattus norvegicus 5-hydroxytryptamine receptor (5HT5a) mRNA,	↓0.66x	--
L08228 RATNMDARI Rattus norvegicus N-methyl-D-aspartate receptor (NMDAR1) gene	↓0.67x	--
E12625cds cDNA encoding a rat novel protein which is expressed with nerve injury	↓0.67x	--

AF075382 Rattus norvegicus suppressor of cytokine signaling-2 (SOCS-2) mRNA	↓0.67x	--
68272 RNU68272 Rattus norvegicus interferon gamma receptor mRNA	↓0.68x	--
M10068mRNA RATCYPOXM Rat NADPH-cytochrome P-450 oxidoreductase mRNA	↓0.70x	--
L27487 Rat calcitonin receptor-like receptor (CRLR) mRNA	↓0.70x	--
AF027954 Rattus norvegicus Bcl-2-related ovarian killer protein (Bok) mRNA,	↓0.70x	--
D00636Poly_Aite#1 RATB5RM Rattus sp. mRNA for NADH-cytochrome b5 reductase	↓0.71x	--
D14014 RATCYCLD1 Rat mRNA for cyclin D1,	↓0.72x	--
X02904cds RNGSTP Rat mRNA for glutathione S-transferase P subunit	↓0.72x	--
AJ132230 RNO132230 Rattus norvegicus mRNA for B1 bradykinin receptor	↓0.74x	--
U90610 Rattus norvegicus CXC chemokine receptor (CXCR4) mRNA	↓0.75x	--
D32249 RATNDAP1 Rattus rattus mRNA for neurodegeneration associated protein 1	↓0.75x	--
X07467 Rat mRNA for glucose-6-phosphate dehydrogenase	↓0.77x	--
Rattus norvegicus Bcl-xalpha mRNA	--	↓0.59x
M72422 Rat glutamic acid decarboxylase (GAD65) mRNA	--	↓0.59x
U11418 Rattus norvegicus NMDAR1 glutamate receptor subunit mRNA	--	↓0.62x
L27112 RATSAPKB Rattus norvegicus stress activated protein kinase alpha II mRNA	--	↓0.63x
D49785 RATPK Rattus norvegicus mRNA for protein kinase (MUK), complete cds	--	↓0.66x
X61381cds RRIIMRNA R. rattus interferon induced mRNA	--	↓0.69x
J04591 Rat dipeptidyl peptidase IV (DPP) mRNA	--	↓0.70x
D14839 Rat mRNA for FGF-9	--	↓0.72x
U73174 RNU73174 Rattus norvegicus glutathione reductase mRNA	--	↓0.72x
D10106 RATPDGFA Rat mRNA for platelet-derived growth factor A chain	--	↓0.74x

a. Table contains ONLY genes identified by using Affymetrix DNA microarrays, which mRNA levels changed significantly after decoy treatment compared to scramble treated brains exposed to hypoxia/ischemia.

b. (↑) means upregulated. (↓) means downregulated. (—) means no significant change was observed. (X) Indicates fold increase/decrease.

CHAPTER 4: DISCUSSION

HI causes cell death in hippocampus and cortex in P7 rat

The results of morphological, histochemical and molecular studies demonstrate neuronal death after cerebral HI injury in different neonatal animal models, including 7-day-old rat pups (Northington et al. 2001; Nakajima et al. 2000), 7-day-old mice (Gibson et al. 2001), newborn piglets (Yue et al. 1997), and infants suffering birth asphyxia (Edwards et al. 1997). Here, we used the Rice-Vannucci 7-day-old rat model with modifications. The original protocol subjected neonatal pups to 8% oxygen for 3 or more hours (Rice et al. 1981). This insult produced an extremely severe injury to the ipsilateral hippocampus, basal ganglia and cortex with a good survival rate. In our study, we intended to characterize the effect of moderate injury on cell death levels and examine possible molecular signaling mechanisms and potential therapeutic strategies after HI injury. Therefore, we subjected pups to 7.8% oxygen for 90 minutes.

One unique feature of apoptosis is the appearance of cytoplasmic histone-DNA complexes, which results from the ordered regulated fragmentation of DNA, its translocation to the cytoplasm and the activation of the executor enzyme caspase-3. In order to characterize cell death after HI, we characterized its temporal and regional features and established an appropriate time to assess the effect of IL-1 by measuring cytoplasmic histone-DNA complexes (ELISA) and caspase 3 activity (colorimetric assay). Using cell death ELISAs and caspase 3 activity assays (Figures 2 and 3), we have shown that HI induced cell death and caspase 3 activation as early as 3h after injury, which reached peak levels from 12 to 48h after HI in the hippocampus and cortex. This extended period of cell death and caspase 3 activation in the neonatal brain after HI would support the possibility for a prolonged window of opportunity for therapeutic interventions.

Analysis of H&E-stained sections allows the identification of morphologic changes of cell death (Figure 4). Analysis of sham animals showed occasional apoptotic cells sporadically distributed throughout the cortex and hippocampus, which is a well

recognized feature of the developing brain. At 24h after HI injury, there were greater numbers of small or large clusters of dying cell seen both in the ipsilateral hippocampus and cortex.

HI induction of IL-1 in P7 pups contributes to hippocampal and cortical cell death. Intracerebroventricular injection of IL-1Ra protects brain against HI injury

The contributions of IL-1 to HI brain damage in rodents have been characterized. There are reports that IL-1 mRNA and protein levels increase as early as 1h after injury and persist during the development of infarction in various adult animal models (Minami et al. 1992; Zhang et al. 1998; Davies et al. 1999). Although an early increase in IL-1 mRNA levels has been reported in a neonatal rat model of ischemia (Hagberg et al. 1996; Szaflarski, Burtrum and Silverstein 1995), there is no information about IL-1 protein levels after HI. We measured IL-1 expression at the mRNA level using RPA techniques and, consistent with the literature, detected significant increases in IL-1α and IL-1β mRNA level in hippocampus 12h after HI (Qiu et al. 2004). The ELISA results presented here show for the first time that IL-1β protein levels increase in cortex and hippocampus as early as 3h after HI in neonatal rats. Regional differences in IL-1β distribution patterns have been observed in normal rodent brain (Ilyin et al. 1998; Vitkovic et al. 2000). We also noticed lower levels of IL-1β in hippocampus when compared to the cortex of sham-treated animals. This variation might reflect endogenous neuromodulatory activities in an untreated rat. In the cortex, IL-1β increases peaked at 6h after HI, then at 12h gradually returned to sham-treated levels by 24h post-HI. In the hippocampus there was a progressive increase in IL-1β protein levels that peaked at 24h post-HI. In contrast to the cortex, IL-1β levels in the hippocampus were less variable over time of survival after HI, although they remained elevated for longer times. This is consistent with there being temporal and spatial differences in IL-1β protein expression after HI, not surprising given similar reports of spatial temporal differences between hippocampus and basal forebrain cell death mechanisms in an adult rodent hypoxia model (Qiu et al. 2001). Thus, it is likely that there are different mechanisms of stress response signal transduction at the

level of IL-1 signaling in the different brain regions affected by HI in the P7 rat. This could also explain some of the particular aspects of long term outcomes in the clinical context and the reported fragility of hippocampus, for example, compared to other brain regions (Yue et al. 1997). Sham-treated animals showed lower expression of IL-1β protein with no difference seen during normal development from P7-P9.

The time course of IL-1β protein levels reported here correlates well with the time course of cell death level and caspase 3 activity observed after HI injury, which prompts us to speculate that IL-1 contributes to HI-induced damage in P7 rats. To test the hypothesis of an involvement of IL-1 in HI-induced brain injury, we first examined the distribution of IL-1RI in neurons and oligodendrocytes in P7 rat brain. Using the techniques of in situ hybridization, RPA and RT-PCR, it has been reported that IL-1RI mRNA is expressed at high levels in the cortex (Wang et al. 1997; Gayle et al. 1997) and at low to moderate levels in the hippocampus (Wong and Licinio 1994). At the cellular level, IL-1RI mRNA has been localized in the cerebrovascular endothelium, astrocytes (Wong and Licinio 1994) and neurons (Takao et al. 1990; Wong and Licinio 1994). However, IL-1RI protein levels need to be determined to characterize the functional distribution of IL-RI in brain cells. In our study, we observed the distribution of IL-1RI on neurons and oligodendrocytes, mainly on membrane and cytoplasm (Figures 7 and 8). This result confirms that IL-1 can bind to its effective receptors and act on P7 rat brain neurons and oligodentrocytes.

To further verify the contribution of IL-1 to HI-induced cell death, recombinant rat IL-1Ra was injected into the ipsilateral cerebroventricle after HI. Significantly protective effects of IL-1Ra have been documented in an adult stroke rat model, where cell death after stroke was significantly reduced when IL-1Ra was administered as a single injection at the time of middle cerebral artery occlusion (MCAO) or 1h, 2h, 3h after MCAO (Mulcahy et al. 2003). The maximal cortical protection occurred after intracerebroventricular injection of IL-1Ra 2h post-MCAO (Mulcahy et al. 2003). Protective effects of IL-1Ra can last for at least 7 days after injury (Garcia et al. 1995; Loddick and Rothwell. 1996). In our study, we injected IL-1Ra 2h after HI injury and

detected markedly decreased cell death level and caspase 3 activity 24h post-HI (Figure 9), in support of the hypothesis that IL-1 contributes to HI-induced cell death in P7 rat. H&E staining (Figure 10) also showed that IL-1Ra injection can markedly reduce the number of dying cells in hippocampus 24h after HI injury. Considering the absence of side effects associated with the IL-1Ra treatment and its safety in clinical trials in rheumatoid arthritis (Calabrese 2002), it is a promising therapeutic strategy for perinatal ischemia.

Intracerebroventricular injection (i.c.v) has been frequently used to deliver IL-1Ra directly into the brain, bypassing the blood brain barrier (BBB). IL-1Ra is a 17.5kDa hydrophilic protein and therefore may have difficulty in crossing an intact BBB. In our study, we noticed an increase in cell death in saline i.c.v animals compared to sham-operated animals (Data not shown). The i.c.v itself causes cell death in the brain, which may confound the effect of IL-1Ra. To better evaluate the effect of IL-Ra, saline i.c.v pups were used as controls instead of sham-operated pups. To be used as a practical therapeutic agent, IL-1Ra would have to be injected systemically as opposed to being injected through a hole drilled in the skull. One study, using radioactively labeled IL-1Ra, IL-1α and IL-1β, showed that these three cytokines share the same saturable transport system to cross the BBB (Gutierrez et al. 1994). Thus, they inhibit each other's transport in a way suggesting that elevated blood IL-1Ra levels would inhibit the entry of IL-1α and IL-1β into the brain while increasing IL-1Ra access. Furthermore, the BBB of perinatal rats is immature, which may facilitate the extent of penetration of IL-1Ra. The HI injury itself may have compromised the BBB of P7 pups and further facilitated the access of IL-1Ra to the injured sites (Vannucci, Christensen and Yager 1993). It should prove useful to test the effect of intravenous IL-1Ra injections after HI in future studies.

HI-induced IL-1 stimulates NF-κB p65/p50 translocation and transcriptional activity

The mechanisms underlying IL-1-induced cell death in neonatal rat brain after HI are not known. One of the most prominent IL-1-inducible signals, acting via IL-1RI,

involves the activation of NF-κB and subsequent induction of multiple genes. NF-κB is constitutively expressed in CNS at low levels (Kaltschmidt et al. 1994), but is stimulated above basal levels by stimuli associated with ischemic insults. In the rodent brain NF-κB activation is stimulated in the forebrain and hippocampus after HI (Koong et al. 1994; Schmidt et al. 1995; Yang et al. 1995; Gabriel et al. 1999; Nurmi et al. 2004). In most of these studies, the expression and activity of p65/p50 was measured and used to represent NF-κB activity, which actually overlooks the role of other NF-κB dimers such as c-Rel/p50. In our study, using probes containing IgG-κB consensus sequences, we observed an increase in NF-κB binding activity 24h after HI injury (Figure 11). Immunodepletion/supershift results confirmed the components of this specific NF-κB dimmer are p65 and p50. We also detected, using western blot, an increase in p65 expression in nuclei and a simultaneous decrease of p65 expression in the cytoplasm 24h post-HI (Figures 12 and 13). Immunohistochemistry staining results demonstrated nuclear translocation of p65 in neurons (Figure 14) and oligodendrocytes (Figure 15) 24h after HI. All these pieces of evidence indicate that p65/p50 NF-κB dimer was activated after HI, which is consistent with the literature. Interestingly, however, our immunodepletion/supershift data (Figure 22) further indicated that endogenous NF-κB protein dimers present in hippocampi bind to the NF-κB binding consensus sequences present on the Bcl-x and IgG-κB promoters with different affinities. NF-κB c-Rel/p50 selectively binds the Bcl-x gene promoter CS4 sequence while p65/p50 preferentially binds the IgG-κB promoter sequence. c-Rel/p50 binding activity decreased 12h after HI, while the p65/p50 binding activity increased. Our data confirm that the different compositions of the active NF-κB dimers convey a degree of NF-κB gene target specificity. Using only NF-κB DNA sequences present in the IgG-κB promoter sequence or measuring nuclear levels of p65 alone as indices of NF-κB activity ignore the differential binding affinities of the different NF-κB dimers to those different sequences present in the promoters of many genes and of the differences in transcriptional activating activities of the different NF-κB "activity" moieties p65 or c-Rel.

NF-κB regulates the expression of anti-apoptotic genes such as Bcl-x_L, Bcl-2, MnSOD, and inhibitor-of-apoptosis proteins; and proinflammatory genes such as IL-1, TNF, matrix metalloproteinase-9, COX-2, and iNOS, thereby playing a dual role in neuronal survival (Mattson and Camandola 2001). Considering the results of recent studies showing that the p65/p50 dimer activates genes coding for proteins with pro-inflammatory properties, while c-Rel/p50 dimer activates genes coding for the Bcl-x_L protein that prevents cell death (Qiu et al. 2001; Pizzi et al. 2002), we believe that some of the present confusion in the field as to the pro-apoptotic or anti-apoptotic nature of NF-κB activities in in vivo lesion paradigms results from a lack of data addressing activation of specific promoters by the different NF-κB dimer species. The activation of different NF-κB dimers under different stimuli and at different time points may be responsible for the different beneficial or detrimental outcomes in cell survival. In our study, we focused on the activation of p65/p50 and its target genes to unravel the mechanism of HI-induced cell death.

Nadjar et al (2003) documented the activation of NF-κB by the visualization of p65 translocation in the cells of adult rat brain after intraperitoneal or i.c.v. IL-1β injection. IL-1RI deficient mice demonstrated impaired NF-κB activation upon the stimulation of IL-1β. Huang et al (2003) documented that decreased NF-κB activity was observed in ischemic ICE null adult mice and suggested that IL-1 signaling contributes to NF-κB activation and subsequent ischemic damage. While studies with adult mice are important, the neonatal rat presents a different spectrum of responses to ischemia given its very high rate of brain growth and metabolic activity. In addition, it is known that both IL-1β and IL-18, another cytokine which has been reported to be important for the development of HI brain injury in neonatal rat (Hedtjarnm et al. 2002), are synthesized as inactive precursors that require cleavage by ICE to become active. ICE deficient mice have neither mature IL-1β nor IL-18 (Wang and Leonardo 2000). Thus we cannot distinguish if IL-1β or IL-18, or both, are involved in the activation of NF-κB after HI using ICE deficient mice. Here, IL-1Ra, which blocks the function of IL-1R, but not IL-

18R, was used to verify the activation of NF-κB by IL-1 after HI in the P7 rat. Our results showed that the increased nuclear p65 and NF-κB p65/p50 binding activity in hippocampus and cortex 24h after HI could be blocked by IL-1Ra injection, in confirmation of the hypothesis that NF-κB p65/p50 is activated by IL-1 after HI.

HI-induced IL-1 increase promotes IκBα degradation and nuclear Bcl-3 levels

To further elucidate the NF-κB transactivating pathway stimulated by HI-induced IL-1 signaling, we measured IκBα and Bcl-3 levels, two molecules important in NF-κB activation. IκBα phosphorylation at Serine-32 and Serine-36 (Traenckner et al. 1995) is a requirement for its ubiquitination and subsequent degradation by the 26S proteasome, an important step in the translocation of NF-κB from the cytoplasm to the nucleus. We measured the expression levels of both IκBα and phosphorylated IκBα (phospho-Ser-32) in cytoplasmic fractions derived from the cortex and hippocampus of HI-treated pups. Phosphorylated IκBα expression increased after HI without a significant change in total IκBα expression, resulting in a marked increase in the Phosphorylated IκBα/IκBα ratio (Figures 18A and 18B). This observation is consistent with there being an ongoing rapid synthesis of IκBα, also known to be positively regulated by NF-κB activation. Thus, by 24 hours the early decreases in total IκBα are over. An in vitro study of IL-1β-challenged C6 (astrocytoma) cells showed that newly synthesized IκBα to be phosphorylated at Ser-32 (Uehara et al. 1999), which may explain the increase of phosphorylated IκBα 24h after HI. After IL-1Ra treatment, the phosphorylated IκBα levels decreased in both the hippocampus and cortex, in support of the hypothesis that IL-1 stimulates NFκB activity via phosphorylation and degradation of IκBα.

Increased nuclear Bcl-3 levels also stimulate NF-κB activation. Western blot analyses (Figures 19 and 20) showed that there was an increase in translocation of Bcl-3 from cytoplasm to nucleus 24h after HI in hippocampus and cortex. After IL-1Ra treatments, nuclear Bcl-3 levels decreased significantly when compared to saline injected pups exposed to HI in both hippocampus and cortex, which would indicate that IL-1

stimulates translocation of Bcl-3 after HI. Not surprisingly, cytosolic Bcl-3 levels also increased significantly after IL-1Ra treatment in cortex. However, to our surprise, the cytosolic Bcl-3 levels remained significantly lower in the hippocampus after IL-1Ra treatments when compared to sham-treated pups, consistent with a decrease in total cellular Bcl-3 levels after the IL-1Ra blockade of IL-1 signaling. These observations are consistent with IL-1 stimulation of both translocation and transcription of Bcl-3. There is a report based on DNA microarray analyses and real time RT-PCR by Elliott et al. (2002) using cultured SW-1353 cells that shows Bcl-3 transcription to be stimulated by IL-1β signaling in support of our interpretation. Thus, Bcl-3 activation of NF-κB would rely on its prompt synthesis and simultaneous translocation to the nucleus. We report here the first evidence that Bcl-3 translocation is regulated by IL-1 and that it is a component of HI-induced NF-κB activation and brain pathogenesis.

IL-1 induces NF-κB- dependent genes expression

There is evidence that nitric oxide (NO) is an important mediator of ischemic and neurodegenerative pathology in the central nervous system (Hara et al. 1996; Mizushima et al. 2002; Brown and Bal-Price 2003). NO is endogenously produced as a byproduct of arginine metabolism by different nitric oxide synthase (NOS) isoforms: neuronal NOS (nNOS), endothelial NOS (eNOS), and inducible NOS (iNOS). Both nNOS and eNOS are constitutively expressed, whereas iNOS is expressed in response to a variety of stimuli. There are reports documenting the relationship between iNOS induction and ischemic lesions in brain (Hara et al. 1996; Mizushima et al. 2002). Also, administration of IL-1β to cultured brain endothelial cells and hippocampal neurons induces expression of iNOS mRNA and increases NO release (Bonmann et al. 1997; Serou et al. 1999). These observations, together with evidence showing that induction of iNOS is regulated by NFκB p65/p50 (Teng et al. 2002), also support our hypothesis that activation of p65/p50 by IL-1 after HI may further stimulate iNOS synthesis and NO formation, which will in turn trigger cell death.

Cyclooxygenase (COX) is an important enzyme in the inflammatory process. COX catalyzes the rate-limiting step in the conversion of arachidonic acid to prostaglandins. There are two isoforms of COX, designated COX-1 and COX-2. COX-1 is expressed constitutively and appears to be responsible for ongoing physiological function, whereas COX-2 is present in only certain tissues where it is transiently induced by growth factors, inflammatory cytokines, tumor promoters and bacterial toxins (Chun et al., 2004). There is evidence to support an involvement of COX2 in HI-induced brain damage (Hara et al. 1998; Sugimoto and Iadecola 2003; Nagayama et al. 1999). IL-1β transcriptional control of COX-2 by NF-κB p65/p50 has been demonstrated in cell culture (Newton et al. 1997), which prompted us to ask if a similar mechanism is activated by HI in the P7 rat. As expected, there was significant iNOS and COX2 expression in the hippocampus and cortex 24h after HI (Figures 16 and 17). Treatment with IL-1Ra reversed the HI-induced increases in iNOS and COX2, a novel finding. Interestingly, sequence analyses of the iNOS and COX2 promoters has shown the presence of DNA binding consensus sequences specific to the p65/p50 binding.

Injected NF-κB decoys permeate hippocampal cells and selectively inhibit p65/p50 binding activity

Because of the importance of NF-κB in the modulation of cell death and survival, the manipulations which alter NF-κB activity may change the fate of cells. Specific inhibition of NF-κB can be accomplished by synthetic double stranded oligonucleotides containing a specific NF-κB consensus sequence, which acts in vivo as a decoy cis element to bind the NF-κB dimer upon release from IκB and competes for the binding to cognate DNA binding sites on specific promoters (Morishita et al. 1997; Yu et al. 1999). In our study, IgG-κB decoy was used to inhibit NF-κB p65/p50 activity, and other two decoys, Bcl-x and scrambled decoys were used as controls.

The pharmacokinetic profiles of phosphothiorated oligonucleotides of varying base composition in rat are similar (Agrawal and Zhao, 1998). Therefore, we used IgGκB decoy sequences as being representative to determine decoy distributions. We

stereotaxically injected fluorescent IgG-κB "decoys" into lateral ventricles and demonstrated cellular incorporation of decoys in hippocampi, as early as two hours after injection, with dissipation taking place by seven hours (Figure 21). Thus we can pulse decoy treatments. The ability to selectively intervene in the binding of different NF-κB binding consensus sequences to cognate NF-κB protein dimers during a fairly short time period should allow for the determination of the role of NF-κB in the regulation of specific genes at specific times after an insult to the CNS, such as HI. It has been proposed that transcriptional injury responses are biphasic and that there are different consequences to delayed transcriptional activation or to persistent vs transient transcriptional factor activation of the NF-κB transcription factor. Our ability to abolish NF-κB binding to selective promoter sites in a transient fashion should provide a useful tool in establishing the role of different injury-induced pathways in cellular commitment to cell death/survival after HI.

Our immunodepletion/supershift data (Figure 22) indicated that endogenous NF-κB protein dimers present in hippocampi bind to the NF-κB binding consensus sequences present on the Bcl-x and IgG-κB promoters with different affinities. NF-κB c-Rel/p50 selectively bind the Bcl-x gene promoter CS4 sequence while p65/p50 preferentially bind the IgG-κB promoters sequence. Our gel shift results showed that IgG-κB decoys selectively inhibited p65/p50 levels and should have repressed transcription of genes whose promoters contain NF-κB sites that preferentially bind p65/p50. Inhibition of c-Rel levels in nuclei by the Bcl-x decoys, on the other hand, should have repressed transcription of genes whose promoters contain NF-κB sites that preferentially bind c-Rel/p50. Clearly the use of decoys could be useful to the characterization of NF-κB transcriptional regulation of selected genes in an in vivo environment.

IgG-κB decoy treatment selectively, compared to Bcl-x decoy, inhibit the transcription of inflammatory cytokines

Since IgG-κB decoy can inhibit p65/p50 binding activity, we speculated that it can inhibit the transcription of inflammatory cytokines, which are the target genes for

NF-κB p65/p50. As expected, we found that at 12h post-HI, IgG-κB decoy treatment selectively down-regulated inflammatory cytokine (IL-1α, TNF-α and TNF-β) mRNA levels of expression (Figure 23), while Bcl-x decoy treatment had effects only on IL-1α expression. On the other hand, using RPA with Rat Apoptosis Multi-probe template sets, we found that the Bcl-x decoy treatment, but not the IgG-κB decoy treatment, had selective inhibitory effects on Bcl-x_L gene expression (Data not shown). These results are consistent with recent reports showing anti-apoptotic features to the stimulation of c-Rel and pro-apoptotic features to the stimulation of p65 DNA binding (Qiu et al. 2001; Pizzi et al. 2002). These results are also consistent with the c-Rel-mediated regulation of Bcl-x gene transcription in response to HI (Qiu et al. 2001). The specific effects of different decoys were demonstrated also in our DNA microarray data (Figures 24A and 24B). Genes that were significantly downregulated by IgG-κB decoys were not affected by Bcl-x decoys, and vice versa. Different decoys have different effects on Bcl-x_L as shown in our DNA microarray data. However, the expression levels of the inflammatory cytokine genes, as shown by RPA, are lower than the detectable levels of the Microarray chips used.

DNA microarray analyses of transcriptional effects of treatment with IgG-κB decoys indicated that the mRNA levels of a large number of genes were affected, confounding the final outcomes

Analysis of the DNA microarray data showed that both IgG-κB and Bcl-x decoy treatments affected mRNA levels of a large number of genes, some of which have not been previously reported to contain NF-κB binding sites, such as the glutamate receptor gene and the FGF-9 gene (Table 1). Considering that there were only 3 microarrays per group and using SAM with false detection rate set at 5%, there probably are many more genes that are differentially affected than those identified in Table 1. The decoy treatments may affect a large number of genes because of the inherent degeneracy of the NF-κB binding DNA consensus sequences. Also, the outcomes may reflect secondary effects on transcription of genes, which in turn regulate transcription of genes lacking a NF-κB DNA binding consensus sequence. Interestingly, the number of genes affected by

the Bcl-x decoy treatments was much smaller than the number affected by the IgG-κB decoy treatments. This might be because: 1) There are fewer genes regulated by c-Rel/p50 as compared to p65/p50; 2) The binding affinity of Bcl-x decoys for c-Rel/p50 is less than the affinity of IgG-κB decoys for p65/p50, which is consistent with previous results in our resrach group demonstrated less relative binding affinity of recombinant p50 for Bcl-x NF-κB binding sequence compared with the IgG-κB NF-κB binding sequence (Glasgow et al. 2000). Should the latter be the case, one would predict that the high affinity of a decoy may sacrifice its specificity, an important consideration when designing a decoy.

We also noticed that there are some controversial effects of IgG-κB decoy treatment. For example, the upregulation of HSP70 mRNA by IgG-κB decoy should be protective since HSP70 has been reported to prevent cell death by inhibiting the release of cytochrome C from mitochondria at early time points after ischemia (Tsuchiya et al. 2003). It is of interest that MnSOD, which has also been reported to attenuate the release of cytochrome C from mitochondria (Fujimura et al. 1999; Noshita et al. 2001), was down regulated by IgG-κB decoy treatment. Thus, the net effect of decoy treatments on HI-induced cell death should integrate all of the individual gene expression changes.

In summary, the data reported here provide evidence that the IL-1 $\rightarrow$ NF-κB pathway contributes significantly to HI-induced cell death (Figure 25). HI induced IL-1 stimulates the degradation of IκBα and the increased nuclear presence of Bcl-3. Thus, IκBα degradation releases p65/p50 dimers for nuclear translocation, binding to cognate promoters and selective gene transactivation. Increased nuclear Bcl-3 levels bind to and sequester p50 homodimers, a non-transactivating dimer, away from the same cognate sequences, vacating these sites and making them available to p65/p50, a transactivating NF-κB dimer. In this way, inflammatory genes – such as, iNOS and COX2 – are induced with increased cell death as an outcome. There are still questions to be answered in this pathway. Jander et al. (2000) identified a role for glutamate receptors in the induction of

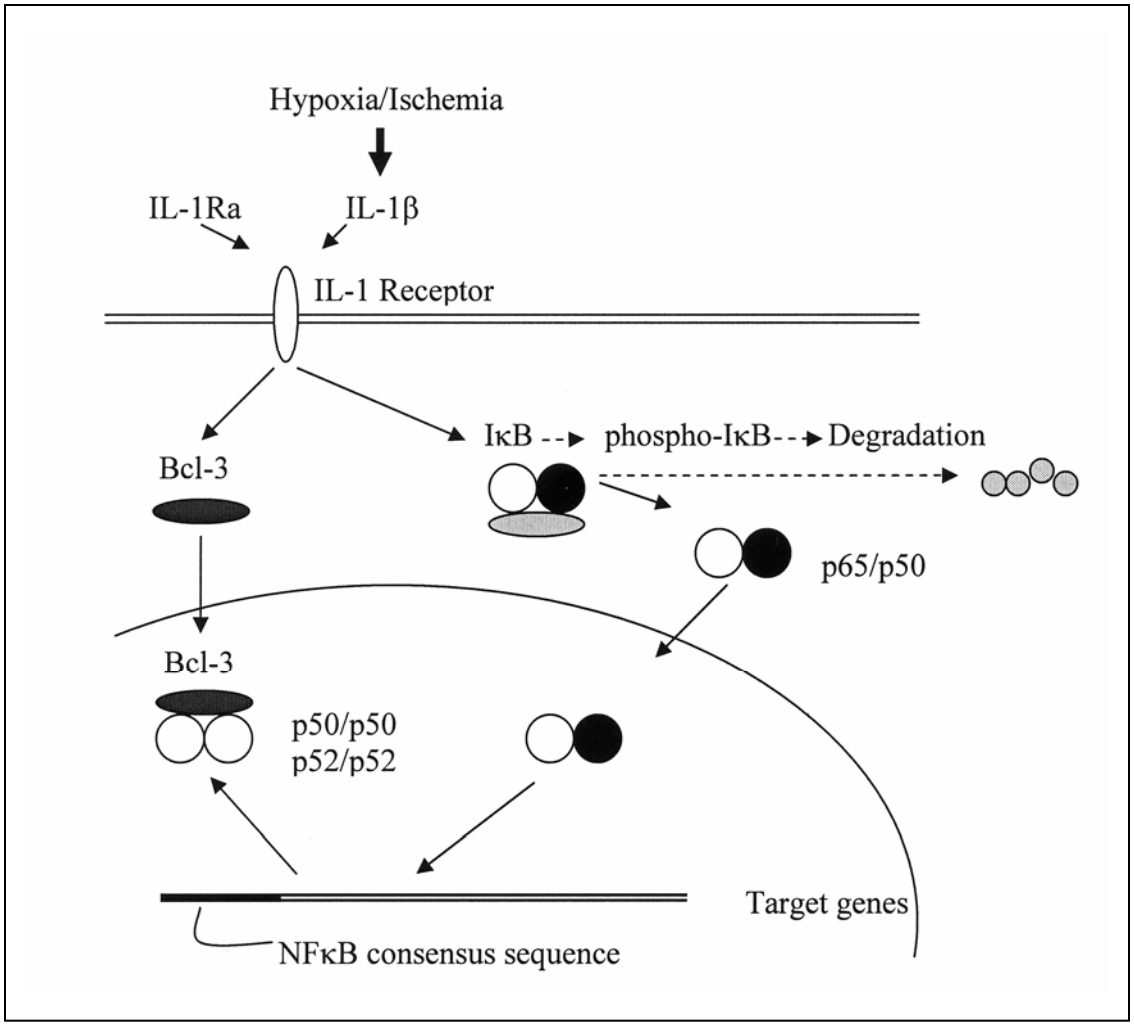

Figure 25. Schematic diagram illustrating the effects of HI-induced IL-1 increases on NF-κB activation. HI-induced IL-1 stimulates degradation of IκBα and increased nuclear levels of Bcl-3. IκBα degradation releases its inhibition on p65/p50 dimers and enables nuclear translocation of p65/p50. Nuclear Bcl-3 binds and dissociates p50 homodimers from cognate NF-κB binding sites enabling p65/p50 dimers to bind and activate target genes.

inflammatory cytokine gene expression in brain after focal ischemic damage. They suggested that NMDA receptor signaling is a dominant mechanism of inflammatory gene induction in the absence of cell death and partial mechanism in the presence of cell death since the production of IL-1β was almost completely inhibited in nonischemic ipsilateral

cortex and partially inhibited in ischemic areas by MK-801, a NMDA antagonist. The function of glutamate surges on IL-1 induction after HI is yet to be determined.

The absence of side effects of IL-1Ra and its safety in clinical trials in rheumatoid arthritis would suggest that this intervention may be applicable to perinatal ischemia. Decoys to NF-κB binding DNA consensus sequences are useful to determine regulatory features affecting individual genes. Use of decoy treatments to alter physiological and pathological outcomes to trauma will require concerted pulsed treatments with "cocktails" made up of different decoy sequences that take into account the large number of genes displaying NF-κB binding sites in their promoters.

REFERENCES

1. Abbadie C, Kabrun N, Bouali F, Smardova J, Stehelin D, Vandenbunder B, Enrietto PJ. (1993) High levels of c-Rel expression are associated with programmed cell death in the developing avian embryo and in bone marrow cells in vitro. *Cell* 75(5): 899-912.

2. Agrawal S, Zhao Q. 1998. Antisense therapeutics. *Curr Opin Chem Biol* 2(4): 519-528.

3. Auron PE. (1998). The interleukin 1 receptor: ligand interactions and signal transduction. *Cytokine Growth Factor Rev* 9(3-4): 221-237.

4. Baeuerle P. (1991) The inducible transcription activator NF-kappa B; regulation by distinct protein subunits. *Biochemica et Biophysica Acta* 1072(1): 63-80.

5. Baichwal VR and Baeuerle PA. (1997) Activate NF-kappa B or die? *Curr Biol* 7(2): R94-R96.

6. Baldwin AS Jr. (1996) The NF-kappa B and I kappa B proteins: new discoveries and insights. *Annu Rev Immunol* 14: 649-683.

7. Barger SW and Mattson MP. (1996) Induction of neuroprotective kappa B-dependent transcription by secreted forms of the Alzheimer's beta-amyloid precursor. *Brain Res Mol Brain Res* 40(1): 116-126.

8. Barger SW, Horster D, Furukawa K Goodman Y, Krieglstein J, Mattson MP. (1995) Tumor necrosis factors alpha and beta protect neurons against amyloid beta-peptide toxicity: evidence for involvement of a kappa B-binding factor and attenuation of peroxide and Ca^{2+} accumulation. *Proc Natl Acad Sci U S A* 92(20): 9328-9332.

9. Betz AL, Yang GY, and Davidson BL. (1995) Attenuation of stroke size in rats using an adenoviral vector to induce overexpression of interleukin-1 receptor antagonist in brain. *J Cereb Blood Flow Metab* 15(4): 547-551.

10. Bonmann E., Suschek C., Spranger M., and Kolb-Bachofen V. (1997) The dominant role of exogenous or endogenous interleukin-1 beta on expression and activity of inducible nitric oxide synthase in rat microvascular brain endothelial cells. *Neurosci Lett* 230(2): 109-112.

11. Bona E, Andersson AL, Blomgren K, Gilland E, Puka-Sundvall M, Gustafson K, Hagberg H. (1999). Chemokine and inflammatory cell response to hypoxia-ischemia in immature rats. *Pediatr Res* 45(4 Pt 1): 500-509.

12. Bours V, Franzoso G, Azarenko V, Park S, Kanno T, Brown K, Siebenlist U. (1993). The oncoprotein Bcl-3 directly transactivates through kappa B motifs via association with DNA-binding p50B homodimers. *Cell* 72(5): 729-739.

13. Bours V, Burd PR, Brown K, Villalobos J, Park S, Ryseck RP, Bravo R, Kelly K, Siebenlist U. (1992) A novel mitogen-inducible gene product related to p50/p105-NF-kappa B participates in transactivation through a kappa B site. *Mol Cell Biol* 12(2): 685-695.

14. Bours V, Villalobos J, Burd PR, Kelly K, Siebenlist U. (1990) Cloning of a mitogen-inducible gene encoding a kappa B DNA-binding protein with homology to the rel oncogene and to cell-cycle motifs. *Nature* 348(6296): 76-80.

15. Brown GC, Bal-Price A. (2003) Inflammatory neurodegeneration mediated by nitric oxide, glutamate, and mitochondria. *Mol Neurobiol* 27(3): 325-355.

16. Bundy DL and McKeithan TW. (1997) Diverse effects of BCL3 phosphorylation on its modulation of NF-kappaB p52 homodimer binding to DNA. *J Biol Chem* 272(52): 33132-33139.

17. Buttini M, Sauter A, and Boddeke HW. (1994) Induction of interleukin-1 beta mRNA after focal cerebral ischaemia in the rat. *Brain Res Mol Brain Res* 23(1-2): 126-134.

18. Cao Z, Henzel WJ, and Gao X. (1996) IRAK: a kinase associated with the interleukin-1 receptor. *Science* 271(5252): 1128-1131.

19. Calabrese LH. (2002) Anakinra treatment of patients with rheumatoid arthritis. *Ann Pharmacother* 36: 1204-1209.

20. Charriaut-Marlangue C, Margaill I, Represa A, Popovici T, Plotkine M, Ben-Ari Y. (1996) Apoptosis and necrosis after reversible focal ischemia: an in situ DNA fragmentation analysis. *J Cereb Blood Flow Metab* 16(2): 186-194.

21. Chen FE, Huang DB, Chen YQ, Ghosh G. (1998) Crystal structure of p50/p65 heterodimer of transcription factor NF-kappaB bound to DNA. *Nature* 391(6665): 410-413.

22. Chen J, Jin K, Chen M, Pei W, Kawaguchi K, Greenberg DA, Simon RP. (1997) Early detection of DNA strand breaks in the brain after transient focal ischemia: implications for the role of DNA damage in apoptosis and neuronal cell death. *J Neurochem* 69(1): 232-245.

23. Cheng Y, Deshmukh M, D'Costa A, Demaro JA, Gidday JM, Shah A, Sun Y, Jacquin MF, Johnson EM, Holtzman DM. (1998) Caspase inhibitor affords neuroprotection with delayed administration in a rat model of neonatal hypoxic-ischemic brain injury. *J Clin Invest* 101(9): 1992-1999.

24. Chun KS, Cha HH, Shin JW, Na HK, Park KK, Chung WY, Surh YJ. (2004) Nitric oxide induces expression of cyclooxygenase-2 in mouse skin through activation of NF-kappaB. *Carcinogenesis* 25(3): 445-454.

25. Clemens JA, Stephenson DT, Dixon EP, Smalstig EB, Mincy RE, Rash KS, Little SP. (1997) Global cerebral ischemia activates nuclear factor-kappa B prior to evidence of DNA fragmentation. *Brain Res Mol Brain Res* 48(2): 187-196.

26. Cogswell PC, Guttridge DC, Funkhouser WK, Baldwin AS Jr. (2000) Selective activation of NF-kappa B subunits in human breast cancer: potential roles for NF-kappa B2/p52 and for Bcl-3. *Oncogene* 19(9): 1123-1131.

27. Cowell RM, Xu H, Galasso JM, Silverstein FS. (2002) Hypoxic-ischemic injury induces macrophage inflammatory protein-1alpha expression in immature rat brain. *Stroke* 33(3):795-801.

28. Davies CA, Loddick SA, Toulmond S, Stroemer RP, Hunt J, Rothwell NJ. (1999) The progression and topographic distribution of interleukin-1beta expression after permanent middle cerebral artery occlusion in the rat. *J Cereb Blood Flow Metab* 19(1): 87-98.

29. Dinarello CA. (1999) Interleukin-18. *Methods* 19 (1):121-32.

30. Dinarello CA, Novick D, Puren AJ, Fantuzzi G, Shapiro L, Muhl H, Yoon DY, Reznikov LL, Kim SH, Rubinstein M. (1998) Overview of interleukin-18: more than an interferon-gamma inducing factor. *J Leukoc Biol* 63(6): 658-664.

31. Dobbing J and Sands J. (1979) Comparative aspects of the brain growth spurt. *Early Hum Dev* 3(1): 79-83.

32. Dunn S, Young E, Hall M, McNulty S. (2002) Activation of astrocyte intracellular signaling pathways by interleukin-1 in rat primary striatal cultures. *Glia* 37 (1): 31-42.

33. Edwards AD, Yue X, Cox P, Hope PL, Azzopardi DV, Squier MV, Mehmet H. (1997) Apoptosis in the brains of infants suffering intrauterine cerebral injury. *Pediatr Res* 42(5):684-689.

34. Eisen M, Spellman P, Brown P, and Botstein D. (1998) Cluster analysis and display of genome-wide expression patterns. *Proc Natl Acad Sci USA* 95(25): 14863-14868.

35. Elliott S, Coon C, Hays E, Stadheim T, Vincenti M. (2002) Bcl-3 is an interleukin-1-responsive gene in chondrocytes and synovial fibroblasts that activates transcription of the matrix metalloproteinase 1 gene. *Arthritis Rheum* 46(12), 3230-3239.

36. Foster-Barber A, Dickens, B and Ferriero D. (2001) Human perinatal asphyxia: correlation of neonatal cytokines with MRI and outcome. *Dev Neurosci* 23(3): 213-218.

37. Franzoso G, Bours V, Azarenko V, Park S, Tomita-Yamaguchi M, Kanno T, Brown K, Siebenlist U. (1993) The oncoprotein Bcl-3 can facilitate NF-kappa B-mediated transactivation by removing inhibiting p50 homodimers from select kappa B sites. *EMBO J* 12(10): 3893-3901.

38. Franzoso G, Bours V, Park S, Tomita-Yamaguchi M, Kelly K, Siebenlist U. (1992) The candidate oncoprotein Bcl-3 is an antagonist of p50/NF-kappa B-mediated inhibition. *Nature* 359(6393): 339-342.

39. French R, VanHoy RW, Chizzonite R, Zachary J, Dantzer R, Parnet P, Bluthe R, Kelley KW. (1999) Expression and localization of p80 and p68 interleukin-1 receptor proteins in the brain of adult mice. *J Neuroimmunol* 93(1-2): 194-202.

40. Fujimura M, Morita-Fujimura Y, Kawase M, Chan P. (1999) Early decrease of apurinic/apyrimidinic endonuclease expression after transient focal cerebral ischemia in mice. *J Cereb Blood Flow Metab* 19(5): 495-501.

41. Fujita T, Nolan GP, Liou HC, Scott ML, Baltimore D. (1993). The candidate proto-oncogene bcl-3 encodes a transcriptional coactivator that acts through NF-kappa B p50 homodimers. *Genes Dev* 7(7B):1354-1363.

42. Gabriel C, Justicia C, Camins A, Planas AM. (1999) Vasculitic neuropathy in association with chronic graft-versus-host disease. *J Neurol Sci* 168(1):68-70.

43. Galley HF, Nelson SJ, Dhillon J, Dubbels AM, Webster NR. (1999). Effect of the nitric oxide inhibitor, L-N(G)-monomethylarginine, on accumulation of interleukin-6 and interleukin-8, and nuclear factor-kappaB activity in a human endothelial cell line. *Crit Care Med* 27(5): 908-912.

44. Garcia JH, Liu KF, Relton JK. (1995) Interleukin-1 receptor antagonist decreases the number of necrotic neurons in rats with middle cerebral artery occlusion. *Am J Pathol* 147(5):1477-1486.

45. Gayle D, Ilyin SE, Plata-Salaman CR. (1997) Interleukin-1 receptor type I mRNA levels in brain regions from male and female rats. *Brain Res Bull* 42(6):463-467.

46. Ghosh S and Baltimore D. (1990). Activation in vitro of NF-kappa B by phosphorylation of its inhibitor I kappa B. *Nature* 344(6267): 678-682.

47. Ghosh S, May MJ, and Kopp EB. (1998) NF-kappa B and Rel proteins: evolutionarily conserved mediators of immune responses. *Annu Rev Immunol* 16, 225-260.

48. Gibson M, Han B, Choi J, Knudson C, Korsmeyer S, Parsadanian M, Holtzman D. (2001) BAX contributes to apoptotic-like death following neonatal hypoxia-ischemia: evidence for distinct apoptosis pathways. *Mol Med* 7(9):644-655.

49. Glasgow JN, Wood T, Perez-Polo JR. (2000) Identification and characterization of nuclear factor kappaB binding sites in the murine bcl-x promoter. *J Neurochem* 75(4):1377-1389.

50. Gozal E, Simakajornboon N, and Gozal D. (1998) NF-κB induction during in vivo hypoxia in dorsocaudal brain stem of rat - effect of MK-801 and L-NME. *J Appl Physiol* 85(1): 312-316.

51. Grafe MR. (1994) Developmental changes in the sensitivity of the neonatal rat brain to hypoxic/ischemic injury. *Brain Research* 653(1-2): 161-166.

52. Grilli M, Chiu J, and Lenardo M. (1993) NF-kappa B and Rel: participants in a multiform transcriptional regulatory system. *Int Rev Cytol* 143:1-62.

53. Grilli M and Memo M. (1999) Nuclear factor-kappaB/Rel proteins: a point of convergence of signalling pathways relevant in neuronal function and dysfunction. *Biochem Pharmacol* 57(1): 1-7.

54. Grimm S, Bauer MK, Baeuerle PA, Schulze-Osthoff K. (1996) Bcl-2 down-regulates the activity of transcription factor NF-kappaB induced upon apoptosis. *J Cell Biol* 134(1): 13-23.

55. Guegan, C and Sola, B. (2000) Early and sequential recruitment of apoptotic effectors after focal permanent ischemia in mice. *Brain Res* 856(1-2): 93-100.

56. Gutierrez EG, Banks WA, Kastin AJ. (1994) Blood-borne interleukin-1 receptor antagonist crosses the blood-brain barrier. *J Neuroimmunol* 55(2):153-160.

57. Hagberg H, Gilland E, Bona E, Hanson LA, Hahin-Zoric M, Blennow M, Holst M, McRae A, Soder O. (1996) Enhanced expression of interleukin (IL)-1 and IL-6

messenger RNA and bioactive protein after hypoxia-ischemia in neonatal rats. *Pediatr Res* 40(4): 603-609.

58. Hara H, Friedlander R, Gagliardini V, Ayata C, Fink K, Huang Z, Shimizu-Sasamata M, Yuan J, Moskowitz M. (1997) Inhibition of interleukin 1beta converting enzyme family proteases reduces ischemic and excitotoxic neuronal damage. *Proc Natl Acad Sci U S A* 94(5): 2007-2012.

59. Hara H, Huang PL, Panahian N, Fishman MC, Moskowitz MA. (1996) Reduced brain edema and infarction volume in mice lacking the neuronal isoform of nitric oxide synthase after transient MCA occlusion. *J Cereb Blood Flow Metab* 16(4): 605-611.

60. Hara K, Kong DL, Sharp FR, Weinstein PR. (1998) Effect of selective inhibition of cyclooxygenase 2 on temporary focal cerebral ischemia in rats. *Neurosci Lett* 256(1): 53-56.

61. Haskill S, Beg A, Tompkins S, Morris J, Yurochko A, Sampson-Johannes A, Mondal K, Ralph P, Baldwin A (1991) Characterization of an immediate-early gene induced in adherent monocytes that encodes I kappa B-like activity. *Cell* 65(7): 1281-1289.

62. Hedtjarn M, Leverin AL, Eriksson K, Blomgren K, Mallard C, Hagberg H. (2002) Interleukin-18 involvement in hypoxic-ischemic brain injury. *J Neurosci* 22(14): 5910-5919.

63. Hill J, Gunion-Rinker L, Kulhanek D, Lessov N, Kim S, Clark WM, Dixon MP, Nishi R, Stenzel-Poore MP, Eckenstein FP. (1999) Temporal modulation of cytokine expression following focal cerebral ischemia in mice. *Brain Res* 820(1-2): 45-54.

64. Hockenbery D. (1995) Defining apoptosis. *Am J Pathol* 146(1):16-19.

65. Hu X, Qiu J, Grafe M, Rea H, Rassin D, Perez-Polo JR. (2003) Bcl-2 family members make different contributions to cell death in hypoxia and/or hyperoxia in rat cerebral cortex. *Int J Dev Neurosci* 21(7): 371-377.

66. Huang F, Wang Z, Wu D, Schielke G, Sun Y, Yang G. (2003) Early NFkappaB activation is inhibited during focal cerebral ischemia in interleukin-1beta-converting enzyme deficient mice. *J Neurosci Res* 73(5): 698-707.

67. Hunter R, Stevenson E, Koncarevic A, Mitchell-Felton H, Essig D, Kandarian S. (2002) Activation of an alternative NF-kappaB pathway in skeletal muscle during disuse atrophy. *FASEB J* 16(6): 529-538.

68. Ilyin S, Gayle D, Flynn MC, Plata-Salaman C. (1998) Interleukin-1beta system (ligand, receptor type I, receptor accessory protein and receptor antagonist), TNF-

alpha, TGF-beta1 and neuropeptide Y mRNAs in specific brain regions during bacterial LPS-induced anorexia. *Brain Res Bull* 45: 507-515.

69. Israel A. (1995) A role for phosphorylation and degradation in the control of NF-kappa B activity. *Trends Genet* 11(6): 203-205.

70. Jander S, Schroeter M, Stoll G. (2000) Role of NMDA receptor signaling in the regulation of inflammatory gene expression after focal brain ischemia. *J Neuroimmunol* 109(2): 181-187.

71. Jung S, Yaron A, Alkalay I, Hatzubai A, Avraham A, Ben-Neriah Y. (1995) Costimulation requirement for AP-1 and NF-kappa B transcription factor activation in T cells. *Ann NY Acad Sci* 766: 245-252.

72. Kaltschmidt C, Kaltschmidt B, Neumann H, Wekerle H, Baeuerle PA. (1994) Constitutive NF-kappa B activity in neurons. *Mol Cell Biol* 14(6): 3981-3992.

73. Kang S, Tran A, Grilli M, Lenardo M. (1992) NF-kappa B subunit regulation in nontransformed CD4+ T lymphocytes. *Science* 256(5062): 1452-1456.

74. Koong A, Chen E, and Giaccia A. (1994) Hypoxia causes the activation of nuclear factor kappa B through the phosphorylation of I kappa B alpha on tyrosine residues. *Cancer Res* 54(6): 1425-1430.

75. Krageloh-Mann I, Toft P, Lunding J, Andresen J, Pryds O, Lou H. (1999) Brain lesions in preterms: origin, consequences and compensation. *Acta Paediatr* 88(8): 897-908.

76. Kuban K and Leviton A. (1994) Cerebral palsy. *N Engl J Med* 330(3): 188-195.

77. Kunsch C, Ruben SM, Rosen CA. (1992) Selection of optimal kappa B/Rel DNA-binding motifs: interaction of both subunits of NF-kappa B with DNA is required for transcriptional activation. *Mol Cell Biol* 12(10):4412-21.

78. Lau L and Yu A. (2001) Astrocytes produce and release interleukin-1, interleukin-6, tumor necrosis factor alpha and interferon-gamma following traumatic and metabolic injury. *J Neurotrauma* 18(3): 351-359.

79. Lawrence C, Allan S, and Rothwell N. (1998) Interleukin-1beta and the interleukin-1 receptor antagonist act in the striatum to modify excitotoxic brain damage in the rat. *Eur J Neurosci* 10(3): 1188-1195.

80. Lenardo M and Siebenlist U. (1994) Bcl-3-mediated nuclear regulation of the NF-kappa B trans-activating factor. *Immunol Today* 15(4): 145-147.

81. Levine S. (1960) Anoxic-ischemic encephalopathy in rats. *American Journal of Pathology* 36: 1-17.

82. Lin R, Gewert D, and Hiscott J. (1995) Differential transcriptional activation in vitro by NF-kappa B/Rel proteins. *J Biol Chem* 270(7): 3123-3131.

83. Lipton S. (1997) Janus faces of NF-kappa B: neurodestruction versus neuroprotection. *Nat Med* 3(1): 20-22.

84. Liu J, Sen R, and Rothstein T. (1993) Abnormal kappa B-binding protein in the cytoplasm of a plasmacytoma cell line that lacks nuclear expression of NF-kappa B. *Mol Immunol* 30(5): 479-489.

85. Liu X, Kwon D, Schielke G, Yang G, Silverstein F, Barks J. (1999) Mice deficient in interleukin-1 converting enzyme are resistant to neonatal hypoxic-ischemic brain damage. *J Cereb Blood Flow Metab* 19(10):1099-1108.

86. Loddick S and Rothwell N. (1996). Neuroprotective effects of human recombinant interleukin-1 receptor antagonist in focal cerebral ischaemia in the rat. *J Cereb Blood Flow Metab* 16(5): 932-940.

87. Majno G, Joris I. (1995) Apoptosis, oncosis, and necrosis. An overview of cell death. *Am J Pathol* 146(1):3-15.

88. Martin D, Chinookoswong N, and Miller G. (1994) The interleukin-1 receptor antagonist (rhIL-1ra) protects against cerebral infarction in a rat model of hypoxia-ischemia. *Exp Neurol* 130(2): 362-367.

89. Martin L, Sieber F, and Traystman R. (2000). Apoptosis and necrosis occur in separate neuronal populations in hippocampus and cerebellum after ischemia and are associated with differential alterations in metabotropic glutamate receptor signaling pathways. *J Cereb Blood Flow Metab* 20(1): 153-167.

90. Matsushita K, Matsuyama T, Kitagawa K, Matsumoto M, Yanagihara T, Sugita M. (1998). Alterations of Bcl-2 family proteins precede cytoskeletal proteolysis in the penumbra, but not in infarct centres following focal cerebral ischemia in mice. *Neuroscience* 83(2): 439-448.

91. Mattson M, Camandola S. (2001) NF-kappaB in neuronal plasticity and neurodegenerative disorders. *J Clin Invest* 107(3):247-254.

92. McMahan C, Slack J, Mosley B, Cosman D, Lupton S, Brunton L, Grubin C, Wignall J, Jenkins N, Brannan C. (1991) A novel IL-1 receptor, cloned from B cells by mammalian expression, is expressed in many cell types. *EMBO J* 10(10): 2821-2832.

93. Minami M, Kuraishi Y, Yabuuchi K, Yamazaki A, Satoh M. (1992) Induction of interleukin-1 beta mRNA in rat brain after transient forebrain ischemia. *J Neurochem* 58(1): 390-392.

94. Mizushima H, Zhou CJ, Dohi K, Horai R, Asano M, Iwakura Y, Hirabayashi T, Arata S, Nakajo S, Takaki A, Ohtaki H, Shioda S. (2002) Reduced postischemic apoptosis in the hippocampus of mice deficient in interleukin-1. *J Comp Neurol* 448(2): 203-216.

95. Morishita R, Sugimoto T, Aoki M, Kida I, Tomita N, Moriguchi A, Maeda K, Sawa Y, Kaneda Y, Higaki J, Ogihara T. (1997) In vivo transfection of cis element "decoy" against nuclear factor-kappaB binding site prevents myocardial infarction. *Nat Med* 3(8): 894-899.

96. Mulcahy N, Ross J, Rothwell N, Loddick S. (2003) Delayed administration of interleukin-1 receptor antagonist protects against transient cerebral ischaemia in the rat. *Br J Pharmacol* 140(3):471-476.

97. Muzio M, Ni J, Feng P, Dixit V. (1997) IRAK (Pelle) family member IRAK-2 and MyD88 as proximal mediators of IL-1 signaling. *Science* 278(5343): 1612-1615.

98. Nadjar A, Combe C, Laye S, Tridon V, Dantzer R, Amedee T, Parnet P. (2003) Nuclear factor kappaB nuclear translocation as a crucial marker of brain response to interleukin-1. A study in rat and interleukin-1 type I deficient mouse. *J Neurochem* 87(4):1024-1036.

99. Nagayama M, Niwa K, Nagayama T, Ross ME, Iadecola C. (1999) The cyclooxygenase-2 inhibitor NS-398 ameliorates ischemic brain injury in wild-type mice but not in mice with deletion of the inducible nitric oxide synthase gene. *J Cereb Blood Flow Metab* 19(11): 1213-1219.

100. Nakajima W, Ishida A, Lange M, Gabrielson K, Wilson M, Martin L, Blue M, Johnston M. (2000) Apoptosis has a prolonged role in the neurodegeneration after hypoxic ischemia in the newborn rat. *J Neurosci* 20(21): 7994-8004.

101. Nelson C and Silverstein F. (1994) Acute disruption of cytochrome oxidase activity in brain in a perinatal rat stroke model. *Pediatr Res* 36(1 Pt 1): 12-19.

102. Newton R, Kuitert L., Bergmann M, Adcock I and Barnes P. (1997) Evidence for involvement of NF-kappaB in the transcriptional control of COX-2 gene expression by IL-1beta. *Biochem Biophys Res Commun* 237(1): 28-32.

103. Nesic O, Xu G, McAdoo D, High K, Hulsebosch C, Perez-Pol JR. (2001) IL-1 receptor antagonist prevents apoptosis and caspase-3 activation after spinal cord injury. *J Neurotrauma* 18(9): 947-956.

104. Nesic O, Svrakic N, Xu G, McAdoo D, High K, Hulsebosch C. and Perez-Polo JR. (2002) DNA Microarray analysis of the Contused Spinal Cord: The effect of NMDA receptor inhibition. *J Neurosci Res* 68(4):406-423.

105. Ni B, Wu X, Su Y, Stephenson D, Smalstig EB, Clemens J, Paul SM. (1998) Transient global forebrain ischemia induces a prolonged expression of the caspase-3 mRNA in rat hippocampal CA1 pyramidal neurons. *J Cereb Blood Flow Metab* 18(3): 248-256.

106. Nitatori T, Sato N, Waguri S, Karasawa Y, Araki H, Shibanai K, Kominami E, Uchiyama Y. (1995) Delayed neuronal death in the CA1 pyramidal cell layer of the gerbil hippocampus following transient ischemia is apoptosis. *J Neurosci* 15(2): 1001-1011.

107. Nolan G, Ghosh S, Liou H, Tempst P, Baltimore D. (1991) DNA binding and I kappa B inhibition of the cloned p65 subunit of NF-kappa B, a rel-related polypeptide. *Cell* 64(5): 961-969.

108. Nolan G, Fujita T., Bhatia K, Huppi C, Liou H, Scott M, Baltimore D. (1993) The bcl-3 proto-oncogene encodes a nuclear I kappa B-like molecule that preferentially interacts with NF-kappa B p50 and p52 in a phosphorylation-dependent manner. *Mol Cell Biol* 13(6): 3557-3566.

109. Northington F, Ferriero D, Flock D, Martin L. (2001) Delayed neurodegeneration in neonatal rat thalamus after hypoxia-ischemia is apoptosis. *J Neurosci* 21(6): 1931-1938.

110. Noshita N, Sugawara T, Fujimura M, Morita-Fujimura Y, Chan P. (2001) Manganese Superoxide Dismutase Affects Cytochrome c Release and Caspase-9 Activation After Transient Focal Cerebral Ischemia in Mice. *J Cereb Blood Flow Metab* 21(5): 557-567.

111. Nurmi A, Lindsberg P, Koistinaho M, Zhang W, Juettler E, Karjalainen-Lindsberg M, Weih F, Frank N, Schwaninger M, Koistinaho J. (2004) Nuclear factor-kappaB contributes to infarction after permanent focal ischemia. *Stroke* 35(4): 987-91.

112. O'Neill LA and Greene C. (1998) Signal transduction pathways activated by the IL-1 receptor family: ancient signaling machinery in mammals, insects, and plants. *J Leukoc Biol* 63(6): 650-657.

113. Perkins N, Schmid R, Duckett C, Leung K, Rice N, Nabel G. (1992) Distinct combinations of NF-kappa B subunits determine the specificity of transcriptional activation. *Proc Natl Acad Sci U S A* 89(5): 1529-1533.

114. Pinteaux E, Parker L, Rothwell N, Luheshi G. (2002) Expression of interleukin-1 receptors and their role in interleukin-1 actions in murine microglial cells. *J Neurochem* 83(4): 754-763.

115. Pizzi M, Goffi F, Boroni F. Perkins S, Liou H, Spano P. (2002) Opposing roles for NF-kappa B/Rel factors p65 and c-Rel in the modulation of neuron survival elicited by glutamate and interleukin-1beta. *J Biol Chem* 277(23): 20717-20723.

116. Pulera M, Adams L, Liu H, Santos D, Nishimura R, Yang F, Cole G, Wasterlain C. (1998). Apoptosis in a neonatal rat model of cerebral hypoxia-ischemia. *Stroke* 29(12): 2622-2630.

117. Przedborski S, Kostic V, Jackson-Lewis V, Cadet JL, Burke R. (1991) Effect of unilateral perinatal hypoxic-ischemic brain injury in the rat on dopamine D1 and D2 receptors and uptake sites: a quantitative autoradiographic study. *J Neurochem* 57(6):1951-1961.

118. Qiu J, Grafe M, Schmura S, Glasgow J, Kent TA, Rassin D, Perez-Polo JR. (2001). Differential NF-kappa B regulation of bcl-x gene expression in hippocampus and basal forebrain in response to hypoxia. *J Neurosci Res* 64(3): 223-234.

119. Qiu J, Hu X, Nesic O, Grafe M, Rassin D, Wood TG, Perez-Polo JR. (2004) Effects of NF-kappaB oligonucleotide "decoys" on gene expression in P7 rat hippocampus after hypoxia/ischemia. *J Neurosci Res* 77(1): 108-118.

120. Ray A, Roberts A, Lee S, Farkas G, Michlin C, Rifkin D, Ostrow P, Krasney J. (2003) Exercise delays the hypoxic thermal response in rats. *J Appl Physiol* 95(1): 272-278.

121. Rice J, III, Vannucci R, and Brierley J. (1981) The influence of immaturity on hypoxic-ischemic brain damage in the rat. *Annals of Neurology* 9(2): 131-141.

122. Rocha S, Martin A, Meek D, Perkins N**.** (2003) p53 represses cyclin D1 transcription through down regulation of Bcl-3 and inducing increased association of the p52 NF-kappaB subunit with histone deacetylase 1. *Mol Cell Biol* 23(13): 4713-4727.

123. Romijn H, Janszen A, van Voorst M, Buijs R, Balazs R, Swaab D. (1992) Perinatal hypoxic ischemic encephalopathy affects the proportion of GABA-immunoreactive neurons in the cerebral cortex of the rat. *Brain Res* 592(1-2):17-28.

124. Rong Y and Baudry M. (1996) Seizure activity results in a rapid induction of nuclear factor-kappa B in adult but not juvenile rat limbic structures. *J Neurochem* 67(2): 662-668.

125. Rothwell N, Allan S, and Toulmond S. (1997) The role of interleukin 1 in acute neurodegeneration and stroke: pathophysiological and therapeutic implications. *J Clin Invest* 100(11): 2648-2652.

126. Ruben S, Dillon P, Schreck R, Henkel T, Chen CH, Maher M, Baeuerle P, Rosen C. (1991) Isolation of a rel-related human cDNA that potentially encodes the 65-kD subunit of NF-kappa B. *Science* 251(5000):1490-1493.

127. Rumpel H, Buchli R, Gehrmann J, Aguzzi A, Illi O, Martin E. (1995) Magnetic resonance imaging of brain edema in the neonatal rat: a comparison of short and long term hypoxia-ischemia. *Pediatr Res* 38(1):113-118.

128. Ryseck R, Bull P, Takamiya M, Bours V, Siebenlist U, Dobrzanski P, Bravo R. (1992) RelB, a new Rel family transcription activator that can interact with p50-NF-kappa B. *Mol Cell Biol* 12(2): 674-684.

129. Sairanen T, Lindsberg P, Brenner M, Siren A. (1997) Global forebrain ischemia results in differential cellular expression of interleukin-1beta (IL-1beta) and its receptor at mRNA and protein level. *J Cereb Blood Flow Metab* 17(10): 1107-1120.

130. Saliba E and Henrot A. (2001) Inflammatory mediators and neonatal brain damage. *Biol Neonate* 79(3-4): 224-227.

131. Schmid R, Perkins N, Duckett C, Andrews P, Nabel G. (1991) Cloning of an NF-kappa B subunit which stimulates HIV transcription in synergy with p65. *Nature* 352(6337): 733-736.

132. Schmidt K, Traenckner E, Meier B, Baeuerle P. (1995) Induction of oxidative stress by okadaic acid is required for activation of transcription factor NF-kappa B. *J Biol Chem* 270(45): 27136-27142.

133. Schneider A, Martin-Villalba A, Weih F, Vogel J, Wirth T, Schwaninger M. (1999) NF-kappaB is activated and promotes cell death in focal cerebral ischemia. *Nat Med* 5(5): 554-559.

134. Seegers H, Grillon E, Trioullier Y, Vath A, Verna JM, Blum D. (2000) Nuclear factor-kappa B activation in permanent intraluminal focal cerebral ischemia in the rat. *Neurosci Lett* 288(3): 241-245.

135. Serou M, DeCoster M, and Bazan N. (1999) Interleukin-1 beta activates expression of cyclooxygenase-2 and inducible nitric oxide synthase in primary hippocampal neuronal culture: platelet-activating factor as a preferential mediator of cyclooxygenase-2 expression. *J Neurosci Res* 58(4): 593-598.

136. Shapiro L, Puren AJ, Barton HA, Novick D, Peskind R, Shenkar R, Gu Y, Su M, and Dinarello C. (1998) Interleukin 18 stimulates HIV type 1 in monocytic cells. *Proc Natl Acad Sci U S A* 95(21): 12550-12555.

137. Shewood N and Timiras P. 1970 A stereotaxic atlas of the developing rat brain. Berkeley, University of California Press.

138. Siebenlist U, Franzoso G, and Brown K. (1994) Structure, regulation and function of NF-kappa B. *Annu Rev Cell Biol* 10: 405-455.

139. Sica A, Tan TH, Rice N, Kretzschmar M, Ghosh P, Young H. (1992) The c-rel protooncogene product c-Rel but not NF-kappa B binds to the intronic region of the human interferon-gamma gene at a site related to an interferon-stimulable response element. *Proc Natl Acad Sci U S A* 89(5):1740-1744.

140. Silverstein F, Naik B, Simpson J. (1991) Hypoxia-ischemia stimulates hippocampal glutamate efflux in perinatal rat brain: an in vivo microdialysis study. *Pediatr Res* 30(6): 587-590.

141. Stephenson D, Yin T, Smalstig E, Hsu M, Panetta J, Little S, Clemens J. (2000) Transcription factor nuclear factor-kappa B is activated in neurons after focal cerebral ischemia. *J Cereb Blood Flow Metab* 20(3): 592-603.

142. Stroemer R and Rothwell N. (1997) Cortical protection by localized striatal injection of IL-1ra following cerebral ischemia in the rat. *J Cereb Blood Flow Metab* 17(6): 597-604.

143. Stroemer R and Rothwell N. (1998) Exacerbation of ischemic brain damage by localized striatal injection of interleukin-1beta in the rat. *J Cereb Blood Flow Metab* 18(8): 833-839.

144. Sugimoto K, Iadecola C. (2003) Delayed effect of administration of COX-2 inhibitor in mice with acute cerebral ischemia. *Brain Res* 960(1-2): 273-276.

145. Svrakic N, Nesic O, Herndon D, and Perez-Polo J.R. (2003) Statistical approach to DNA chip analysis. *Recent Progress in Hormone Research* 58:75-93.

146. Szaflarski J, Burtrum D, and Silverstein F. (1995) Cerebral hypoxia-ischemia stimulates cytokine gene expression in perinatal rats. *Stroke* 26(6): 1093-1100.

147. Takao T, Tracey D, Mitchell W, De Souza E. (1990) Interleukin-1 receptors in mouse brain: characterization and neuronal localization. *Endocrinology* 127(6):3070-3078.

148. Teng X, Zhang H, Snead C, and Catravas J. (2002) Molecular mechanisms of iNOS induction by IL-1 beta and IFN-gamma in rat aortic smooth muscle cells. *Am J Physiol Cell Physiol* 282(1): C144-C152.

149. Thompson J, Phillips R, Erdjument-Bromage H, Tempst P, Ghosh S. (1995) I kappa B-beta regulates the persistent response in a biphasic activation of NF-kappa B. *Cell* 80(4): 573-582.

150. Tomita N, Morishita R, Tomita S, Gibbons GH, Zhang L, Horiuchi M, Kaneda Y, Higaki J, Ogihara T, Dzau VJ. (2000) Transcription factor decoy for NFkappaB inhibits TNF-alpha-induced cytokine and adhesion molecule expression in vivo. *Gene Ther* 7(15): 1326-1332.

151. Tomita N, Morishita R, Tomita S, Kaneda Y, Higaki J, Ogihara T, Horiuchi M. (2001) Inhibition of TNF-alpha, induced cytokine and adhesion molecule. Expression in glomerular cells in vitro and in vivo by transcription factor decoy for NFkappaB. *Exp Nephrol* 9(3): 181-190.

152. Tomita N, Morishita R, Tomita S, Yamamoto K, Aoki M, Matsushita H, Hayashi S, Higaki J, Ogihara T. (1998) Transcription factor decoy for nuclear factor-kappaB inhibits tumor necrosis factor-alpha-induced expression of interleukin-6 and intracellular adhesion molecule-1 in endothelial cells. *J Hypertens* 16(7): 993-1000.

153. Touzani O, Boutin H, Chuquet J, Rothwell N. (1999) Potential mechanisms of interleukin-1 involvement in cerebral ischaemia. *J Neuroimmunol* 100(1-2): 203-215.

154. Towfighi J, Mauger D, Vannucci R, and Vannucci S. (1997) Influence of age on the cerebral lesions in an immature rat model of cerebral hypoxia-ischemia: a light microscopic study. *Brain Res Dev Brain Res* 100 (2)**,** 149-160.

155. Traenckner E, Pahl H, Henkel T, Schmidt K, Wilk S, Baeuerle P. (1995) Phosphorylation of human I kappa B-alpha on serines 32 and 36 controls I kappa B-alpha proteolysis and NF-kappa B activation in response to diverse stimuli. *EMBO J* 14(12): 2876-2883.

156. Tsuchiya D, Hong S, Matsumori Y, Shiina H, Kayama T, Swanson R, Dillman W, Liu J, Panter S, Weinstein P. (2003) Overexpression of rat heat shock protein 70 is associated with reduction of early mitochondrial cytochrome C release and subsequent DNA fragmentation after permanent focal ischemia. *J Cereb Blood Flow Metab* 23(6): 718-727.

157. Tusher V, Tibshirani R, Chu G. (2001) Significance analysis of microarrays applied to the ionizing radiation response. *Proc Natl Acad Sci U S A* 98(9): 5116-5121.

158. Uehara T, Matsuno J, Kaneko M, Nishiya T, Fujimuro M, Yokosawa H, and Nomura Y. (1999) Transient nuclear factor kappaB (NF-kappaB) activation stimulated by interleukin-1beta may be partly dependent on proteasome activity, but not phosphorylation and ubiquitination of the IkappaBalpha molecule, in C6 glioma cells. Regulation of NF-kappaB linked to chemokine production. *J Biol Chem* 274(22): 15875-15882.

159. Vannucci R, Christensen M, Yager J. (1993) Nature, time-course, and extent of cerebral edema in perinatal hypoxic-ischemic brain damage. *Pediatr Neurol* 9(1):29-34.

160. Vannucci R, Connor J, Mauger D, Palmer C, Smith M, Towfighi J, Vannucci S. (1999). Rat model of perinatal hypoxic-ischemic brain damage. *J Neurosci Res* 55(2): 158-163.

161. Vannucci R and Perlman J. (1997). Interventions for perinatal hypoxic-ischemic encephalopathy. *Pediatrics* 100(6): 1004-1014.

162. Vaux D, Strasser A. (1996) The molecular biology of apoptosis. *Proc Natl Acad Sci U S A* 93(6):2239-44.

163. Vexler Z and Ferriero D. (2001) Molecular and biochemical mechanisms of perinatal brain injury. *Semin Neonatol* 6(2): 99-108.

164. Vitkovic L, Bockaert J, Jacque C. (2000) "Inflammatory" cytokines: neuromodulators in normal brain? *J Neurochem* 74(2): 457-471.

165. Wang J, Lenardo M (2000) Roles of caspases in apoptosis, development, and cytokine maturation revealed by homozygous gene deficiencies. *J Cell Sci* 113(Pt 5): 753-757.

166. Wang X, Barone F, Aiyar N, Feuerstein G. (1997) Interleukin-1 receptor and receptor antagonist gene expression after focal stroke in rats. *Stroke* 28(1):155-161.

167. Wesche H, Korherr C, Kracht M, Falk W, Resch K, Martin M. (1997) The interleukin-1 receptor accessory protein (IL-1RAcP) is essential for IL-1-induced activation of interleukin-1 receptor-associated kinase (IRAK) and stress-activated protein kinases (SAP kinases). *J Biol Chem* 272(12): 7727-7731.

168. Wong M, Licinio J. (1994) Localization of interleukin 1 type I receptor mRNA in rat brain. *Neuroimmunomodulation* 1(2):110-115.

169. Xu H, Barks J, Schielke G, and Silverstein F. (2001) Attenuation of hypoxia-ischemia-induced monocyte chemoattractant protein-1 expression in brain of neonatal mice deficient in interleukin-1 converting enzyme. *Brain Res Mol Brain Res* 90(1): 57-67.

170. Yang G, Liu X, Kadoya C. Zhao Y, Mao Y, Davidson B, Betz A. (1998) Attenuation of ischemic inflammatory response in mouse brain using an adenoviral vector to induce overexpression of interleukin-1 receptor antagonist. *J Cereb Blood Flow Metab* 18(8): 840-847.

171. Yang K, Mu X, and Hayes R. (1995) Increased cortical nuclear factor-kappa B (NF-kappa B) DNA binding activity after traumatic brain injury in rats. *Neurosci Lett* 197(2): 101-104.

172. Yu Z, Zhou D, Bruce-Keller A, Kindy MS, Mattson M. (1999) Lack of the p50 subunit of nuclear factor-kappaB increases the vulnerability of hippocampal neurons to excitotoxic injury. *J Neurosci* 19(20): 8856-8865.

173. Yue X, Mehmet H, Penrice J, Cooper C, Cady E, Wyatt JS, Reynolds EO, Edwards AD, Squier MV. (1997) Apoptosis and necrosis in the newborn piglet brain following transient cerebral hypoxia-ischaemia. *Neuropathol Appl Neurobiol* 23(1):16-25.

174. Zabel U and Baeuerle P. (1990). Purified human I kappa B can rapidly dissociate the complex of the NF-kappa B transcription factor with its cognate DNA. *Cell* 61(2): 255-265.

175. Zhang M, Harhaj E, Bell L, Sun S, Miller B. (1998) Bcl-3 expression and nuclear translocation are induced by granulocyte-macrophage colony-stimulating factor and erythropoietin in proliferating human erythroid precursors. *Blood* 92(4): 1225-1234.

176. Zhang Z, Chopp M, Goussev A, Powers C. (1998) Cerebral vessels express interleukin 1beta after focal cerebral ischemia. *Brain Res* 784(1-2): 210-217.

VITA

Xiaoming Hu was born on May 12th, 1972 in Beijing, P. R. China. On June 7th, 2003, Xiaoming proudly married Ye Peng. They currently reside in Galveston, Texas and have one daughter.

After graduating in 1991 from Beijing August the first High School, Xiaoming entered Beijing Meidical University, where she received the degree of Bachelor of Medicine in 1996.

In August 1998, Xiaoming began working toward a Master's degree at China-Japan Friendship Institute of Medical Sciences, Beijing. Her thesis was titled *The Immune balance and immune suppression status in cancer patients*. Xiaoming earned a Master's of Medical Science degree in Immunology in August 2001.

Immediately following completion of her Master's degree, Xiaoming entered Ph.D. Neuroscience Graduate Program of UTMB Graduate School of Biomedical Sciences at Galveston, Texas.

Education

M.D., July 1996, Beijing Medical University, Beijing, P.R.China
M.S., July 2001, China-Japan Friendship Institute of Medical Sciences, Beijing, P.R.China

Publications

1. Hu X, Nesic-Taylor O, Qiu J, Rea HC, Fabian R, Rassin D, Perez-Polo JR (2005) Activation of Nuclear Factor-κB signaling pathway by Interleukin-1 after hypoxia/ischemia in neonatal rat hippocampus and cortex. *J of Neurochem*. 93(1): 25-37.

2. Qiu J*, Hu X*, Nesic O, Rassin D, Wood T, Perez-Polo JR. (2004) Effects of NF-κB oligonucleotide "decoys" on gene expression in P7 rat hippocampus after hypoxia/ischemia. *J neurosci. res*. 77(1):108-118. (* co-first author)

3. Hu X, Qiu J, Grafe M, Rea H, Rassin D, Perez-Polo JR. (2003) Different contributions of Bcl-2 family members to cell death in hypoxia and/or hyperoxia in rat cerebral cortex. *International Journal of Developmental Neuroscience*. 21(7):371-377.

4. Hua Z, Zhang Y, Hu X, Jia Z. (2003) Loss of DPC4 expression and its correlation with clinicopathological parameters in pancreatic carcinoma. *World J Gastroenterol.* 9(12):2764-2767.

5. Hu X, Zhao WS, Cong X. (2003) The immune balance in cancer patients. *Journal of Chinese Clinical Medicine*. 4(9): 42-45.

6. Hu X. (2003) IL-10 suppresses tumor immunity. *Foreign Medical Sciences*. 26 (2):107-110. Review.

7. Hu X, Zhao WS, Cong X. (2003) Changes of AgNORs expression of T lymphocytes and helper T cell subsets in peripheral blood mononuclear cells from cancer patients. Chinese Journal of Medical Laboratory Sciences. 26 (1): 34-36.

8. Wang HC, Zhang H, Zhou T, Qiao J, Hu X, Zhao WS. (2002) Protective effect of Hydrophilic Salvia Monomer on liver ischemia/reperfusion injury induced by pro-inflammatory cytokines. *Chinese Journal of Integrated Traditional and Western Medicine*. 22(3): 207-210.

9. Hu LY, Wang F, Hu X. (2002) Investigation of iodine nutritional status of 0-6 year-old children. *Chinese Journal of medical theory and practice*. (2): 169-170.

Published Abstract:

1. Hu X and Perez-polo JR. (2004) IL-1 activation of NF-kappaB signaling pathway in neonatal rat after hypoxia/ischemia. *J of Neurochem*. 90 (suppl. 1): 14.

2. Hu X, Cong X, Ye LY, Zhao WS. (2001) The Th1/Th2 imbalance in cancer patients. *Journal of Tumor Marker oncology* 16(4): 337.

3. Hu LY, Chen JL, He RX, Yan H, Hu X. (1995) Application of determination of BALP to diagnosis, prevention and treatment of rickets. *Chinese Journal of Child Health Care* 3 (S): 24.